A SYNERGISTIC APPROACH TO TRANSTIBIAL SOCKET INTERFACE MECHANICS: EXPERIMENTS AND MODELING

By

Amy Lorraine Lenz

A DISSERTATION

Submitted to
Michigan State University
in partial fulfillment of the requirements
for the degree of

Engineering Mechanics – Doctor of Philosophy

2017

ABSTRACT

A SYNERGISTIC APPROACH TO TRANSTIBIAL SOCKET INTERFACE MECHANICS: EXPERIMENTS AND MODELING

By

Amy Lorraine Lenz

Prosthetics is a clinical field in need of further investigation for the improvement of patient care. Engineering principles can be used in collaboration with clinical expertise to quantify key mechanical issues occurring at the residual limb to prosthetic socket interface. Deep penetrating ulcers can form on the residual limb within the socket and the formation is not understood in the current research regarding interface mechanics. Quantitative data on limb motion within the socket, shear forces at the interface, and propagation of these loads to the skin level and deeper tissues are all lacking in current literature. The broad goal of this research was to understand the interface mechanics of the gel liner on the residual limb relative to the prosthetic socket to improve our understanding of displacements, loads and gel liner slip or no slip conditions.

This work consisted of four aims. Objective 1: Develop a quantitative method for assessing motions between the prosthetic device and gel liner on the residual limb for patients with transtibial amputation. Objective 2: Determine limb displacements, strains, relative socket to limb displacements and angular rotations of transtibial limbs within a prosthetic socket during gait. Objective 3: Quantify normal and shear force within the prosthetic socket for use in modeling. Objective 4: Determine the level of tissue stresses within a layered finite element model including gel liner interactions, constrained with experimental conditions of displacement and normal force.

First, a method to obtain kinematics within a socket was developed using motion capture thin-disc markers beneath the surface of a clear prosthetic socket. Results comparing motion capture with gold standard measurements statistically supported the use of this method.

Secondly, the newly developed method was used to obtain limb displacements, strains, relative socket to limb displacements and angular rotations within a prosthetic socket during gait from eight participants. Reflective markers with motion capture were used to track displacements of the gel liner located within the clear prosthetic socket device. Results provide the most comprehensive data set of interface kinematics in a transtibial amputee population and significantly contribute to knowledge of interface mechanics which are a direct predictor of ulcer formation.

Thirdly, a single transtibial prosthetic socket was instrumented with a two axis load cell to measure kinetics at the internal socket wall. The participant walked in three conditions: gel liner, three ply sock and a hole cut through the liner to measure forces at the skin. Shear and normal force data were obtained during walking for these three conditions.

Lastly, simulations of tissue layers in transtibial amputees were modeled with Finite Element Methods in FEBio. The gel liner to skin interface was modeled for two situations 1) gel liner slips on the skin or 2) does not slip relative to the skin. Kinematic and kinetic conditions obtained in earlier objective served as boundary conditions. The purpose was to further understand tissue stresses that may lead to pressure ulcer development and evaluate the influence of various liner stiffness and thicknesses on underlying tissue stresses.

The presented research benefits the biomechanical community by addressing multiple gaps in the literature and our understanding of the interface mechanics associated with prosthetics. These data also further our understanding of how pressure ulcer formation may progress due to internal resulting stresses.

This dissertation is dedicated to the pursuit of worldwide dreams.

ACKNOWLEDGEMENTS

As a wise mentor once told me, the path to a PhD is a sinusoidal road with a fair share of hills and valleys. As I reflect on those key moments, I am grateful and blessed to have such wonderfully supportive people in my life who have each contributed to my success on this difficult path.

This PhD research would not have been possible without the guidance of my advisor, Tamara Reid Bush. Thank you for believing in me and giving me the opportunity to work on such a novel and stimulating project. Combining your background in pressure ulcers and mine in human gait mechanics lead to a fun adventure in prosthetics for both of us. I greatly appreciate all you have taught me over the years, especially the important skill of saying no. It has been very rewarding learning from you. I will always be grateful for your willingness to work with me as a non-traditional PhD student and be fond of the work we completed during this time.

I would like to thank my wonderful committee members Dr. Roccabianca, Dr. Kwon and Dr. Bix for their support throughout my dissertation development. It has been a pleasure learning from them and receiving their feedback to improve my dissertation. Thank you for their generous time given to support my research.

A huge thank you is owed to all of my lab members (Wu Pan, Amber Cussen, Josh Drost, Jessica Buschman and Justin Scott) for supporting me during my soap opera life throughout these past years and providing a helpful ear with meaningful advice to successfully make it through.

Funding support made the success of this work possible, especially the gracious fellowship contributions from Michigan State University Graduate Office and Michigan State University Mechanical Engineering Department. I am extremely thankful for this support which helped me through challenging unexpected downturns financially. The Society of Women

Engineers have always been a source of encouragement and their scholarship support contributed to my success as well. Thank you also to the School of Engineering at Grand Valley State University for their support in my professional development through equipment and resources. Lastly, my dissertation could not have been possible without the collaboration at Mary Free Bed Rehabilitation Hospital and clinical collaborators, especially Katie Johnson and Patrick Logan. All the staff and management in the Orthotics and Prosthetics division have been supportive in supplying resources for my experimental designs including thermoplastics, scrap materials and duplication of prosthetic sockets.

To my loving dog, Crystal: Here's to the long nights of you watching me work at my desk (both at home and in the lab). Your continuous snuggles, kind kisses and gazing eyes of belief have gotten me through years of school. Your never ending support is worth far more than the small adoption fee I once paid, because you're part of me in life and spirit. We've moved mountains together and gotten through many moves across valleys. The support of a dog is unparalleled when it comes to selflessness. "A dog is the only thing on earth that loves you more than she loves herself."

To my mom, Karen, and dad, Russell: I cannot thank you enough for all the support and encouragement you've given me over the years. Mom, you have been my partner in crime, my steady rock, my personal cheerleader and my tireless source of inspiration. Thank you for always coming to my endless rescue at the drop of a dime. We've had so many priceless memories that have gotten me through the ten years of school. Here's to more of them and forever being appreciative of your contributions to my career success. Dad, you have always been my tinkering inspiration that began my journey as an engineer at a very young age. Thank you for instilling such great qualities in me which have allowed me to grow as a successful engineer. Even when you didn't realize, you were teaching me how to think outside the box, critically evaluating problems and developing creative solutions. This dissertation was developed on a clinical

curiosity that I believed engineering could help to solve. Thank you dad for having encouraged me at a young age to think in this manner. It will forever be useful and essential to my career in research and engineering.

To my irreplaceable friend, John: Thank you for being such as support as an expert in SolidWorks, stable tower of strength and late night sounding board. You've been essential to the success of my research, passing qualifying exams and motivating homework for the entire length of this degree and treacherous road. I wouldn't have been able to do it without you.

To my amazing engineering interns, Alex, Dayna, Alyssa, Kate, Sydney, Curtis, Alyna and Brooke: It was extremely rewarding mentoring you and working with you over the years. I'm so proud to see how you've grown, developed professionally and are all succeeding so well in your engineering careers. You each contributed to my dissertation research by stimulating valuable technical questions, being an extra set of hands for data collection, processing in Vicon, having fun in MATLAB and troubleshooting in FEBio. I'm thankful to have had the opportunity to work with all of you.

TABLE OF CONTENTS

LIST OF TABLES

LIST OF FIGURES

KEY TO ABBREVIATIONS

CAD	Computer aided design
CAM	Computer aided modeling
CT	Computed tomography
FE	Finite element
FEA	Finite element analysis
FEBio	Finite Elements for Biomechanics
FEM	Finite element methods
kPa	Kilopascals
LCS	Local coordinate system
MRI	Magnetic resonance imaging
O_{LCS}	Origin of local coordinate system
UTS	Ultimate tensile strength

1. INTRODUCTION

1.1 Overview

Prosthetics is a clinical field in need of further investigation for the improvement of patient care due to the complex nature of device development. Engineering principles can be used in collaboration with clinical expertise to quantify key mechanical issues occurring at the residual limb to prosthetic socket interface. Deep penetrating wounds in the skin called ulcers can form on the residual limb within the socket. The formation of ulcers is not understood as the interface mechanics have not been well researched.

Previous research has aimed to address certain portions of prosthetics which can influence improvements of prosthetic design, specifically alignment and fit. However, numerous gaps still exist in the basic knowledge of what boundary conditions are occurring at the socket to limb interface. Quantitative data on limb motion within the socket, motion relative to the socket, shear forces at the interface, and propagation of these loads to the skin level and deeper tissues are all lacking in current literature.

The goal of this research was to study limb interface mechanics of the prosthetic/limb boundary for better understanding of pressure ulcer formation. This work includes the following aims:

Specific Aim 1: Develop and validate a quantitative method for assessing motions between the prosthetic device and gel liner on the residual limb for patients with transtibial amputation.

Method: Transtibial rigid and deformable replica models were used in the development of a novel method to validate measurement of motion capture thin-disc markers beneath the surface of a clear prosthetic socket. Markers were placed beneath the surface of the clear transparent prosthetic socket and used to measure inter-marker distances which were compared statistically to caliper inter-marker distance measurements.

Specific Aim 2: Determine limb displacements, strains, relative socket to limb displacements and angular rotations of transtibial limbs within a prosthetic socket during gait.

Method: Eight participants consisting of nine limbs with below knee amputation were recruited for the study. Reflective markers were placed on bony and soft tissue anatomical landmarks throughout the residual limb beneath the surface of a clear duplicated prosthetic socket. A motion capture system was used to track the markers. Displacements and strains were analyzed during walking. Anatomical locations were additionally used to compute relative limb to socket displacements and relative rotation of the limb within the socket.

Specific Aim 3: Experimentally quantify longitudinal shear force and normal force within the prosthetic socket for a transtibial amputee during walking in a single case study.

Method: A single transtibial prosthetic socket was instrumented with a two axis load cell to measure forces at the internal socket wall. The participant walked in three conditions: gel liner, three ply sock and a hole cut into the liner to measure forces at the skin. Force data located at the mid fibular region of the residual limb was desired for constraining finite element models and to further investigate interface mechanics in a pin locking suspension with gel liner interface.

Specific Aim 4: Determine the level of tissue stresses within a layered model including gel liner interactions, constrained with experimental conditions of displacement and normal force.

Method: Numerically model the tissue layers in transtibial amputees with Finite Element Methods (FEM) in Finite Elements for Biomechanics (FEBio). The residual limb section was defined as a multi-layer model with different material properties for each layer based on literature. Layers included bone, muscle, skin and the prosthetic gel liner. Non-linear hyperelastic materials were used for the muscle and skin. This model simulated tissue layer stresses within the residual limb in response to boundary conditions occurring at the socket interface. Boundary conditions used were from experimentally collected displacement and force data.

This document has been formatted with a literature review plus four chapters, one chapter per aim, followed by a conclusion chapter. Each chapter has been formatted as a publication. A list of chapters can be seen as follows:

Chapter 1 Literature Review

Chapter 2 A New Method to Quantify Residual Limb Motion within a Prosthetic Socket for Below Knee Amputees

Chapter 3 Understanding Displacements and Strains of the Gel Liner for Below Knee Prosthetic Users

Chapter 4 Instrumented Transtibial Socket for Evaluating Shear and Normal Force: A Case Study

Chapter 5 Finite Element Analysis of the Socket to Limb Interface with Experimental Data Inputs

Chapter 6 Conclusions

1.2 Limb Loss Statistics

In the United States, approximately 1.7 million people are living with limb loss (Ziegler-Graham et al. 2008). Additionally, an estimated 185,000 new amputations are performed each year (Owings & Kozak 1998), with 120,000 of these amputations non-traumatic in nature (Armstrong et al. 1997). Fifty-four percent of amputations are a result of complications from vascular diseases such as diabetes, followed by 45% due to traumatic amputation (Ziegler-Graham et al. 2008). Additionally with this many individuals undergoing amputation each year, further amputation due to infection or ulceration particularly in the vascular patients is a clinical concern. Progression to higher level amputations occurred 35% of the time when patients had originally undergone a foot or ankle amputation (Dillingham et al. 2005). Furthermore, diabetic amputees had a higher frequency of progression to a higher amputation than those nondiabetic amputees (Dillingham et al. 2005). When analyzing racial differences in amputee rates, African Americans exhibited greater risk for amputation, reportedly ranging from two to four times more likely than Caucasians (Collins et al. 2002; Dillingham et al. 2005). Those patients who underwent revascularization prior to the necessity for amputation were more often Caucasian, with elderly African Americans receiving care at a significantly lower rate than Caucasians (Holman et al. 2012). In a study focused on Oklahoma Indians, the incidence rate of lower extremity amputation was 1.8% of the population each year with males being twice as frequent as females with significant co-morbidity being diabetes (Bahr et al. 1993). Regardless of race, gender or co-morbidities, if limb health is not maintained, the 5-year rate of mortality for patients with lower extremity amputation can be as high as 74% (Robbins et al. 2008).

1.3 Skin Disorders in Amputees

Persistent dermatologic concerns in amputees can restrict typical use of a prosthesis. Maintaining a healthy residual limb is essential for preventing further amputation or pressure ulcer formation. Studies have investigated the range of skin disorders seen in a population of amputees. In a sampling of patients with amputation, 34% experienced a skin problem including epidermoid cysts, follicular hyperkeratoses, verrucous hyperplasia, calluses, ulcers, bacterial folliculitis, tinea infection, eczema, dermatitis, transient erythema caused by friction, or unexplained rashes (Lyon et al. 2000). These dermatologic problems can be classified by: physical effects of wearing their prosthesis, allergic contact dermatitis, infection and constitutional skin disease. Type of prosthetic design can also contribute to the frequency of skin disorders with significantly more patients experiencing issues in soft socket prostheses (Koc et al. 2008) as compared to those using silicon prostheses, regardless of suspension type. In the prosthetic-user population investigated by Koc et al., 74% of patients experienced a skin problem and of the 142 patients enrolled in the study, the most common level of amputation was transtibial (n = 113). Any of these skin complications can limit the patient's use of their prosthesis, cause more serious irritation or complications and potentially lead to reasons for further amputation.

1.4 Pressure Ulcer Statistics

Pressure ulcers are regional tissue damage areas from habitual excessive loading on the skin from various body-interface conditions. Ulcers can be either superficial or deep in nature depending on the loading conditions (Mak et al. 2010). Superficial pressure ulcers often result from primarily frictional and abrasive rubbing of the skin relative to the prosthetic device. Deep ulcers originate within a close proximity to bony prominences which can become massive lesions from within before appearing at the surface. These bony prominences are particularly relevant and troublesome in lower extremity amputees where loading is concentrated within the prosthetic socket. During daily activities, amputees wearing prosthetic devices experience high loads between the prosthetic socket and the soft tissue around the residual limb; however, few studies have actually quantified this loading.

In a systematic review, primary patient risk factors for pressure ulcer development were identified as patient activity level/mobility, blood perfusion (including diagnoses such as diabetes), and status of existing ulcers on skin (Coleman et al. 2013). Mobility factors include sub-categories of bedfast, chair fast, walking with limitations and walking with no limitations (Coleman et al. 2013). The most prevalent site on the lower limb is the posterior aspect of the heel, which unhealed heel ulcerations commonly lead to amputation (Arao et al. 2013). Important to note are the morphological characteristics in skin when pressure ulcers develop. The tissue becomes less tolerant to ischaemia and therefore less resilient to increased external forces (Arao et al. 2013). The role of skin blood flow dynamics are key in understanding pressure ulcers because blood flow function determines the ability of skin to respond to ischemic stress (Liao et al. 2013). Due to reduced blood flow, the tissues of the extremities cannot receive adequate oxygen and nutrients from the blood stream. Necrosis of the tissue begins, and infections often result (Bouten et al. 2003). Reduction of blood flow can be caused by different changes in load applied to the skin and has been proven to differ under normal or shear loads (Manorama et al. 2010). Transcutaneous oxygen and blood perfusion levels decreased when shear loads were applied in addition to normal loads (Manorama et al. 2010; Manorama et al. 2013). Understanding of load on the skin, such as that due to a prosthetic, is important to understanding and preventing ulcer formation. Particularly in the case of amputees, blood flow dynamics can be compromised due to the loading conditions at the socket to limb interface. Ultimately, pressure ulcers are a great clinical concern, increasing infection and leading to additional amputations.

1.5 Peripheral Arterial Disease: Risk Factors for Foot Ulceration and Implications in Diabetic Patients

1.5.1 Importance of Restructuring Blood Flow After Amputation

Peripheral arterial disease is prevalent in 20-30% of diabetic patients (Marso & Hiatt 2006). Patients with peripheral arterial disease and diabetes are at a higher risk of lower extremity amputation than those without diabetes (Jude et al. 2001). Many considerations need to be taken into account when amputation is indicated. The following review will outline factors that relate to amputation including peripheral arterial disease, foot ulcerations and the importance of understanding blood flow patterns (angiosomes). All relate to reasons individuals have amputations and lead to prosthetic use.

Lower extremity peripheral arterial disease (PAD) is commonly associated with increases in morbidity. In worst cases, 1-2% of patients need major amputation (Khan et al. 2014). Epidemiological studies have confirmed an association between diabetes and increased prevalence of peripheral arterial disease (Marso & Hiatt 2006). The vessels often involved in diabetic PAD patients are the tibial vessels and the distribution of pathology is located more distally than in patients with PAD (Haltmayer et al. 2001). The abnormal metabolic state that coincides with diabetes directly contributes to the development of atherosclerosis in PAD patients with an increase in vascular inflammation. Amputation as a result of PAD is common for patients experiencing treatments that have been unsuccessful to control infection (Marso & Hiatt 2006).

1.5.2 Diabetic Foot

Chronic foot ulcers are a result of foot lesions commonly in diabetic patients which persist and contain complications often due to infection. Over 85% of amputations are preceded by an active foot ulcer as these conditions are closely inter-related in diabetes (Boulton 2008). Patients with a combination of infection and ischemia who presented with foot ulcers were 90 times more likely to undergo midfoot or higher amputation compared to those with better wound management (Prompers et al. 2007). If occlusion occurred, lengthened duration of blood occlusion was a characteristic associated with poor prognosis for amputation (Fagundes et al. 2005). Experimental modeling of engineering mechanics related to arteries has provided understanding of arterial wall density, poisson ratio, compliance, internal volume, pulse wave velocity and wall thickness (Langewouters et al. 1984); however, computational modeling that addresses impaired patient populations are missing from the literature and are essential for further understanding of ulcer formation.

1.5.3 Reasons for Amputation

When limb salvaging methods are no longer viable, amputation may be the best option for preserving ambulation capabilities. For individuals who are being considered for amputation, a few considerations must be assessed. If the patient has a low chance of ambulation post amputation, a through-knee-amputation is often indicated to prevent long term knee flexion contractures which may develop in prolonged seated postures (Brown et al. 2012). For those patients who have the potential to ambulate, appropriate surgical procedures are considered for ample blood flow to the residual limb as well as ease for fitting into a prosthesis (Brown et al. 2012). Regardless of care taken to preserve healthy blood flow to the residual limb, re-amputation can be necessary if wound ulcerations form or persist (Brechow et al. 2013).

1.5.4 Angiosomes

Blood flow patterns are complex and especially important to understand during amputation. Vascular surgery is complicated when preserving adequate nourishment to the residual tissue. Surgeons are mindful of vascular territories, also known as angiosomes. Angiosomes are regional subdivisions of branching arteries that supply regions of tissue. These areas need to be considered during vascular surgery, especially limb salvaging surgeries or in the worst case, amputation. Compromised blood flow to a residual limb can lead to poor nourishment of the residual limb and could predispose tissue necrosis. One study investigated angiosomes by using fresh cadavers where regions of the lower extremities could be dissected to separate muscles while preserving blood vessel connections (Taylor & Pan 1998). This allowed for specific knowledge of which muscle was supplied with blood regionally as the arteries bifurcated. Taylor and Pan et al., showed that the anterior leg compartment muscles were exclusively supplied by the anterior tibial artery. It was clinically an important finding because with a common vessel supplying one muscle followed by another in a narrow passage, this group of muscles is particularly vulnerable to ischemia because the compartment is highly constricted and has few vascular connections. When amputation is indicated, careful consideration of the angiosome regions should be utilized (Attinger et al. 2006). As noted earlier, even with careful consideration of blood vessels, and successful surgery, in many prosthetic users, ulcers continue to form. Thus, further consideration of the prosthetic socket design to account for patient specific blood occlusion regional concerns may decrease ulcerations in regions where vessels could be easily occluded over bony prominences.

1.6 Prosthetic Device Components: Fabrication Selections

Prosthetics are designed to mimic anatomical function. In order to accomplish this task with a variety of clinical limb presentations, there are numerous componentry options and fabrication methods. The wide selection for prosthetic interface and suspension options (Figure 1-1 and 1-2) creates a complex prescription process for developing and selecting a definitive device for a patient.

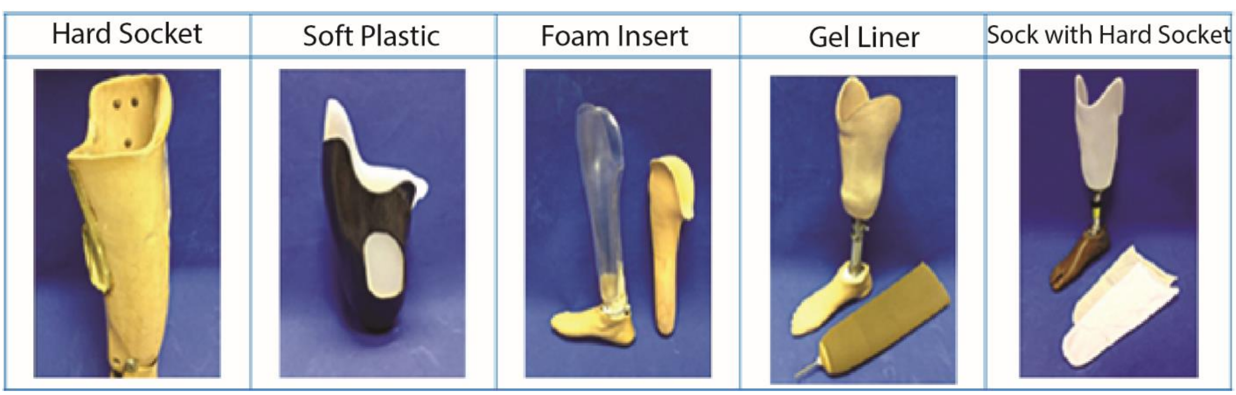

Figure 1-1. Various prosthetic interface options available for patients with transtibial amputation (Spires et al. 2014).

Figure 1-2. Transtibial suspension types (Spires et al. 2014)

1.6.1 Sockets

The design of a prosthetic socket is always patient specific. Within a transtibial socket, controlling the limb motion is essential for minimizing skin friction which could lead to pressure ulcers. Additionally, minimizing excessive motion of the residual limb relative to the socket is important for optimizing gait efficiency (Gard 2006; Fergason & Smith 1999). Three main types of transtibial socket types are: patella tendon bearing (PTB), total surface bearing, and hydrostatic (Spires et al. 2014). The PTB socket design became popular in the late 1950s (Radcliffe & Foort 1961). In a PTB socket, the device is meant to bear loads through pressure tolerant areas such as the gastrocnemius, anterior tibialis, medial tibial flare, lateral shaft of fibula and patella tendon; while it relieves pressure from sensitive areas such as the tibial crest, fibular head, hamstrings and distal ends of the tibia and fibula (Spires et al. 2014). Advantages of a PTB socket are that it creates a triangulation to control rotation of the socket relative to the residual limb but this is difficult to implement in short residual limbs. Generally, the PTB style socket is thought of as widely successful for transtibial amputees with reportedly 90% of below knee amputees functioning well with a PTB socket (Galdik 1955; Pirouzi et al. 2014). Secondly, the total surface bearing socket design loads the entire residual limb and is typically donned over a liner (Spires et al. 2014). The gel liner can provide cushioning and absorption of rotational and shear forces while aiming to provide equal distribution of loads over the residual limb. Lastly, a hydrostatic suction socket generally provides less motion of the residual limb within the socket because it elongates the soft tissue to increase stiffness between the bone and soft tissues for augmented stability during gait (Kahle 1999). The most commonly implemented socket type is a PTB or modified PTB and therefore was the focus of this dissertation research.

1.6.2 Socket Interface

The socket interface with the residual limb ranges from direct skin contact to gel liner interfaces. In a direct socket interface, individuals need to have a limb with adequate soft tissue covering bony prominences because no barrier exists between the skin and hard socket (Spires et al. 2014). For patients requiring a cushioned interface, soft materials comprising of either a soft plastic flexible inner liner or foam inserts can be used within the socket (Spires et al. 2014). These provide manufacturing adaptation capabilities for anatomical changes and sensitive areas to improve comfort but they require daily cleaning as they can absorb perspiration. Lastly, a gel liner typically made of urethane, silicone or thermoplastic elastomer can decrease friction and shear forces against the skin and can also provide cushioning (Spires et al. 2014). Gel liners are most commonly prescribed for persons with below knee amputations (Boutwell et al. 2012) and therefore the following research includes the use of a gel liner.

1.6.3 Suspension

Numerous factors are taken into account when considering a suspension type, these include skin condition, volume, limb length, available range of motion (intact knee health), patent's activity level, comorbidities (peripheral neuropathy, vascular disease, cardiac disease) and an individual's cognitive level (ability to maintain device) (Kapp 1999; Pritham 1979). Seven typical suspension options include (Figure 1-2): joint and corset, sleeve, supracondylar cuff, supracondylar suprapatellar, supracondylar, gel liner with pin, and subatmospheric (Spires et al. 2014).

First, joint and corset suspension provides an above the knee brace system to help with knee medial/lateral instability with an increased weight-bearing surface. However, this adds weight to the prosthetic device with potential for increased pistoning of the residual limb relative to the socket. Pistoning is when the prosthetic device translates vertically with respect to the residual limb due to the suspension of the limb (H. Gholizadeh et al. 2014). Further disadvantage is potential thigh musculature atrophy from not using the muscles for stability (Spires et al. 2014).

Secondly, sleeve suspension consists of a frictionous tightly fit outer sleeve that encompasses the socket with the above knee residual limb. It is excellent for patients with a long residual limb, stable knee ligament structures, good hygiene and no vascular comorbidities. Yet, sleeve suspension can restrict knee motion, causing skin problems and it can be difficult to don.

The next set of suspension types (supracondylar cuff, supracondylar suprapatellar, and supracondylar) function based on the ability to use bony anatomic landmarks for suspension and occasionally additional straps. They are generally easy to don, provide increased medial/lateral stability by crossing the knee joint but can be difficult to fit in obese patients (Spires et al. 2014).

Then there are gel liners with pin suspension set ups. These utilize a locking mechanism on the distal end of the gel liner which attaches to the socket to hold the liner inside the socket (Fergason & Smith 1999). The gel liner provides a frictional interface to suspend the complete device off of the residual limb. A gel liner with pin suspension allows for less restriction of knee range of motion, absorption of rotational forces, allows for volume fluctuations by adding socks within the socket, and added cushioning within the socket (Spires et al. 2014).

Lastly, subatmospheric pressure suspension provides excellent suspension with decreased pistoning at the residual limb, added proprioception and shown to help wound healing (Brunelli et al. 2009). Major disadvantages to a subatmospheric pressure suspension though are high maintenance for adequate function with expensive equipment cost and added weight to the prosthesis. The most frequently implemented suspension type consists of the pin locking mechanism with liner interface and therefore was a focus when designing this dissertation research in a prospective experimental study.

1.6.4 Combinations of Socket Interface and Suspension

A recent worldwide systematic review concluded there is no singular clinical standard for suspension methods in transtibial amputees; however, the most favored setup by users consisted of the total surface bearing socket with gel liner interface pin/lock suspension system (H. Gholizadeh et al. 2014). The implementation of soft gel/silicone inner layers with pin locks has greatly improved the function of artificial limbs by allowing a more comfortable prosthetic solution with greater movement at the proximal joint (Heim et al. 1997). Notable however is the large friction between the gel or silicone interface and residual limb skin which is clinically stated to reduce the pistoning motion when the artificial foot contacts the ground (Narita, Yokogushi, Shii, Kakizawa & Nosaka 1997). While this friction interface stability allows for functional clinical benefits, understanding the skin surface during ambulation is important as it may be the source of tissue breakdown which has become covered by the gel liner. Therefore, liner motion should be monitored as it has become a common and preferred method of suspension interface in transtibial amputees.

1.7 Experimental Literature on Lower Extremity Amputees

1.7.1 Interface Pressures

Numerous studies have experimentally assessed the pressure distribution within the socket (Muller & Hettinger 1952). Key studies have documented pressure distributions for many years, using this technology to assess stump-socket pressure and comparisons between different socket types (Pearson 1974; Meier 1973; Leavitt et al. 1970; Appoldt et al. 1969; Naeff & van Pijkeren 1980; van Pijkeren et al. 1980). For example, pressure distributions during self-selected over ground flat walking are not predictable of pressures during walking on stairs, slopes and uneven ground (Dou et al. 2006). Regardless of task, regional pressure differences can be observed over the residual limb when comparing the regions of the patellar tendon, lateral tibia, medial tibia, anterodistal tibia and popliteal depression. Highest pressures were observed in normal gait at the popliteal depression (back of the knee joint), followed by the anterodistal tibia and patellar tendon (Dou et al. 2006). Most recently, pressure distribution at the socket to limb interface has been implemented to compare differences in prosthetic componentry, suspension types, and liners (Beil et al. 2002; Hossein Gholizadeh et al. 2014; Ali, Abu Osman, et al. 2012; Wolf et al. 2009; Boutwell et al. 2012; Eshraghi et al. 2013; Gholizadeh et al. 2015; Ali, Osman, et al. 2012).

One study followed a single patient and found that the anterior distal residual limb peak pressures were almost 10 times higher in the patellar tendon bearing socket and the patient reported increased comfort in the total surface bearing socket (Gholizadeh et al. 2015). For another study with twelve unilateral transtibial amputees, greatest peak pressures occurred at the mid-posterior location (Wolf et al. 2009; Ali et al. 2013). These regions however were not consistent with Dou et al., where in stair climbing they found notable changes when compared to walking in the anterior and proximal areas above the patellar tendon region.

Prosthetic liner differences can also influence limb comfort and perceived pressure distribution within the socket. Liners provide a layer of cushion between the limb and the socket; depending on the limb architecture, more padding over bony landmarks may be desired to reduce high peak pressures. In one study, fibular head peak pressures were significantly reduced with a thicker liner, and resulted in increased patient comfort (Boutwell et al. 2012). Further mechanics based research needs to be conducted to address the correlation of liner selection with increased risk of pressure ulcer development.

1.7.2 Shear Stress at Interface

Pressure distribution is describing the compressive nature of the limb tissue, however, a combination of normal and shear stresses are more valuable for describing tissue break down due to skin blanching and blood occlusion. First published in 1992, the development of strain based transducers established a method to measure shear stresses in two orthogonal directions on the plane flush with the inside of the socket (Sanders et al. 1992). Three participants were recruited for the study in which custom total-contact patellar-tendon-bearing prosthesis were designed and fabricated for each transtibial amputee. Each socket was lined with a Pelite interface which was custom designed to fit without the use of an additional sock or nylon sheath and was suspended by a latex sleeve. This allowed for shear stresses to be measured directly at the skin surface.

To further the understanding of shear stresses at the surface of the residual limb, Sanders et al. improved on the original work expanding shear stress measurement to thirteen locations on two patients with transtibial amputation (Sanders et al. 1997). Pressures as well as resultant shear stress maxima were recorded during gait and the resulting timings of these loads. Areas of highest shear stress were consistently at the anterior distal location (Sanders et al. 1997). Timings of when maxima resultant shear stresses occurred were variable (Sanders et al. 1997).

This socket interface measurement was implemented in numerous studies to quantify differences in shear stresses over time at daily and six month time points as well as changes due to prosthetic alignment or various prosthetic componentry options (J. E. Sanders et al. 1998; Sanders et al. 2000; Sanders et al. 2005). Most recently Schiff et al. instrumented load cells into a transtibial socket to further explore shear forces for amputees with and without distal tibia-fibular bone bridges (Schiff et al. 2014). Further understanding of load transfer between the residual limb and the prosthetic socket is not only important in ulcer formation but also in surgical decision making of best amputation practices (Schiff et al. 2014). Extensive shear force information is currently lacking, more experimental work combined with finite element modeling can further this understanding of shear throughout the limb and implications loading on deep tissue stresses.

1.7.3 Friction and Prosthetic Liners

In order to better understand the interaction of prosthetic gel liners at the residual limb interface, detailed descriptions of the material properties of commonly used interface materials have been researched (Emrich & Slater 1998; J E Sanders et al. 1998; Sanders et al. 2004). It was discovered that normal force versus shear force curves were nonlinear and the coefficient of friction increased with higher applied force (J E Sanders et al. 1998). Later, the Sanders group improved upon their previous work testing 15 products for classification of material performance under compressive, frictional, shear and tensile loading conditions (Sanders et al. 2004). Understanding liner materials is essential in optimizing prosthetic fits, tailoring prosthetic needs based on a patient’s limb structure and preventing ulcer formation. These data in conjunction with a finite element model optimizing gel liner materials will be helpful for understanding interface forces and movements between different interfaces of the skin and liner or the liner and prosthetic socket.

1.7.4 Pylon to Socket Interface: Load Cells, Forces, Moments, Inverse Dynamics

Load cells have been used in prosthetic research to instrument the junction of the prosthetic pylon to the base of the prosthetic socket. Neumann et al. instrumented a load cell at the base of the prosthetic socket in a portable manner to test three below knee amputees walking on various terrains and curved pathways to measure real world situations of transverse plane moments within the pylon (Neumann et al. 2013). Their purpose of analyzing this planar moment was to hypothesize the contributing factors within the socket to these transverse plane moments. The transverse moments represent when the residual limb and socket are attempting to rotate relative to each other possibly generating shear forces at contact points within the socket. Higher reported transverse moments were recorded when patients were asked to walk in a curved circular path (Neumann et al. 2013). Similar studies instrumented load cells for above knee amputees to measure forces and moments for multi-body simulation and inverse dynamics during gait (Dumas et al. 2009; Schwarze et al. 2013). Schwarze et al., successfully validated a multi-body simulation for calculating loads on the prosthesis interface for above-knee amputees. However, none of these data directly assess loads and boundary conditions occurring at the limb to socket interface for understanding localized regions of common tissue breakdown. These data are necessary to fully model the liner to skin to device interface.

1.7.5 Kinematics: Whole body and Limb within Socket

Numerous experimental studies have investigated aspects of kinematic changes of amputee gait in a whole body analysis as well as within socket kinematics. One approach used stereogrammetric analysis to quantify skeleton relative to socket motion and skin strain during strenuous motions such as a sudden stop and stepping down from stairs (Papaioannou et al. 2010). Roentgenological technology has been used to quantify movement between the stump and socket (Erikson & Lemperg 1969). However, these analyses were limited to a small imaging view due to the instrumentation. Key findings included maximum relative strain of proximally located markers to be 8-10%, which is important for clinicians to know for optimizing prosthetic design fit (Papaioannou et al. 2010). Before this more complex experimental study had been developed for dynamic use, x-rays were initially used to quantify static positioning of the residual limb bone structure within the socket (Friberg 1984; Newton et al. 1988; Lilja et al. 1993).

Ultrasound has also been used to measure planar motion of the femur relative to socket in trans-femoral patients (Convery & Murray 2001; Convery & Murray 2000). The ultrasound technique was compared to x-ray methods of determining frontal and sagittal plane angles of the femur relative to socket and results were inconclusive (Convery & Murray 2001; Convery & Murray 2000). Attempts to use ultrasound were creative however, this application would not work due to the presence of the tibia and fibula. Alternative experimental methods need to be developed to quantify limb motion within the socket.

Dynamic analysis of socket relative to limb motion during walking is important to measure for improving prosthetic device fit. A noncontact sensor was developed from a lightweight photoelectric sensor positioned beneath the socket to assess pistoning within the socket (Sanders et al. 2006). Displacements during swing relative to stance phases of gait were obtained, proximal displacements averaged 41.7 mm across multiple gait cycles for a single transtibial amputee (Sanders et al. 2006). Motion was greater than expected of the socket relative to the residual limb and therefore further exploration should quantify this in more patients and more regions within the prosthetic limb.

Lastly, motion capture has been utilized to quantify limb motion within the socket (Childers & Siebert 2015; Gholizadeh et al. 2012). Gholizadeh et al. assessed vertical displacement of the limb relative to the socket along the lateral aspect of the residuum for two different liners. However this was not conducted during walking but rather a progression of full-weight bearing, semi-weight bearing, non-weight bearing and with 30, 60 or 90 N loads. Key findings compared the two liners demonstrating the Seal-In X5 liner decreased pistoning by 71% compared to the Iceross Dermo liner (Gholizadeh et al. 2012). Another study drilled holes in the prosthetic socket of a single subject to allow for three motion capture markers to be placed on the gel liner which extended out from the prosthetic socket (Childers & Siebert 2015). Residual limb movement relative to the prosthetic socket demonstrated about 5 mm differences proximally versus distally; however this only represented one person, and three locations with respect to the prosthetic socket (Childers & Siebert 2015). The limb may be moving in uneven displacements depending on the soft tissue or bony anatomical structure; therefore, further investigation should evaluate motion capture methods in more regions of the residual limb during walking.

1.7.6 Residual Limb Volume Changes

Throughout an amputee's life, management of their residual limb volume is essential for maintaining proper socket fit and accounting for within day volume changes for the purpose of minimizing pressure ulcers and wounds (Sanders & Fatone 2011). Numerous reasons for amputation exist, but regardless of initial etiology the residual limb during the first 12-18 months changes considerably in shape, tissue structure and volume (Prosthetists 2004). Immature limbs, just after amputation, undergo extensive edema and muscle atrophy, therefore socket volume must be adjusted frequently (Golbranson et al. 1988). After this period of initial healing the limb is then considered a mature limb; however, daily fluctuations in volume still occur and can often be problematic (Zachariah et al. 2004; Sanders et al. 2009). Daily volume changes in mature limbs are thought to be a product of pooling of blood in the venous compartment, arterial vasodilatation and changes in interstitial fluid volume (Zachariah et al. 2004; Sanders et al. 2009). The amount of daily volume fluctuation is also thought to be a function of comorbidities, prosthesis fit, activity level, ambient conditions, body composition, dietary habits and for women, menstrual cycle. A prosthetists' role in volume management is essential for determining proper socket design, prescription of within socket accommodations for volume fluctuation and determination of the need for a new socket. Shape and volume changes in the residual limb are believed important to changes in limb-socket interface pressure and shear stress distributions, which may in turn lead to socket fit problems, including gait instability and skin breakdown (Sanders et al. 2005).

1.8 Finite Element Modeling of Residual Limb and Deep Tissue Injury

Finite element analysis and computer-aided design have improved upon a once purely artisan field with increasing knowledge of within socket mechanical interactions, deep tissue responses to loading, and improved socket design. First, in the late 1980s, FE modeling was introduced as a potential instrument for prosthetic socket design (Krouskop et al. 1987). While the model was simplistic, it was the first step towards future work aimed to address mechanics within the socket that could not be seen with the eye. Other models quickly immerged using CT, MRI and simplified geometries of amputee limbs with a generic layer of tissue, rigid bone structure and an encompassing socket bound by external loads were implemented to investigate socket interface mechanics (Brennan & Childress 1991; Reynolds & Lord 1992; Sanders & Daly 1993; Steege & Childress 1988; Silver-Thorn 1991; Quesada & Skinner 1991; Zhang et al. 1995).

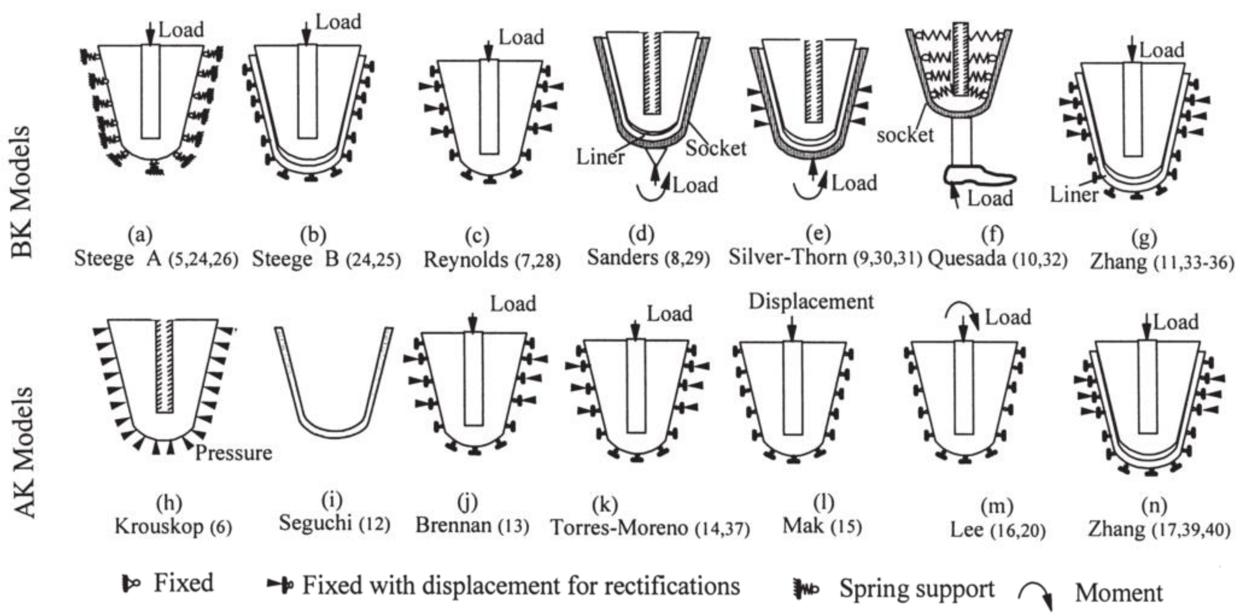

Figure 1-3. Previous FE models for residual limb and prosthetic socket. Below knee (BK) and above knee (AK) model examples (Zhang et al. 1998)

While theoretically any model can be solved under the correct series of parameters, the value of a FE model improves with experimental validation. During novel model development, comparison with experimental data is essential to confirm a realistic clinical situation is being represented by the model.

More recent models have refined tissue layers, interactions between those layers and included mathematical constitutive models of elastic non-linear material properties to mimic biological tissues. Real-time patient specific finite element analyses have been conducted to assess internal stresses of soft tissue for the continued purpose of improving prosthetic fit (Portnoy et al. 2007). The development of these models allowed for the investigation of deep tissue injury when applied to loading of a transtibial's limb (Portnoy et al. 2008; Portnoy, Siev-Ner, Shabshin, et al. 2009; Portnoy, Siev-Ner, Yizhar, et al. 2009; Portnoy et al. 2010; Portnoy et al. 2011; Gefen et al. 2008). Key findings have discovered higher stresses accumulating at the tissue-to-bone interface rather than more superficial tissue layers, indicating close monitoring of limb health is essential in this clinical population. Pressure ulcers may be forming in the deep layers of tissues far before they present at the skin surface. Further detailed refinement of FE models is needed to mathematically account for the limb's complexity as well as customized model inputs based on experimental data. Finally, validation of a FE approach with experimental data will strengthen usage for predicting the onset of pressure ulcers and help to indicate the prosthetic componentry that will minimize certain boundary conditions leading to limb wounds.

1.9 Conclusions

The medical complexity of blood flow dysfunction, prosthetic device design, experimental methods in amputees and finite element models have been described in this literature review. Many considerations need to be addressed when amputating an infected and poorly nourished diabetic limb. Extensive research and collaboration with engineering should be considered to understand the mechanical limitations of arterial wall strength, blood flow to peripheral regions and remapping of blood flood pathways during amputation. Specific research methods to address these topics in amputated limbs is necessary to define the primary factors which may lead to ulceration on the residual limb from poor tissue nourishment.

With extensive componentry options for making transtibial prosthetic devices, there is not one clinically perfect answer with a proven algorithm to have optimized performance using a particular device. The clinical judgement and crafted skill of developing a prosthetic device is extremely complex. However, experimental research will continue to contribute quantitative data to the field of prosthetics to guide appropriate device development.

A variety of research studies have investigated crucial questions relevant to the transtibial patient population focusing on prosthetic componentry, pressure distribution, walking kinematics, within socket fit and forces measurement. However, in such a complex field with reoccurring problems of pressure ulcers, more research is needed to address numerous unknowns. As prosthetics transitions from an artisan field to an integrated computerized technical trade, biomedical engineering research can be at the forefront of new methods, prosthetic designs and improved quality of life for patients living with amputations.

As a result of the above literature review, experimental and modeling aims have been developed to address areas of research needed to quantify limb motion beneath the surface of a transtibial socket including measurement of displacements, strains and shear forces throughout the residual limb with understanding of deep tissue response. These novel studies to address these research questions have been outlined in the following chapters.

2. A NEW METHOD TO QUANTIFY RESIDUAL LIMB MOTION WITHIN A PROSTHETIC SOCKET FOR BELOW KNEE AMPUTEES

2.1 Abstract

Many amputees who wear a leg prosthesis develop significant skin wounds, called pressure ulcers, on their residual limb. The exact cause of these wounds is unclear as little work had studied the interface between the prosthetic device and the limb. Our research objective was to develop a quantitative method for assessing limb displacement patterns during walking for patients with transtibial amputation. Using a reflective marker system and a custom clear socket, three evaluations were conducted: 1) a clear transparent test socket mounted over a replica of a patient's leg cast in plaster, 2) a deformable leg model and 3) a patient's leg. Using a motion capture system, distances between markers were measured with a digital caliper and compared with the motion capture system. Dynamic trials were then collected while the non-human limbs were vertically displaced to measure changes in inter-marker distance due to vertical elongation of the gel liner. Static inter-marker distances within day and across days confirmed the ability to accurately capture displacements using this new approach. Furthermore, a single human subject was tested with this approach and larger displacements were found distally as compared to proximally. Uneven deformation is an interesting finding because clinicians may be underestimating the displacement particularly at the distal end, where ulcers commonly occur. These results encourage this novel method to be applied to a larger sample of amputee patients during walking to assess displacements and the distribution of limb deformation within the socket.

2.2 Introduction

In the United States, approximately 1.7 million people are living with limb loss (Ziegler-Graham et al. 2008). In addition, there are roughly 185,000 new amputations performed each year (Owings & Kozak 1998). Fifty-four percent of amputations are a result of complications from vascular diseases such as diabetes, followed by forty-five percent due to traumatic amputation (Ziegler-Graham et al. 2008). Following amputation, wound management and healing is essential because further amputation is a clinical concern due to infection or ulceration (Dillingham et al. 2005).

Pressure sores or ulcers are deep penetrating wounds that frequently occur on the residual limb at the socket interface (Figure 2-1). These wounds are painful, prone to infection, and disruptive to the patient (Mak et al. 2010). Numerous factors contribute to the formation of pressure ulcers both in clinical comorbidities and anatomical residual limb architecture. A recent systematic review concluded there is no singular risk factor to explain the occurrence of pressure ulcers (Coleman et al. 2013). Clinical comorbidities leading to ulcers often include poor circulation, venous insufficiency, diabetes, kidney insufficiency, hypertension, lymphedema, and inflammatory diseases (Nixon et al. 2006; Coleman et al. 2013).

Figure 2-1. Distal anterior tibia region skin break down and ulceration.

Wound healing throughout the clinical care process is essential and often challenging as there are many complications. Clinical factors that contribute to ulcer formation include: time since amputation, degree of tissue remodeling, presence of bony prominences close to the surface of the skin, quality of socket fit, and distribution of forces on the limb (Koc et al. 2008;

Lyon et al. 2000). Wound infection and poor healing are the frequent culprits leading to re-amputation. In the case of trans-tibial amputations, sixty percent of patients undergo transfemoral amputation, contralateral limb amputation, or pass away (Dillingham et al. 2005; Robbins et al. 2008; Ziegler-Graham et al. 2008).

In order to maintain ambulation, patient-specific prosthetic devices are designed and manufactured (Johnson & Davis 2014; Edwards 2000; Narita et al. 1997). Prosthetists can connect the socket to the residual limb through numerous means of suspension. A recent review concluded there is no singular standard for suspension method in transtibial amputees; however, the most favored setup by users was the total surface bearing socket with gel liner interface pin/lock suspension system (H. Gholizadeh et al. 2014). Prosthetists implement this type of system because it provides a less restricted knee range of motion, is believed to decrease pistoning of the residual limb, increases proprioception between the limb and socket, and can provide cushioning (Kapp & Fergason 2004; Johnson & Davis 2014; Kapp 1999).

The implementation of soft gel/silicone inner layers with pin/locks has greatly improved the function of artificial limbs by allowing a more comfortable prosthetic solution with greater movement at the proximal joint (Heim et al. 1997). Notable however, is the large friction between the gel or silicone interface and residual limb skin which is clinically stated to reduce the pistoning motion (Narita et al. 1997). Pistoning is when the prosthetic device translates vertically with respect to the residual limb due to the suspension of the limb (Gholizadeh et al. 2012). While this high friction interface allows for clinical benefits, understanding its effects at the skin surface during ambulation is important as this interface may be a source of tissue breakdown. Therefore, a need exists to understand how the liner moves relative to the prosthetic device and relative to the skin.

Skin movement and residual limb loading are ongoing throughout the day for prosthetic users, this loading, coupled with deformation and strain on the skin plays a role on ulcer formation

(Gefen et al. 2008). In particular, for lower-leg prosthetic users, we hypothesize that there is uneven displacement of the limb within the socket with larger displacements occurring distally. Resulting from uneven displacements, non-uniform strains or slippage of one surface to another may result in regions of high shear forces on the skin and deeper tissues. Other researchers have shown that shear loads on the skin significantly reduce blood flow to the loaded region (Manorama et al. 2010; Manorama et al. 2013). A reduction of blood flow, over a duration of time leads to skin necrosis and formation of an ulcer (Bouten et al. 2003). Additionally, loads at the skin level can lead to deeper tissue stresses, again causing tissue damage and ulcer formation (Gefen et al. 2008). To study the relative movement between the skin and the prosthetic device we must first develop a method that permits this assessment.

Previous research has provided limited information on the movement that occurs between the socket and liner interface (Childers & Siebert 2015; Gholizadeh et al. 2012). Dynamic roentgen stereogrammetric analysis was also utilized to assess skin movement within the socket however this study was limited to small movements so the participate remained within the small capture region of the 3D digitizer (Papaioannou et al. 2010). None of these methods have studied the complete displacement field of limb motion within the socket. In particular, research is needed to compare longitudinal and transverse displacements between the socket and the residual limb during regular activities such as walking. In order to perform this comparison, first a method must be developed.

Motions occurring within the socket are not measured by prosthetists because the interface region is not visually accessible and a method for quantifying these motions is not readily available. Thus, the objective of this work was to develop and validate a quantitative method for assessing limb displacement patterns for patients with transtibial amputation while wearing a prosthetic device. This method used a clear prosthetic socket and motion capture markers to obtain displacement data sets.

2.3 Methods

For the development of this method, research was focused on transtibial prostheses with a gel liner interface and pin locking suspension (Figure 2-2).

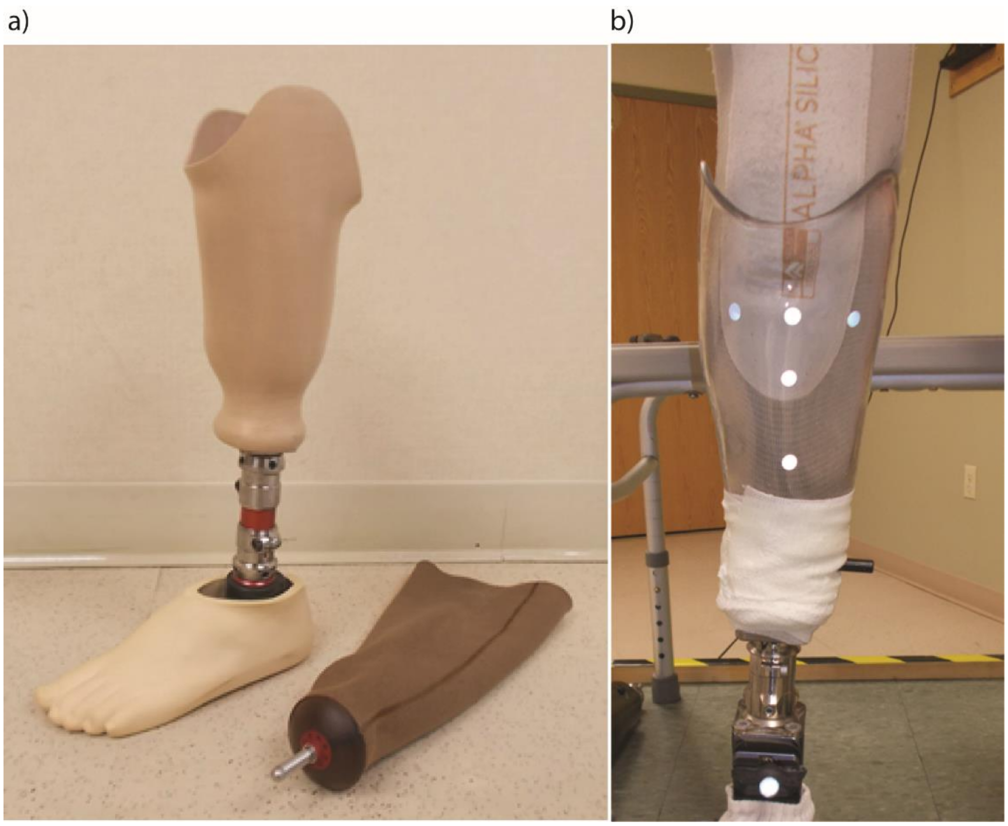

Figure 2-2. a) Below knee prosthesis with pin suspension and gel liner. b) Clear Thermolyn prosthesis developed for this research.

2.3.1 Test Configuration

Two replicas of an amputee’s transtibial limb were used in the development of the experimental method: 1) an anatomical replica made of rigid plaster and 2) a deformable limb model which mimics the anatomical structure and deformable nature of a transtibial limb (Burner et al. 2013; Dombroski et al. 2014). The deformable limb has material components representing bones, soft tissue and skin (Burner et al. 2013; Dombroski et al. 2014).

Using standard clinical prosthetic socket manufacturing methods, appropriate sized sockets were fabricated, custom to each unique limb model. The model limbs were casted, positive plaster models were modified, sockets were pulled using thermoplastic, and anatomical trim lines were cut and smoothed. To allow for measurement and capture of the limb motion and anatomical landmarks, the socket was manufactured out of a clear material called Thermolyn. Thermolyn is a transparent, thermoplastic material commonly used in fabrication of prosthetic "test sockets" for clinical use leading up to a definitive prosthetic socket. The limb and socket with pin locking mechanism were then rigidly affixed to a metal base through the linkage of a prosthetic pylon. This provided a stable base of support for the test configuration (Figure 2-3).

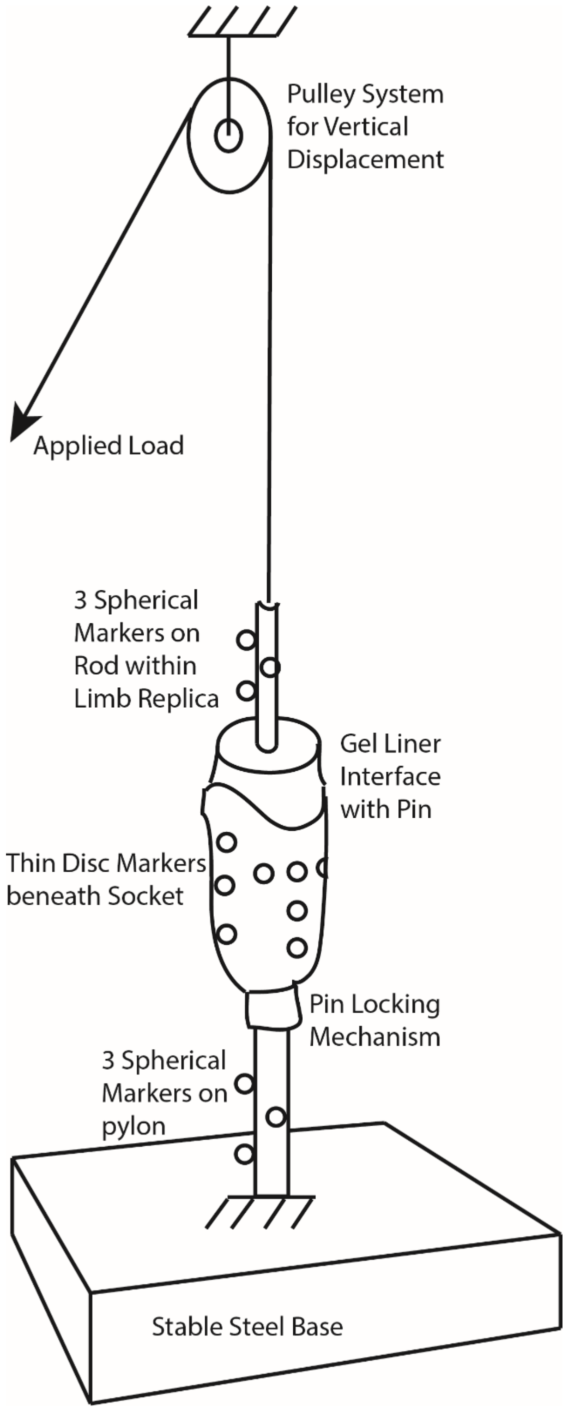

Figure 2-3. Experimental setup of replica limb and reflective markers beneath the socket with pulley system application of force to the limb. Distal markers are closer to the pin locking mechanism.

2.3.2 Markers

The production of the clear sockets allowed reflective thin-disc motion capture markers to be positioned inside on the gel liner directly beneath the surface of the transparent socket and spherical markers on the outside of the socket so that static anatomical locations could be measured. Anatomical locations of interest included: anterior tibial tuberosity, anterior tibial crest, distal end of the tibia, lateral proximal fibular head, distal fibula, intersegmental locations along the lateral fibula, medial tibial condyl, soft tissue medial limb border to distal end, and gastrocnemius muscle soft tissue locations on posterior calf are shown on Figures 2-4 and 2-5 while the displacement measures are presented in Table 2-1.

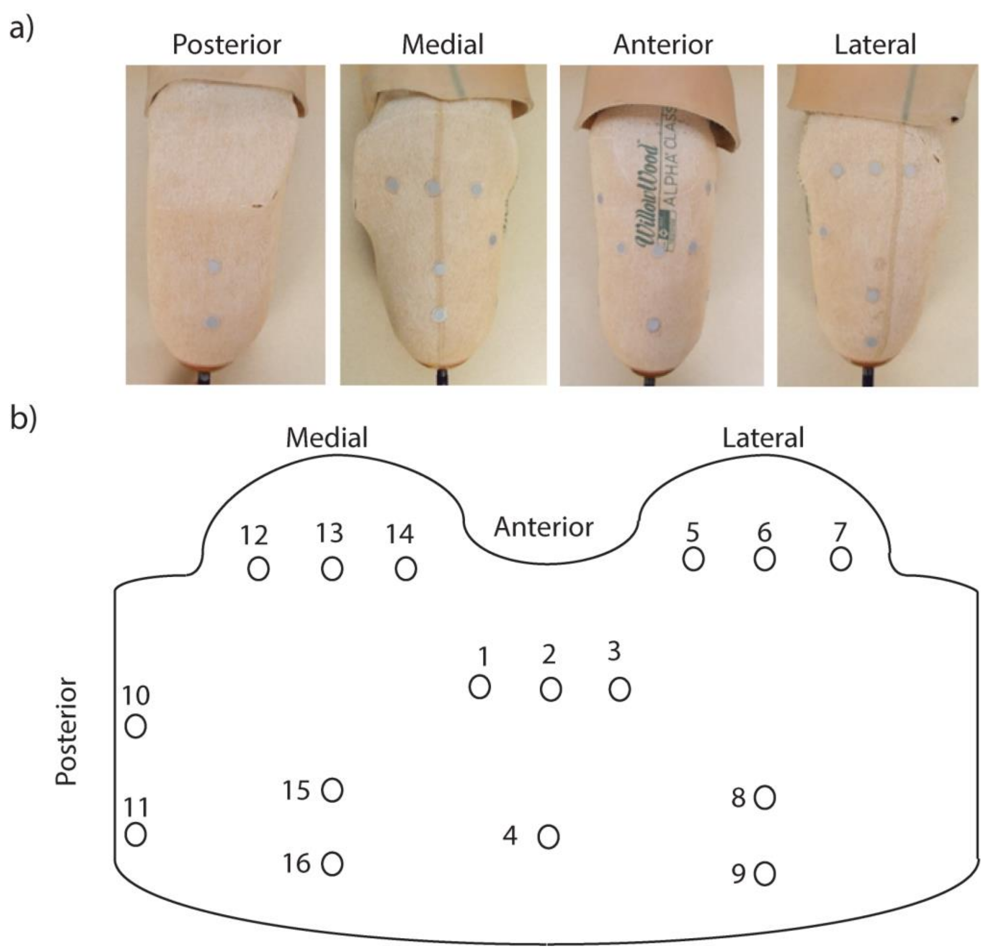

Figure 2-4. a) Marker placement over gel-liner interface for the plaster limb. b) Marker definitions on the plaster limb.

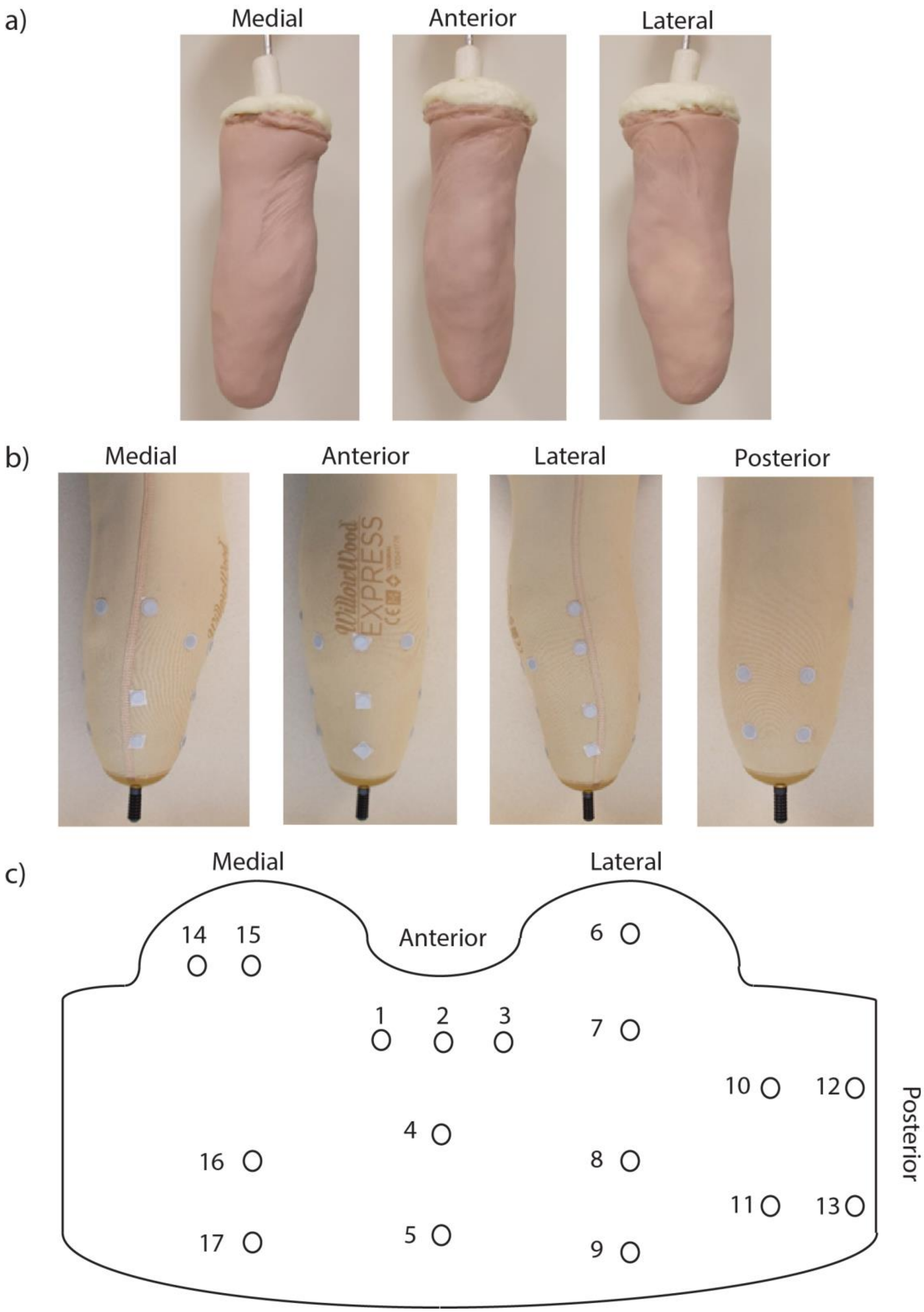

Figure 2-5. a) Replica of trans-tibial limb used in deformable limb testing. b) Marker placement over gel-liner interface for the deformable limb. c) Marker definitions on the deformable limb.

Table 2-1. Displacement definitions. |12| indicates the distance between markers 1 and 2. The left indicates the distances measured on the plaster limb and on the right the deformable limb.

Plaster Limb Intermarker Distance Definitions	**Deformable Limb Intermarker Distance Definitions**
Transverse	Transverse
|12| Proximal Anterior: Medial Tibial Tuberosity	|12| Proximal Anterior: Medial Tibial Tuberosity
|23| Proximal Anterior: Laterial Tibial Tuberosity	|23| Proximal Anterior: Laterial Tibial Tuberosity
|56| Proximal Lateral: Anterior Tibial Condyle	|10 12| Proximal Posterior: Gastroc Muscle
|67| Proximal Lateral: Fibular Head	|11 13| Distal Posterior: Gastroc Muscle
|12 13| Proximal Medial: Tibial Medial Condyle	|14 15| Proximal Medial: Tibial Medial Condyle
|13 14| Proximal Medial: Tibial Medial Condyle	
Longitudinal	Longitudinal
|24| Proximal Anterior: Tibial Crest	|24| Proximal Anterior: Tibial Crest
|89| Distal Lateral: Residual Fibula	|45| Distal Anterior: Tibial Boarder
|10 11| Posterior: Gastrocnemius Muscle	|67| Proximal Lateral: Fibular Head
|15 16| Distal Medial: Residual Soft Tissue	|89| Distal Lateral: Residual Fibula
	|10 11| Posterior: Gastrocnemius Muscle
	|12 13| Posterior: Gastrocnemius Muscle
	|16 17| Distal Medial: Residual Soft Tissue

The plaster limb model was tested first with an initial marker set-up consisting of sixteen reflective thin-disc markers beneath the clear, transparent socket (Figure 2-4). Following data collection and analysis from the plaster limb, the deformable limb model had marker placements adjusted to improve the representation of transverse and longitudinal inter-marker distances. Therefore, in the deformable limb seventeen reflective thin-disc markers were used (Figure 2-5). Markers were positioned to represent bony anatomical landmarks because these locations are related to clinically known pressure intolerant areas and soft tissue areas likely to show larger deformation. Three external spherical reflective markers were placed on the rod attached within the limb replica and an additional three markers were placed on the pylon to track motion of the external prosthetic device relative to internal marker locations.

2.3.3 Data Collection and Processing

A twelve camera motion capture system (Vicon Motion Systems Ltd.; Oxford, UK) recorded the locations of all markers in three-dimensional space; the system was calibrated before each data collection. Accuracy of this motion capture system is +/- 0.5 mm for inter-marker distance calculations. Inter-marker distance calculations were conducted between pairs of markers and a relative displacement field was calculated based on the locations of individual markers moving relative to each other. Inter-marker distances were computed as the magnitude of the vector between the two markers. Thus, |12| indicates the magnitude between markers one and two. Reported inter-marker distance definitions on the limb relative to their anatomical representation can be found in Table 2-1.

2.3.4 Static Analysis

For each limb model, rigid and deformable, three static motion capture trials were collected. In both limbs, inter-marker distances reported longitudinal and transverse limb distances. Specific to each limb, these same anatomically defined inter-marker distances were also measured with a digital caliper in millimeters to the hundredths place with measures being repeated three times, and averaged. Thus comparisons could be made to see if the plastic device caused distortion of marker distances with the motion capture system. For both limbs, this test protocol was conducted on three separate days to test within day accuracy and across testing day repeatability.

2.3.5 Dynamic Analysis

To ensure movement through the motion capture volume would not negatively influence intersegmental dimensions, the plaster model was moved in biplanar motions. Multiple dynamic trials simulated a walking motion through the capture volume and inter-marker distances were computed and compared.

To simulate pistoning, a dynamic condition was created that displaced the limb upward. The limb and socket with pin locking mechanism were rigidly affixed to a metal base through the linkage of a prosthetic pylon. This provided a stable base of support for the test configuration (Figure 2-3). A rope-pulley system was used to induce pistoning while the marker data were used to compute inter-marker distances. The prosthetic socket was securely mounted via a pylon to a steel base. This fixed approach was used to mimic the contact phase of the foot during walking. Our hypothesis was that larger displacements would be observed distally on the residual limb due to pistoning.

2.3.6 Statistical Analysis

For data collected within the same day, repeated measures t-tests (SPSS Statistical Analytics, Armonk, New York) were performed to compare static motion capture marker distances with caliper measured distances. Separate analyses were run for the rigid and deformable limbs. One-way analysis of variance (ANOVA) statistical tests were performed for motion capture distances measured across the three testing days. Significant differences for all statistical analyses were defined with a P value of 0.05 or less. Dynamic displacement distances were reported regionally in both limb setups as an average maximum displacement over three cyclical vertical displacements. Biplanar dynamic inter-marker distances were compared with static motion capture inter-marker distances using a t-test (SPSS Stastical Analytics, Armonk, New York) to statistically quantify measured differences through the clear socket when movement was introduced.

2.3.7 Human Subject Data

Finally, our experimental method was implemented with a single human subject during a walking cycle. This work was conducted under an approved Human Subject's IRB protocol (#14-089M).

A prosthetic device identical to the patient's original was formed with the clear, transparent Thermolyn. The patient's limb length and circumferential dimensions were smaller than either the plaster or deformable models. In order to avoid merging of markers, the placement was modified to fourteen thin-disk reflective markers (Figure 2-5). However, this setup still allowed displacement measurements along the same anatomical regions. Marker distances were evaluated relative to the patient's gait cycles (Miller 2009). The maximum and minimum inter-marker distances were reported within a single gait cycle and five independent trials of one gait cycle were each evaluated.

2.4 Results

2.4.1 Static Analysis

First reported are inter-marker distances for the plaster replica limb (Table 2-2A). Next, data are reported for the static inter-marker distances for the deformable limb replica (Table 2-2B). The differences for the plaster limb between caliper and motion data ranged from the lowest of 0.00 to the highest of 0.46 mm. Differences between caliper and motion capture for the deformable limb ranged from 0.01 to 0.50 mm. No statistically significant differences were found between the motion capture and caliper distances for the plaster leg with regard to the measurements obtained using the different techniques. This was also true for the deformable limb.

Table 2-2. A. Comparison of caliper measured inter- marker distances to motion analysis data for plaster limb replica with gel liner pin suspension interface. Measured distances represent average +/- standard deviations of the three trials performed each day. The difference between measured and caliper is the difference between measurement method averages. No statistically significant differences were identified between measured and caliper data. B. Comparison of caliper measured inter-marker distances to motion analysis data for deformable limb replica with gel liner pin suspension interface. Measured distances represent average +/- standard deviations of the three trials performed each day. The difference between measured and caliper is the difference between measurement method averages. No statistically significant differences were identified between measured and caliper data.

A)

Plaster Limb Intermarker Distances	Caliper Measurement (mm ± SD)	Static Measurement w/Motion Capture (mm ± SD)	Difference Between Measured and Caliper (mm)	Dynamic Range of Motion Max/Min (mm)
|12|	34.84 ± 0.38	34.67 ± 0.47	0.17	34.62 - 35.89
|23|	35.79 ± 0.31	35.99 ± 0.65	0.20	35.09 - 37.45
|24|	48.22 ± 0.29	48.19 ± 0.45	0.03	46.21 - 51.63
|56|	37.70 ± 0.18	38.16 ± 0.19	0.46	37.89 - 39.33
|67|	34.12 ± 0.24	34.16 ± 0.70	0.04	33.58 - 35.47
|89|	45.31 ± 0.19	45.31 ± 0.50	0.00	45.25 - 49.54
|10 11|	33.64 ± 0.22	33.67 ± 1.67	0.04	33.59 - 36.21
|12 13|	39.15 ± 0.45	39.31 ± 0.38	0.16	39.02 - 41.68
|13 14|	39.91 ± 0.17	39.61 ± 0.29	0.30	39.46 - 41.16
|15 16|	41.19 ± 0.21	41.20 ± 0.25	0.01	41.03 - 45.62

B)

Deformable Limb Intermarker Distances	Caliper Measurement (mm ± SD)	Static Measurement w/Motion Capture (mm ± SD)	Difference Between Measured and Caliper (mm)	Dynamic Range of Motion Max/Min (mm)
|12|	39.06 ± 0.27	38.56 ± 0.25	0.50	38.32 - 41.31
|23|	44.25 ± 0.25	44.33 ± 0.25	0.08	44.17 - 47.92
|24|	45.17 ± 0.21	45.26 ± 0.40	0.08	45.14 - 49.47
|45|	54.72 ± 0.44	54.53 ± 0.50	0.19	54.36 - 59.69
|67|	33.80 ± 0.21	34.12 ± 0.64	0.31	33.88 - 37.98
|89|	38.28 ± 0.32	38.21 ± 0.21	0.07	37.79 - 44.46
|10 11|	46.62 ± 0.24	46.82 ± 0.44	0.21	46.51 - 49.63
|10 12|	54.52 ± 0.28	54.36 ± 0.33	0.16	46.75 - 47.95
|11 13|	47.78 ± 0.23	47.56 ± 0.43	0.22	47.45 - 49.14
|12 13|	46.45 ± 0.24	46.52 ± 0.50	0.07	46.48 - 48.93
|14 15|	42.71 ± 0.31	42.60 ± 0.47	0.10	42.59 - 44.89
|16 17|	44.57 ± 0.28	44.56 ± 0.20	0.01	43.78 - 49.62

Repeated measures paired t-tests revealed no significant differences for within day measurements for either the plaster or deformable limb. Additionally, an ANOVA revealed no statistically significant differences between caliper and motion capture data for either the plaster or deformable limb across testing days.

2.4.2 Dynamic Analysis

Inter-maker distance and range of dynamic motion of the gel liner were also analyzed for the rigid plaster and deformable amputee limb replicas. These inter-marker distances are reported in Table 2-2, and are the minimum and maximum range of displacement over five vertical displacement trials. Dynamic ranges were greatest in distal and vertical inter-marker locations for both limbs yet even greater displacements were observed in the deformable limb than the plaster. The average applied load for vertical displacement was 119.7 ± 23.1 N with resulting range of 10-20 mm of displacement between the markers on the rod attached to the limb replica and the pylon (Figure 2-3).

For biplanar dynamic motion of the model through the capture volume, statistical analysis using a t-test compared static and dynamic inter-marker distances. No statistically significant differences were found between the motion capture static trials and motion capture dynamic trials for calculated distances using the plaster leg.

2.4.3 Human Subject Analysis

Dynamic measurement of inter-marker distances during walking for one patient resulted in larger displacements distally versus proximally, with the largest regions of displacement at the distal tibia and distal fibula (Table 2-3). Specifically, marker distances |45| and |89| which represent the locations on the distal tibia and distal fibula showed displacements of 7.34-7.41 mm longitudinally. Transverse marker distances corresponding to |12| and |23| which were along the tibial tuberosity to the medial and lateral directions averaged displacements of 3.82-3.9 mm. The human subject data reported displacements greater than observed in the non-human models with human data exhibiting approximately 3-5 mm more displacement throughout the limb.

Table 2-3. Human subject data for displacements of marker locations beneath the prosthetic socket. Standing data represents static weight bearing data. Walking ranges represent the minimum to maximum displacement observed over five gait cycles. The reported difference is the average and standard deviation of within trial dynamic differences averaged across five gait cycles.

	Transverse (mm)		Longitudinal (mm)			
	Lateral Tibal Tub	Medial Tibial Tub	Proximal Tibia	Distal Tibia	Fibular Head	Distal Fibula
Standing	34.6	42.36	35.65	50.64	68.48	57.25
Walking	32.44 - 38.15	39.49 - 44.2	33.34 - 43.3	44.88 - 54.75	66.2 - 74.1	52.2 - 63.3
Difference AVE ± SD	3.82 ± 1.14	3.9 ± 0.37	6.5 ± 2.11	7.34 ± 1.66	4.5 ± 1.97	7.41 ± 2.40

2.5 Discussion

In an effort to understand residual limb movement within the prosthetic, a method was developed using thin disc markers located on the gel liner beneath clear plastic prosthetic sockets. The measurement technique was validated by comparing motion capture data and digital caliper data for static trials. Results showed that no statistically significant differences between measured caliper inter-marker distances and those acquired by the motion capture system existed for either the rigid or deformable limb models. Absence of statistically significant differences indicated that motion capture system markers mounted beneath a clear thermoplastic prosthetic test socket could accurately capture movement of the gel liner. Additionally, data were compared across multiple sessions within a day, and across three days. No differences were found.

Limited data are available for quantification of limb motion within the socket (Childers & Siebert 2015; Gholizadeh et al. 2012). Gholizadeh et al. assessed vertical displacement of the limb relative to the socket along the lateral aspect of the residuum for two different liners. However this was not conducted during walking but rather a progression of full-weight bearing, semi-weight bearing, and non-weight bearing. Comparisons showed that liner type affected the magnitude of pistoning; specifically, the Seal-In X5 liner decreased pistoning as compared to the Iceross Dermo liner (Gholizadeh et al. 2012). Another study drilled holes in the prosthetic socket to allow for three motion capture markers to be placed on the gel liner (Childers & Siebert 2015; Gholizadeh et al. 2012). This work demonstrated approximately 5 mm differences proximally versus distally; however the prosthetic device was altered, potentially affecting the fit and they were only able to measure a few locations (Childers & Siebert 2015). Our new method allows for a much larger evaluation of limb displacement measurements across the entire lower leg and this approach can be used during dynamic activities such as walking, stair climbing or even running.

Our study also used a lab set-up with a plaster and deformable limb to emulate pistoning, where the liner elongated beneath the rigid socket. Both the plaster and deformable limb models showed displacement changes with larger displacements distally. Additionally, the deformable limb yielded larger displacements than the rigid plaster limb. The plaster limb data set provided insight into the liner response as there were no soft tissues below the liner. Based on the plaster and deformable limb model results, it was hypothesized a human limb with soft tissue would demonstrate even greater displacements than either the plaster or deformable limbs.

A clear prosthetic was manufactured for a single subject and our approach was used to provide an initial indicator of what displacements would occur in a human data set. This initial participant showed uneven displacement occurring within the prosthetic socket during walking. The two highest regions of displacement were measured at the distal tibia and fibula. This result was likely due to the combination of the soft tissue at the distal end of the leg and the pin/lock suspension mechanism which “pulls” at the distal end due to the mass of the foot during swing. The entire prosthesis is suspended from the distal pin on the gel liner, therefore it must carry the load of the pylon/foot during swing. Increased movement at the distal end of the limb may lead to higher friction at the skin surface leading to tissue irritation and the formation of ulcers. Prosthetists are unable to measure these within socket displacements, therefore, this new method will increase data available for prosthetists and will help support improved prosthetic device design.

Based on these results, it is likely that the larger distal displacements will lead to higher shear forces and stresses in deeper tissues. Once the motions of the gel liner relative to the prosthetic device are quantified, then engineering principles can be used in a model to understand the stresses, strains, deformations and stretch occurring on the skin and in deeper tissues. This mechanics-based information, combined with clinical information, will allow us to understand the local loading and provide further insight regarding localized tissue breakdown and ulcer formation.

Limitations of this study are a function of the type of prosthetic suspension being studied. While gel liner interface with pin/lock mechanism suspension is a commonly used setup in transtibial amputees, it does not allow for measurement directly at the surface of the skin. Without the gel liner type of suspension method, there would be no stable form of suspension in the prosthesis without extending the device above the knee (i.e. joint corset design). The large friction between the gel liner and residual limb skin has been clinically stated to reduce the pistoning motion (Narita et al. 1997). While this friction interface stability allows for functional clinical benefits, understanding the skin surface during ambulation is important as it may be the source of tissue breakdown which has become covered by the gel liner.

Clinically impact of this new method is high. Obtaining these quantitative data and understanding the distribution and magnitude of displacements can potentially explain regions where in incidence of pressure ulcer formation is high, commonly observed at the distal tibia and distal fibula. Further, these data are likely to lead to improved patient-specific socket designs for prosthetic devices that reduce local loads and minimize ulcerations on the residual limb. Future research will apply this experimental method to more patients presenting with transtibial amputations during walking to understand the displacement field occurring within the socket.

2.6 Conflict of Interest Statement

The authors do not have any conflicts of interest to disclose.

2.7 Acknowledgements

The authors would like to thank Patrick Logan, CPO and Leo DelCarmen for their support and encouragement of the research. Also a special acknowledgement goes to the Orthotics and Prosthetics School at Eastern Michigan University for the gracious use of their transtibial deformable limb model without any financial involvement.

3. UNDERSTANDING DISPLACEMENTS AND STRAINS OF THE GEL LINER FOR BELOW KNEE PROSTHETIC USERS

3.1 Abstract

Many people with amputation utilize a prosthetic device to maintain function and ambulation. During the use of the prosthetic device, their residual limbs can develop wounds called pressure ulcers. The formation of these wounds has been linked to deformation and loading conditions of the skin and deeper tissues. Our research objective was to develop a complete profile of displacements and strains of the residual limb within the socket during walking in transtibial amputees. Seven regions within the limb were evaluated for calculated displacements and strains in addition to six calculations of displacement and three rotations relative to the prosthetic socket. Greatest displacements were observed in the distal region of the residual limb, near the pin locking mechanism on the gel liner. Calculated displacements were uneven throughout the residual limb and reportedly greater than previous research, indicating a potential problem with current prosthetic device design methods. This mechanics-based information, combined with clinical information, will allow us to understand the local skin and muscle displacements, the associated forces and will provide insights regarding localized tissue breakdown. Knowledge of limb movement within the prosthetic socket can help also help prosthetists modify prosthesis design to reduce these displacements and strains.

3.2 Introduction

With improved safety mechanisms more people are surviving auto or military related accidents and therefore living with a missing limb (Ziegler-Graham et al. 2008). In the United States alone, 1.7 million individuals have had a foot or leg amputation; in general, 45% are due to traumatic amputation and 54% are a result of complications from vascular diseases such as diabetes (Ziegler-Graham et al. 2008). In 35% of individuals with amputation, a second amputation further up the leg occurs due to clinically unmanageable infections (Dillingham et al. 2005). Furthermore, diabetic amputees have higher frequency of secondary amputation than nondiabetic amputees (Dillingham et al. 2005).

One cause for infection and a second amputation, are pressure ulcers. Pressure ulcers are regional tissue damage caused by loading on the skin from body-device interface conditions, particularly common over bony prominences (Le et al. 1984). Ulcers can be either superficial or deep depending on the loading conditions (Mak et al. 2010). Common regions of ulcer formation have been clinically noted to occur at the distal end of the tibial crest, lateral tibial flare, fibular head and distal fibula (Dudek et al. 2006; Henrot et al. 2000).

Following transtibial amputation, a prosthetic socket is utilized to maintain ambulation for patients. Understanding the limb to socket interface is essential for creating a well fit prosthetic device and to minimize tissue damage and the potential for the development of pressure ulcers. Pressure distribution analysis has been performed for over six decades, analyzing regions of high and low pressure primarily during gait (Muller & Hettinger 1952; Gholizadeh et al. 2015). However, pressure measurement usually requires thin-film sensors that suffer from errors with changes in temperature, curvature, and humidity. Pressure also does not provide a complete evaluation of loading conditions within the socket. To obtain a comprehensive understanding of the limb-device interface, a better understanding of how the limb deforms and movement of the limb with respect to the prosthesis is needed.

Understanding movement of the socket relative to limb during walking is important for improving prosthetic device fit, however, few studies have tackled this problem. One study created a noncontact sensor positioned beneath the socket to assess pistoning within the socket; but this was limited to a single measurement at the distal end of the limb (Sanders et al. 2006). Pistoning is when the prosthetic device translates vertically with respect to the residual limb due to the suspension of the limb (H. Gholizadeh et al. 2014). Two other studies used motion capture to quantify limb motion within the socket (Childers & Siebert 2015; Gholizadeh et al. 2012). Gholizadeh et al. assessed vertical displacement of the limb relative to the socket along the lateral aspect of the residuum for two different liners, however this was not conducted during walking but rather for partial to full weight bearing positions. Another study drilled holes in the prosthetic socket of a single subject to allow for three motion capture markers to be placed on the gel liner; yet this did not represent a wide range of locations within the prosthetic socket (Childers & Siebert 2015). Uneven displacements are likely because of limb structure, soft tissue regions and the walking movement. Therefore, further investigations are necessary to evaluate displacements around the entire residual limb during dynamic daily activities such as walking.

Therefore, the objective of this work was to determine 1) limb displacements, 2) strains, 3) relative displacements between the limb and socket, and 4) angular rotations of transtibial limbs within a prosthetic socket during walking. We hypothesized that larger localized displacements and strains would occur in the distal region due to pistoning of the gel liner. We also believe this pistoning will lead to higher shear forces on the skin and in deeper tissues influencing the stresses making tissue damage more likely. Once the motions of the gel liner relative to the prosthetic device are able to be quantified, then engineering principles can be used to model the resulting stresses, strains, deformations, and stretch occurring on the skin and in deeper tissues. This mechanics-based information, combined with clinical information, will allow us to understand the local skin and muscle displacements, the associated forces and will provide insights regarding localized tissue breakdown. Further, these data are likely to lead to improved patient-specific socket designs for prosthetic devices that reduce local loads and minimize ulcerations on the residual limb.

3.3 Methods

The previously developed method to capture a displacement field of thin-disc reflective markers beneath the surface of a prosthetic socket (Lenz, Johnson, and Bush, in review; Lenz, Johnson, and Bush 2016) was implemented in a group of transtibial amputees. This work was conducted under an approved Human Subject's IRB protocol with informed consent (#14-089M).

3.3.1 Participants

Participants included eight transtibial amputees, one with bilateral amputation and seven with unilateral amputation. All amputations occurred at least one year prior to the study. Reasons for amputation included traumatic injury, diabetes, and infection. None of the participants had any other disabilities or needed the use of an assistive device such as a walker or cane. At the time of testing, participants were free of any sores on their residual limb.

3.3.2 Prosthetic Componentry

All participants had been seen within six months by a certified prosthetist who deemed their current prosthesis was fitting well and had a proper alignment and fit. All participants were using the same type of prosthetic suspension; a gel liner interface with pin/lock mechanism.

3.3.3 Test Procedure

The testing procedure consisted of two parts. First, to allow for measurement and capture of the limb motion and anatomical landmarks, a duplicate socket was manufactured out of a clear proprietary thermoplastic material commonly used in fabrication of prosthetic “test sockets” for clinical use leading up to a definitive prosthetic socket (Figure 3-1 a, b). The duplicates were developed to match the alignment and fit of the participant's prosthetic socket.

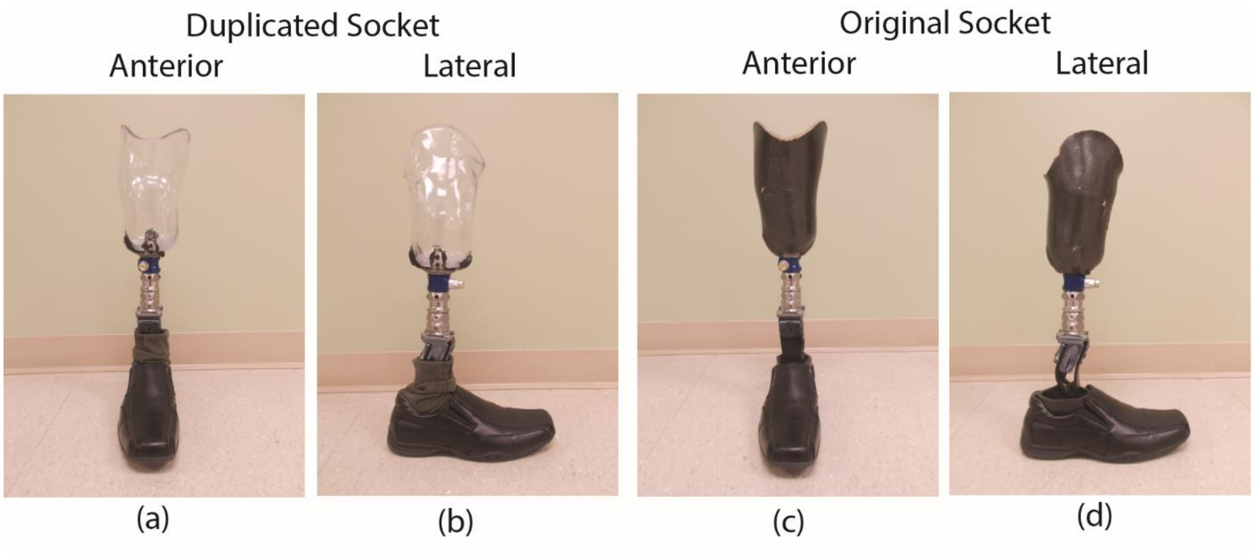

Figure 3-1. Example of clear thermoplastic duplicated socket (a, b) for one participant compared with their original opaque prosthesis. Componentry and alignment was maintained with only the socket exchanged for the experimental test configuration (a, b). The duplicated socket allowed the cameras to track the markers within the socket whereas the original socket does not.

The second portion of the study was a kinematic assessment. First a comparison of their gait was made between the original device and the new duplicated clear socket. Kinematics data were obtained so residual limb motions within and relative to the socket could be computed.

3.3.3.1 Comparison of Devices

To ensure the duplicated socket yielded identical walking patterns, a kinematic assessment was completed with both the original and duplicated sockets. Kinematics were obtained for the lower extremity and trunk joint angles during walking. From this, a Gait Deviation Index was calculated for the walking trials (Schwartz and Rozumalski 2008). Secondly, the participant's duplicated prosthetic was assembled with their existing pylon, foot and suspension components and data of lower extremity and trunk kinematics were captured with the same Gait Deviation Index. The two data sets were compared to determine if significant changes were introduced between prosthetic devices within a participant.

3.3.3.2 Measurement of Limb Motion within the Socket

The production of the clear sockets allowed reflective thin-disc motion capture markers (9.5 mm diameter and 0.2 mm thick) to be positioned inside on the gel liner. Spherical markers were also placed outside on the socket so that static anatomical locations and movement of the limb relative to the socket could be calculated. Anatomical locations of interest included: anterior tibial tuberosity, anterior tibial crest, distal tibial cut end, lateral proximal fibular head, distal fibular cut end, intersegmental locations along the tibia/fibula and soft tissue medial limb proximal to distal (Figure 3-2). All markers were positioned the same on all participants except two. On the second participant, the limb contained a shorter fibula and only two markers were placed along the lateral aspect of the limb, omitting the mid fibula. Participant eight had an even shorter and in this case the mid fibula and mid tibial crest markers were omitted.

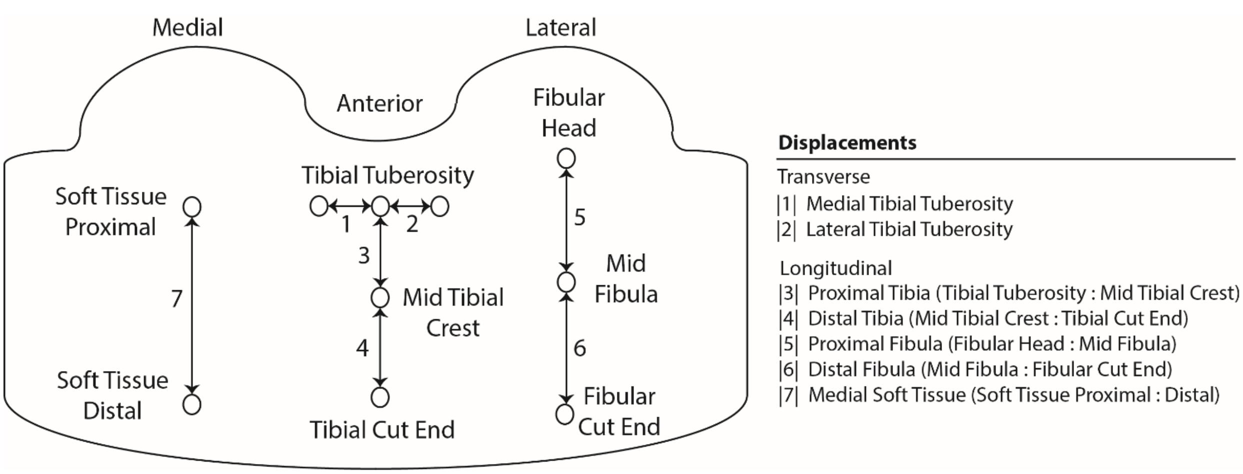

Figure 3-2. Calculation of displacements from anatomical marker locations on the gel liner within the prosthetic socket

3.3.4 Analysis

A twelve camera motion capture system (Vicon Motion Systems Ltd.; Oxford, UK) tracked the locations of all markers in three-dimensional space; the system was calibrated before each data collection. Locations of markers were reconstructed using Vicon Nexus 2.3 to determine the three-dimensional location of each individual marker within the global coordinate system.

Four parameters were developed for quantification of the residual limb within the prosthetic socket: displacement, strain, displacement relative to the prosthetic socket, and rotation of the limb relative to the prosthetic socket. With these data sets movements of the gel liner within the socket and relative to the socket were calculated.

A displacement field was calculated based on how individual markers moved relative to each other on the gel liner. Inter-marker distances were computed as the magnitude of the vector between two markers. Inter-marker distance definitions on the limb relative to their anatomical representation can be found in Figure 3-2. Inter-marker distances were tracked during an individual gait cycle and the displacement was defined as the maximum inter-marker distance minus the minimum inter-marker distance during a single gait cycle. This was repeated for five gait cycles per participant, averaged within participants, and also averaged across all participants.

Following inter-marker displacements, calculation of strain was completed. Strain was defined by the change in length (i.e. the calculated displacement) divided by an original inter-marker distance that was measured in a static standing trial of the participant.

To determine if the prosthetic device was moving relative to the residual limb, relative socket displacement calculations were conducted. First, a local coordinate system (LCS) was defined. The origin of the local coordinate system O_{LCS} was defined as the midpoint between the malleoli. The local coordinate system was created by a superior unit vector in the z direction based on an axis passing from the distal end, local coordinate system origin, to the midpoint of the knee joint center (Equation 1). This was achieved from medial and lateral markers on the femoral epicondyles and the malleoli taken during the static standing trial.

$$\hat{k} = \frac{0.5*(\overrightarrow{Knee_{Lat}} + \overrightarrow{Knee_{Med}}) - \vec{O}_{LCS}}{|0.5*(\overrightarrow{Knee_{Lat}} + \overrightarrow{Knee_{Med}}) - \vec{O}_{LCS}|} \tag{1}$$

Next, a unit vector passing from the medial malleolus to the lateral malleolus was created, $\hat{v}$ (Equation 2).

$$\hat{v} = \frac{(\overrightarrow{Ankle_{Lat}} - \overrightarrow{Ankle_{Med}})}{|(\overrightarrow{Ankle_{Lat}} - \overrightarrow{Ankle_{Med}})|} \tag{2}$$

Next an anterior unit vector was created from the cross product of $\hat{k}$ and $\hat{v}$ unit vectors. The third lateral unit vector was created from the cross product of $\hat{j}$ and $\hat{k}$ unit vectors. Finally a rotation matrix was created from unit vectors of the local coordinate system (Robertson et al. 2014).

$$R_{shank} = \begin{bmatrix} \widehat{i_x} & \widehat{i_y} & \widehat{i_z} \\ \widehat{j_x} & \widehat{j_y} & \widehat{j_z} \\ \widehat{k_x} & \widehat{k_y} & \widehat{k_z} \end{bmatrix} \tag{3}$$

This rotation matrix was multiplied by x, y, z global coordinates of all markers to transform into the local coordinate system (Equation 3). Also, appropriate sign conventions were applied depending upon direction of walking or whether it was a right or left residual limb.

3.3.4.1 Relative Motion

Following transformation into the local coordinate system, six locations were tracked relative to the socket during walking. The locations corresponded to the tibial tuberosity, tibial cut end, fibular head, fibular cut end, medial proximal soft tissue and medial distal soft tissue (Figure 3-2). The six marker locations were with respect to a marker placed on the prosthetic pylon to track the relative movement between the device and the residual limb in the local z direction, which was along the shank (Figure 3-3). In the local coordinate system, a vector was defined as the difference in z direction components of one of the six markers within the socket minus the z component of the prosthetic pylon marker. Throughout a single gait cycle the maximum distance and minimum distances were located and the limb displacement relative to the prosthesis was defined as the maximum minus minimum distance in the local z direction (Figure 3-3).

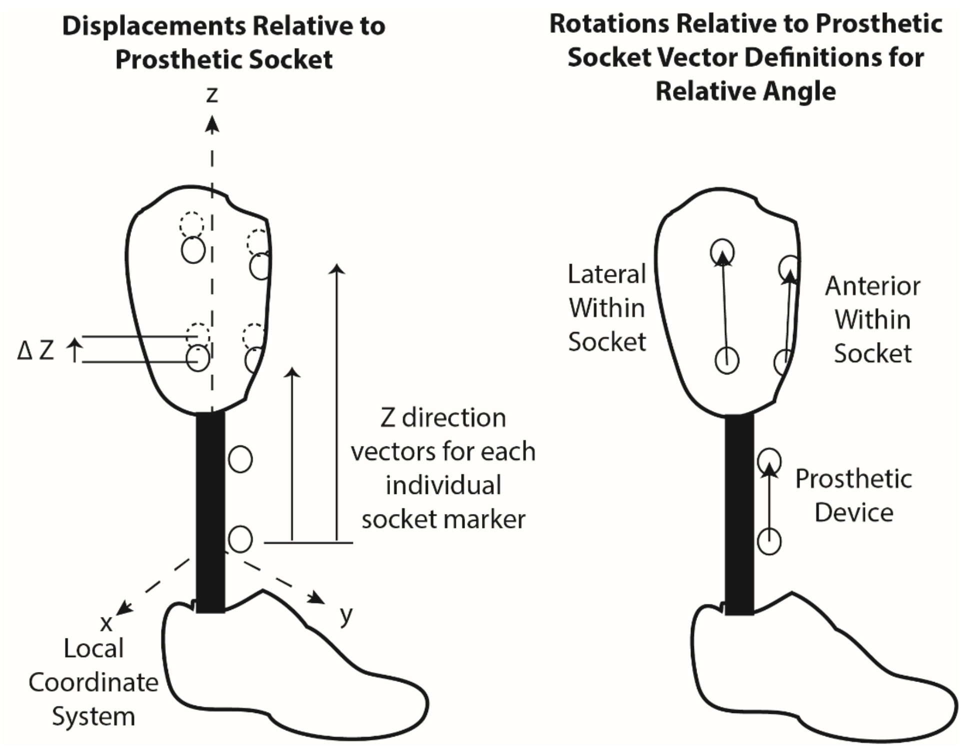

Figure 3-3. Analysis of vertical displacement and rotation relative to the prosthetic socket during a gait cycle. Δ Z symbolizing the change in marker location for relative displacement.

Rotation of the limb with respect to the socket was calculated for three regions on the limb in the anterior, medial and lateral aspects. A vector was created between the two markers located on the prosthetic pylon as a reference vector for the rigid body. Then, three independent vectors were created in the anterior, medial and lateral regions of the residual limb by using the tibial tuberosity and distal tibia markers for the anterior vector, followed by fibular head and distal fibula for the lateral region vector, with lastly the two medial markers located proximally and distally for the medial vector. Each of these vectors was used to calculate the angle between the limb vector and the prosthetic pylon vector using Equation 4 where $\vec{A}$ represents the pylon vector and $\vec{B}$ represents one of the three region vectors of the limb. This was repeated for five gait cycles within each participant and across all participants consistently.

$$\theta = \arctan\left(\frac{\vec{A}\,x\,\vec{B}}{\vec{A}\cdot\vec{B}}\right) \tag{4}$$

All reported measures were analyzed in five gait cycles per participant, reported as an average with standard deviation within all individual limbs.

3.3.5 Statistical Method

Statistical comparisons were conducted within the four key parameters of displacement, strain, relative strain and relative rotation. A one-way analysis of variance (ANOVA) followed by Tukey's post-hoc test was conducted to compare differences between the displacements and separately to compare between the strains (MATLAB, 2012a). Statistical analysis using a one-way ANOVA with Tukey's post-hoc was conducted on all nine limbs to compare displacements and rotations relative to the prosthetic socket (MATLAB, 2012a).

3.4 Results

3.4.1 Participants

Mean participant age was 57.9 +/- 8.2 years and on average 14.5 years since amputation. Table 3-1 provides details of participants. Two participants (2 and 8) had different shaped limbs which did not allow for the same marker placement. The slightly changed marker set only changed calculations for two measures: displacements and strains. Therefore, individual analysis for these two patients were performed but were not included in the statistical analysis.

Table 3-1. Participant characteristics. Residual limb length defined as inferior edge of patella to distal end of the stump. Mobility grade scale classifies an individual's ability to ambulate or navigate their environment. (Gailey et al. 2002). Level K3 is defined as the participant has the ability or potential for ambulation with variable cadence - a typical community ambulator with the ability to traverse most environmental barriers and may have vocational, therapeutic, or exercise activity that demands prosthetic use beyond simple locomotion.

Participant	Age (Years)	Height (cm)	Mass (kg)	Gender	Cause of Amputation	Amputated Side	Time Since Amputation (Years)	Residual Limb Length (cm)	Mobility Grade
1	61	187.96	88.99	Male	Trauma	Left	16.0	19.0	K3
2	51	177.80	85.45	Male	Trauma	Right	27.0	16.5	K3
3	54	160.02	63.91	Female	Infection	Bilateral	1.5	12 (R) 15 (L)	K3
4	62	187.96	88.27	Male	Diabetic	Left	2.5	18.0	K3
5	64	172.72	86.36	Male	Infection	Right	1.5	17.0	K3
6	44	180.34	135.45	Male	Trauma	Right	10.0	24.0	K3
7	57	187.96	80.91	Male	Auto-Immune	Right	6.5	15.5	K3
8	70	166.37	59.6	Female	Trauma	Left	51.0	11.5	K3

3.4.2 Displacements on the Residual Limb

Highest displacements in the residual limb analysis were observed at the distal fibula, distal tibia and medial side (Table 3-2 a). These areas including the fibular head had significantly more displacement compared with transverse direction displacements as assessed by the one-way ANOVA and Tukey's post hoc for seven participant limbs with consistent displacements measured ($p < 0.05$). On average the distal tibia, distal fibula and medial soft tissue regions showed 5.83, 5.93 and 6.34 mm of displacement respectively.

3.4.3 Strains on the Residual Limb

Greatest strains occurred in the proximal tibia, distal tibia and distal fibular regions (Table 3-2 b). These were statistically significant differences when compared to the transverse direction strains by statistical analysis of a one-way ANOVA followed by Tukey's post hoc ($p < 0.05$). Distal tibia and distal fibula region values were on average 11% strain followed by 10% strain in the proximal tibia region, with a lowest strain of 6% occurring in the proximal fibula region.

Table 3-2. (a) Displacements for participants. Reported as average of five gait cycles plus or minus standard deviation. (b) Strains for participants. Reported as average of five gait cycles plus or minus standard deviation.

(a)

	Transverse Displacements (mm)		Longitudinal Displacements (mm)				
P#	Lateral Tibial Tuberosity	Medial Tibial Tuberosity	Proximal Tibia	Distal Tibia	Proximal Fibula	Distal Fibula	Medial Soft Tissue
1	2.49 ± 0.41	2.64 ± 0.69	3.23 ± 0.82	4.69 ± 0.76	2.96 ± 0.51	5.53 ± 1.41	2.62 ± 1.21
3 R	1.91 ± 0.53	2.58 ± 0.24	4.07 ± 0.65	5.72 ± 0.93	2.81 ± 1.02	4.72 ± 0.85	7.64 ± 2.98
3 L	3.27 ± 0.67	2.99 ± 0.66	4.36 ± 1.79	5.55 ± 0.53	2.59 ± 0.83	4.82 ± 1.35	10.02 ± 2.05
4	3.51 ± 0.67	3.42 ± 0.43	5.16 ± 1.37	6.46 ± 0.96	4.12 ± 1.34	6.34 ± 2.54	5.22 ± 0.68
5	3.04 ± 0.48	2.53 ± 0.71	4.17 ± 0.54	6.17 ± 0.77	3.72 ± 0.89	6.15 ± 0.86	3.5 ± 1.30
6	2.57 ± 0.79	2.45 ± 0.59	4.68 ± 1.28	4.85 ± 1.16	3.73 ± 1.04	6.53 ± 1.10	10.33 ± 2.59
7	3.82 ± 1.14	3.90 ± 0.37	6.50 ± 2.11	7.34 ± 1.66	4.51 ± 1.97	7.41 ± 2.40	5.04 ± 2.06
Avg	2.94	2.93	4.60	5.83	3.49	5.93	6.34
SD	0.89	0.72	1.55	1.27	1.26	1.74	3.39

(b)

	Transverse Strains (mm/mm)		Longitudinal Strains (mm/mm)				
P#	Lateral Tibial Tuberosity	Medial Tibial Tuberosity	Proximal Tibia	Distal Tibia	Proximal Fibula	Distal Fibula	Medial Soft Tissue
1	0.05 ± 0.01	0.06 ± 0.01	0.05 ± 0.01	0.06 ± 0.01	0.05 ± 0.01	0.07 ± 0.02	0.04 ± 0.02
3 R	0.06 ± 0.02	0.07 ± 0.01	0.09 ± 0.01	0.12 ± 0.02	0.07 ± 0.03	0.11 ± 0.02	0.08 ± 0.03
3 L	0.09 ± 0.02	0.08 ± 0.02	0.09 ± 0.04	0.11 ± 0.01	0.05 ± 0.02	0.09 ± 0.03	0.11 ± 0.02
4	0.08 ± 0.02	0.09 ± 0.01	0.11 ± 0.03	0.11 ± 0.02	0.09 ± 0.03	0.15 ± 0.06	0.07 ± 0.01
5	0.07 ± 0.01	0.06 ± 0.02	0.08 ± 0.01	0.11 ± 0.01	0.07 ± 0.02	0.11 ± 0.01	0.06 ± 0.02
6	0.05 ± 0.02	0.05 ± 0.01	0.08 ± 0.02	0.09 ± 0.02	0.05 ± 0.01	0.10 ± 0.02	0.06 ± 0.02
7	0.11 ± 0.03	0.09 ± 0.01	0.18 ±0.06	0.15 ± 0.03	0.07 ± 0.03	0.13 ± 0.04	0.06 ± 0.02
Avg	0.07	0.07	0.10	0.11	0.06	0.11	0.07
SD	0.03	0.02	0.05	0.03	0.02	0.04	0.03

3.4.4 Displacements Relative to the Prosthetic Socket

Lateral and medial anatomical landmarks had the largest displacements relative to the prosthetic socket. On average, the greatest relative displacement of 30.7 ± 11.4 mm was observed in the medial proximal soft tissue region, followed by the fibular head with 27.3 ± 10.7 mm. In comparison, anterior displacements of 11.0 ±6.3 to 13.3 ± 6.4 mm at the tibial tuberosity and distal tibial prominence exhibited significantly less displacement relative to the prosthetic socket. Furthermore, the distal fibula displaced statistically less than the fibular head and medial proximal soft tissue regions ($p < 0.05$). Additionally, “gapping”, or a space between the socket and residual limb was observed visually in six participants and can be seen for one participant in Figure 3-4.

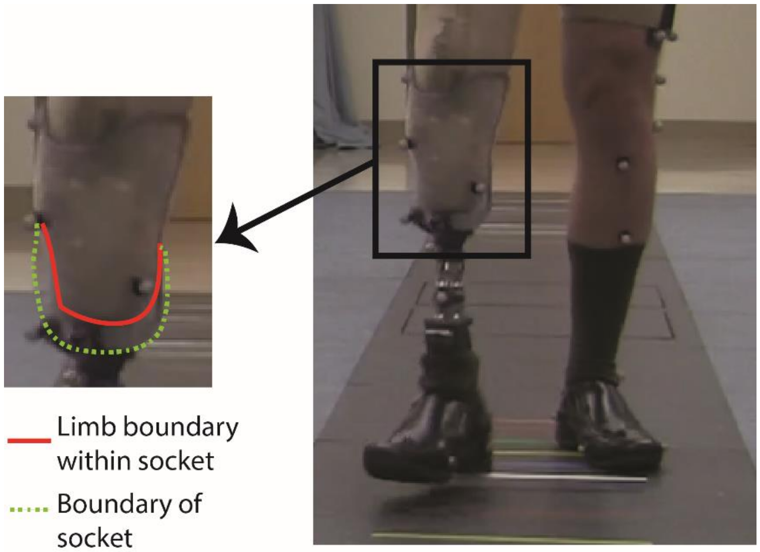

Figure 3-4. Demonstration of distal gap between residual limb and prosthetic socket within the socket just prior to initial contact and loading during walking

3.4.5 Angular Rotation of Limb Relative to the Socket

Angular rotation along the anterior, lateral and medial regions of the residual limb relative to the prosthetic socket showed rotations ranging from 0.8 to 10.8 degrees across all participants. On average the anterior, lateral and medial rotations were 5.3 ± 3.6, 5.2 ± 3.5, and 5.4 ± 3.9 degrees respectively. These data did not yield statistically significant differences when compared using a one-way ANOVA across all participants. Overall all regions uniformly rotated relative to the socket as measured as a change in rotational displacement during a gait cycle.

3.5 Discussion

The goal of our study was to investigate residual limb displacements within the socket, and displacements and rotations relative to the prosthetic socket in transtibial amputees during walking. Results overall confirmed that higher displacements and strains were observed distally as compared to proximally. The reason for this increased distal displacement and strain is related to the suspension method. At the base of the gel liner, a pin system locks to the prosthetic socket, leg and foot. This causes elongation of the gel liner due to the suspended weight. Our displacement data are the most comprehensive data set currently available; we have computed displacements at six regions in the longitudinal direction, two in the transverse direction, three regions of rotation of the prosthetic relative to the leg and relative displacement of the prosthetic to the leg.

Gholizadeh et al. utilized motion capture to assess vertical displacement of the limb relative to the socket along the lateral aspect of the residuum (Gholizadeh et al. 2012). However this was not conducted during walking but rather a progression of full-weight bearing, semi-weight bearing, and non-weight bearing. Gholizadeh et al. reported 0-6 mm change in displacements which are 25 mm lower than our study. The controlled loadings in Gholizadeh's study are believed to result in the lower displacement values because the limb did not experience inertial dynamics typical during the gait cycle.

Our data indicates that highest displacements occurred in the regions of the distal fibula, distal tibia and medial soft tissue. These regions are all close to the insertion point of the pin to the locking mechanism. Thus, the entire weight of the prosthetic device is suspended from the pin at the distal end of the gel liner and is the cause of these larger distal displacements. Assuming the gel liner is moving with the skin surface, these high gel liner displacements are would also cause high displacements of the skin. In some cases, it was clinically observed that a clear separation occurred between the distal limb and the prosthetic socket. Knowing the gel liner displaces, there are two possible interactions that can occur between the liner and the skin: 1) no slip occurs or 2) the liner slips with respect to the skin. If it is assumed that the gel liner is moving with the skin surface, these high gel liner displacements would also cause high displacements of the skin. If the gel liner is, however, slipping with respect to the skin, a suction hematoma at the distal residual limb may be creating erythemas or dilatation of the blood capillaries (Levy 1995; Levy & Barnes 1956). Both cases of stretch, or slip of the liner on the skin will lead to increased forces on or within the tissue which have been shown to reduce regional blood flow and lead to conditions that produce ulcers (Manorama et al. 2010; Manorama et al. 2013).

Displacements were converted to strains in the study. Both displacement and strain data create a sense of where elongation of the liner occurs. Sanders et al. documented different responses of liners in tensile test experimental setups and results were reported in kPa, noting significant differences between gels, elastomers and urethane based liners (Sanders et al. 2004). While many variables were constrained in our recruitment of participants, gel liners were not controlled for, but all were documented. One previous study reported maximum relative strain of proximally located markers to be about 8-10% in participants during stepping down activities which is similar to what we found (Papaioannou et al. 2010). Prosthetists should consider liner material properties when determining selection for patients experiencing high strains distally. Clearly, significant movement occurs distally with the gel liner. Clinically, this is important to note. Although a stiffer liner could be used to decrease displacement/strain, it may cause other issues. For example a stiffer liner could result in higher loads over bony prominences because it is less forgiving.

One limitation of this study is that only one type of prosthetic suspension was studied. To achieve pin locking suspension, a gel liner interface is required. Therefore, another limitation is that residual limb movements described are always with respect to gel liner motion because measurement was taken from the surface of the gel liner, not the skin surface itself. We are unable to state definitively what the underlying tissue is doing with respect to the gel liner. Two possible assumptions are that 1) the liner moves and stretches with the skin and 2) the liner slides along the skin. Both of these scenarios will be studied computationally in future work.

Limb displacement relative to the prosthetic socket revealed less displacement on the proximal and distal anterior tibial locations as compared to medial and lateral locations. This statistically significant finding indicates the socket is constraining anteriorly which may be related to the fact that we are evaluating gait which is a sagittal plane motion with loading from the prosthetic onto the leg primarily in the anterior/posterior regions which would reduce shifting of the device. The lateral sides of the residual limb/ prosthetic device are less constrained during gait. High displacements in the proximal fibula region are clinically concerning because prosthetists often create reliefs for the fibular head when designing a modified PTB style socket. The clinical thought is to allow this bony prominence some extra room for comfort, however with on average 27.3 mm of vertical displacement relative to the prosthetic socket, it is likely the fibular head prominence is displacing outside of the designated relief and potentially contributing to this regions common formation of ulcerations. We hypothesized higher displacements and the data provided a more detailed view of limb displacement than had been previously documented but within the documented ranges in the literature. Displacement during swing relative to stance phases of gait, proximal displacements averaged 41.7 mm across multiple gait cycles for a single transtibial amputee (Sanders et al. 2006). Another study compared two liners demonstrating the Seal-In X5 liner decreased vertical pistoning by 71% compared to the Iceross Dermo liner (Gholizadeh et al. 2012). No statistically significant differences in residual limb rotation throughout the gait cycle, confirms our hypothesis that the within socket motion is primarily a vertical pistoning motion rather than twisting motion of the limb relative to the socket. This study presents a larger sample size with more refined detail than previously existed to our knowledge, positively contributing to the knowledge of transtibial limb motion within a prosthetic socket with the utilization of pin/lock mechanism suspension. These data provide a comprehensive set of information on the interface displacements and can be implemented clinically to design systems with reduced pistoning which in turn has the potential to decrease skin wounds.

3.6 Acknowledgements

The authors would like to thank Patrick Logan, CPO for his support and encouragement of the research. Additionally, Sarah Veldman, Kate Clarke and Curtis Ackermann are thanked for their assistance in data extraction and marker tracking.

3.7 Funding

Michigan State University Graduate Office Fellowship and Michigan State University Mechanical Engineering Fellowship

4. INSTRUMENTED TRANSTIBIAL SOCKET FOR EVALUATING SHEAR AND NORMAL FORCE: A CASE STUDY

4.1 Introduction

Pressure ulcers are areas of tissue damage caused by loading on the skin from various body-interface conditions. Ulcers can be either superficial or deep in nature depending on the loading conditions (Mak et al. 2010). Within an amputee's transtibial socket, controlling the friction is essential for minimizing shear loads on the skin which could lead to the formation of pressure ulcers. The socket interface with the residual limb ranges from direct skin contact to gel liner interfaces. A gel liner is typically made of urethane, silicone or thermoplastic elastomer and is used to provide cushioning with respect to the rigid socket (Spires et al. 2014). Gel liners are most commonly prescribed for persons with below knee amputations (Boutwell et al. 2012). When a patient's limb fluctuates in volume throughout the day, additional sock layers are prescribed to be worn to fill extra space within the socket for a more comfortable fit. However, additional layers are not always necessary and could increase interface loads if worn when not indicated. Experimental investigation of loading within the prosthetic socket is needed in these conditions to understand the loading mechanics occurring at this interface.

Studies have documented pressure distributions using pressure sensor technology within the socket and to compare different socket types (Pearson 1974; Meier 1973; Leavitt et al. 1970; Appoldt et al. 1969; Naeff & van Pijkeren 1980; van Pijkeren et al. 1980). Most recently, pressure distribution at the socket to limb interface has been used to compare differences in prosthetic componentry, suspension types, and liners (Beil et al. 2002; Hossein Gholizadeh et al. 2014; Ali, Abu Osman, et al. 2012; Wolf et al. 2009; Boutwell et al. 2012; Eshraghi et al. 2013; Gholizadeh et al. 2015; Ali, Osman, et al. 2012). These studies only addressed pressure which is related to the normal loading. Shear forces have been shown to be more detrimental to skin health (Manorama et al. 2010; Manorama et al. 2013), however, none of these studies addressed shear and normal forces at the socket to limb interface.

Load cells have been used in prosthetic research to understand moments at the interface between the pylon and the base of the prosthetic socket. Neumann *et al.* instrumented a load cell at the base of the prosthetic socket to obtain moment data for below knee amputees walking on various terrains and curved pathways to measure real world situations (Neumann et al. 2013). In one study, transducers were also used to measure shear stresses in two orthogonal directions on a plane flush with the inside of the socket (Sanders et al. 1992). Three participants were tested and each socket was lined with a custom molded foam insert, designed to fit without the use of an additional sock or nylon sheath. This allowed for shear stresses to be measured directly at the skin. To further the understanding of shear stresses at the surface of the residual limb, Sanders *et al*. improved on the original work expanding shear stress measurement to thirteen locations on two patients with transtibial amputation (Sanders et al. 1997). In the type of suspension method used by Sanders *et al*., a gel liner interface was not required and the effect of multiple liners was not addressed.

Most recently Schiff *et al*. instrumented load cells into a transtibial socket utilizing sleeve suspension to further explore shear forces for amputees with and without distal tibia-fibular bone bridges (Schiff et al. 2014). However, sleeve suspension systems function mechanically different than gel interfaced pin suspension by gripping the prosthetic device from the outside of the prosthetic socket rather than at a single distal pin location. Additionally, pin suspension systems with gel liner interface are the most common attachment for below knees amputees and as such warrant investigation (H. Gholizadeh et al. 2014). Extensive shear force information for prosthetic users is currently lacking, more experimental work is needed to understand interface mechanics to improve our understanding of ulcer formation (Schiff et al. 2014). Force data gathered experimentally also has the potential to be used an input to a finite element modeling so deep tissue stresses can be obtained and multiple conditions studied.

The objective of this research was to instrument a single transtibial prosthetic socket with a two axis load cell to measure longitudinal shear force and normal force during walking. Force data located at the mid fibular region of the residual limb was desired as input for a finite element model and to further investigate interface mechanics of a gel liner interface. Experimental data comparisons were also evaluated with a gel liner, additional sock ply and removal of gel liner to allow contact with the skin. It was hypothesized that normal and shear forces would increase with increasing sock ply due to the added thickness within the socket allowable volume.

4.2 Methods

One male right unilateral transtibial amputee, 1.77 m in height, mass of 85.5 kg and mobility grade of K3 (Gailey et al. 2002), participated in this study. The participant provided written consent to complete the study. He underwent amputation twenty-nine years prior due to a traumatic accident. His current prosthetic device componentry included a 9 mm Alpha Willowwood gel interface liner with pin locking suspension. At time of testing, no pain or discomfort with his prosthetic device was reported. He had been seen within a month by a certified prosthetist who deemed his socket interface to be appropriate and alignment of his prosthesis to be acceptable.

First, to allow for force measurement, a duplicate socket was manufactured out of a clear thermoplastic material commonly used in fabrication of prosthetic "test sockets" for clinical use leading up to a definitive prosthetic socket. The duplicate was developed to match the alignment and fit of the participant's prosthetic socket. A duplicated socket was required for the insertion of a load cell within the inner socket surface. A hole was cut in the wall of the prosthetic socket in order to mount the load cell flush within the inner surface which contacted the limb. The participant's original socket would have been compromised if used for the experimental procedure.

Prior to load cell instrumentation a kinematic assessment was completed with both the original and duplicated sockets to ensure the duplicated socket yielded identical walking patterns. Kinematics were obtained for the lower extremity and trunk joint angles during walking. From this, a Gait Deviation Index was calculated for the walking trials (Schwartz & Rozumalski 2008). Secondly, the participant's duplicated prosthetic was assembled with their existing pylon, foot and suspension components and data of lower extremity and trunk kinematics were captured with the same Gait Deviation Index. The two data sets were compared to determine if significant changes were introduced between prosthetic devices within a participant.

To install the multi-axis load cell, a 4 cm diameter hole was created in the duplicated prosthetic socket. The hole's center was located 8.5 cm below the patient's fibular head on the lateral aspect of the residual limb. This location was selected because of the presence of muscle, complete contact with the load cell and avoidance of a bony prominence. The absence of contact would not allow for force measurement with the mounted load cell.

An OptoForce HEX-70-CE load cell (OptoForce; Budapest, Hungry) was mounted securely to the prosthetic socket as seen in Figure 4-1. The removed material from the prosthetic socket wall was mounted to the recording surface of the load cell with counter sunk screws. Mounting the removed piece to the load cell allowed for a consistent coefficient of friction across the entire socket. Additionally, it maintained the original curvature of the internal socket surface therefore preserving the clinically developed design of the socket. Shear load was measured along the long axis of the socket. Normal force was perpendicular to the internal curvature of the socket and designated as the z direction of force.

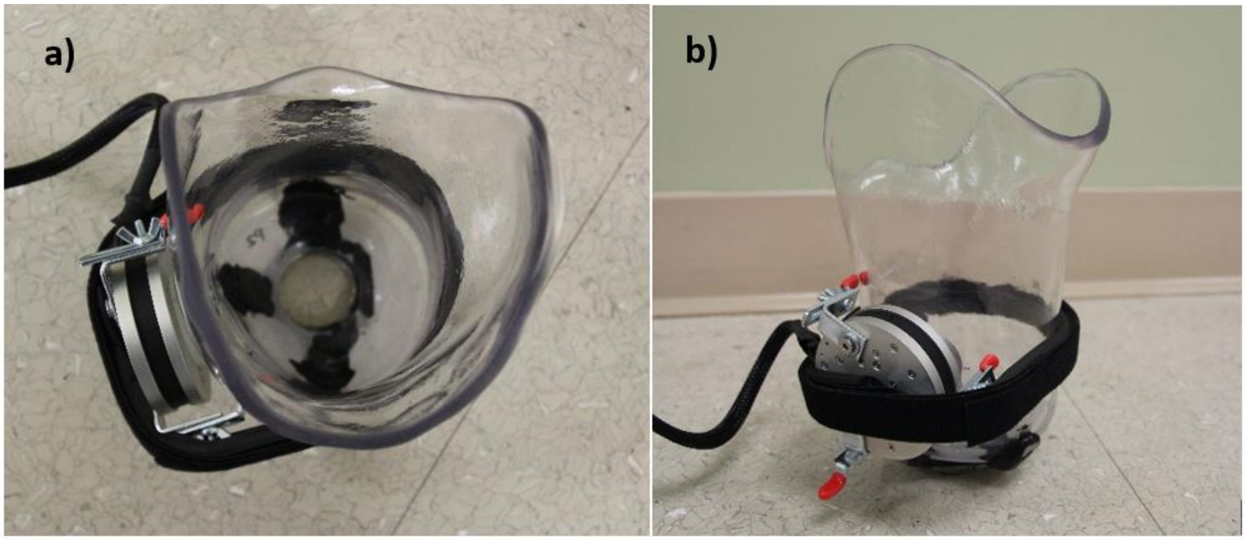

Figure 4-1. a) Top view of instrumented socket demonstrating flush internal curvature. b) Oblique view of load cell securely affixed from the outside of the prosthetic socket.

The instrumented prosthetic was assembled with the patient's every day original componentry from below the socket to pylon interface, maintaining the alignment of the device as a whole (Figure 4-2). The patient walked with the instrumented socket for an adjustment period.

Figure 4-2. Assembled instrumented prosthesis as worn by the participant.

Three walking conditions were conducted while two axes of force data were collected from within the socket. First, the participant wore his original gel liner within the socket, which was a 9 mm Alpha Willowwood gel liner (E = 50050 Pa). Secondly, a 3 ply sock was added over the gel liner. Lastly, a hole was cut in the 9 mm gel liner, exposing the patient's skin which allowed direct force measurement at the skin surface during walking (Figure 4-3). The hole was slightly larger than the recording surface on the load cell to ensure only skin contact was being recorded. The skin protruded through the hole to the outer region of the liner and the mounting of the load cell was not changed. For all three testing conditions, multiple self-selected walking trials were collected from which eight gait cycles were analyzed in each condition. Data were collected from the load cell at a 100 Hz sampling frequency.

Figure 4-3. Whole in gel liner to allow for contact and force measurement at the skin surface.

Force data were analyzed in gait cycles with respect to heel contacts and toe offs defined as gait events for the residual and sound limbs. Motion capture and force systems were synchronized with an external trigger so that force data could be split into gait cycles based on motion capture gait events. This analysis was performed using a custom Matlab code based on motion capture data for landmarks defined on the bilateral calcanei and second metatarsal heads (Miller 2009). Within each condition, shear and normal force data from eight gait cycles were normalized with respect to the gait cycle and averaged together. Force data during the gait cycle were selected for each condition corresponding to the peaks during initial contact, early stance, single support and swing. Based on the circular four centimeter diameter contact area, stresses were also calculated for the three conditions.

Four statistical comparisons were conducted using an ANOVA followed by a Tukey's posthoc for each analysis (MATLAB, 2016a). Three way comparisons analyzed the experimental normal and shear differences in force values across the three conditions including 1) gel liner alone 2) three ply sock worn over the gel liner, and 3) a hole cut in the gel liner exposing the skin. Separate peak force statistical analyses were conducted for these three comparisons within the four regions of the gait cycle defined earlier: initial contact, early stance, single support and swing. Level of significance was set to a p value of $p < 0.05$.

4.3 Results

The results obtained from experimental data collection using the instrumented socket revealed differences in force throughout the gait cycle across condition types (Figure 4-4). First, shear force data averaged across eight gait cycles revealed statistically significant differences across all comparisons which included four ANOVA results across the three conditions (gel liner alone, 3 ply sock with gel liner and the hole in the liner) with respect to the peaks identified during the gait cycle (Table 4-1). During all four analyzed regions (initial contact, early stance, single support and swing) of the gait cycle, shear force was greatest for the condition with the addition of a 3 ply sock and least in the hole in liner condition with the gel liner alone falling in between ($p < 0.05$).

Comparing normal forces, there were only two comparisons which were not found statistically significant as a result of the ANOVA analysis within periods of the gait cycle (Table 4-2). First, during initial contact, the gel liner and hole in liner conditions were not statistically different from each other but the three ply sock was significantly different from both. Secondly during early stance, the three ply sock did not demonstrate a statistical increase in normal force when compared with the gel liner alone condition, however later in single support all conditions were statistically different from each other for normal force ($p < 0.05$). It is also notable that a residual normal force during swing phase of gait were highest with the 3 ply sock addition, which was statistically significant when compared with the gel liner and hole in liner conditions ($p < 0.05$).

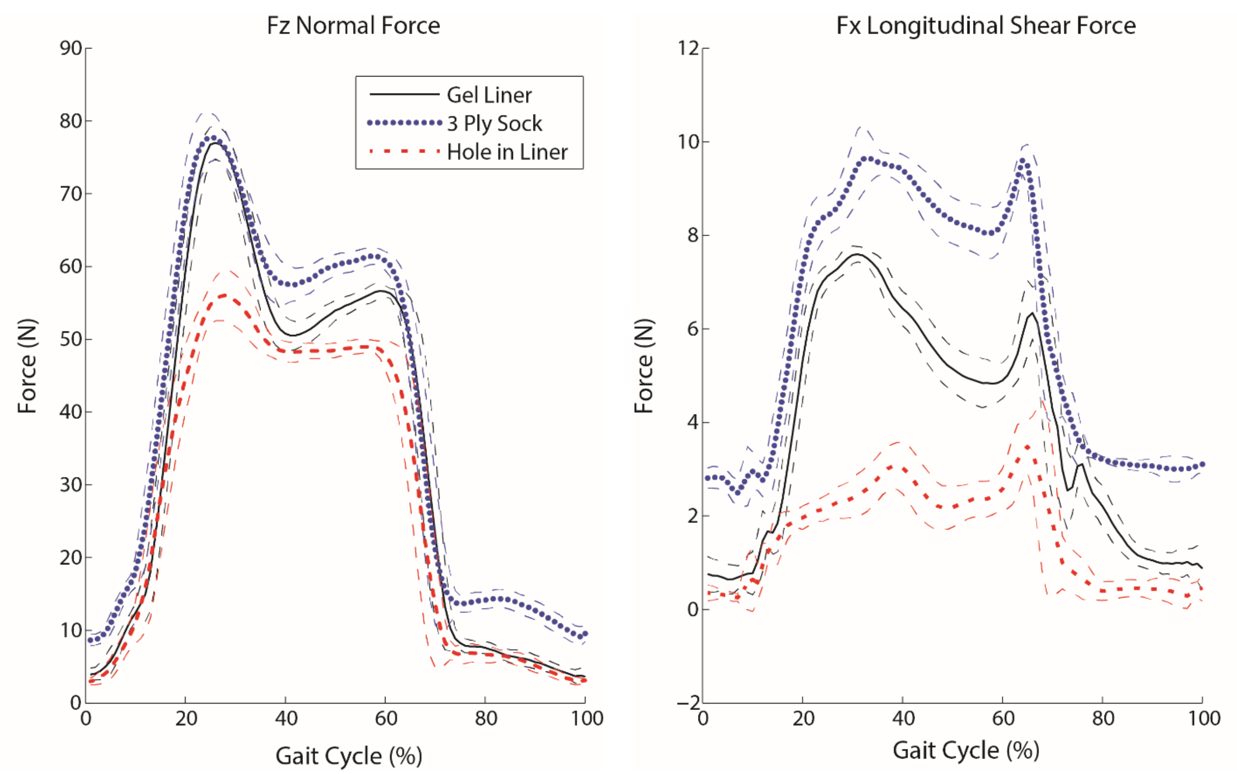

Figure 4-4. Three conditions of normal and shear force during walking from heel contact to heel contact on the right residual limb. Sashed lines in the same condition color represent the ± standard deviation of force data as it was analyzed across 8 gait cycles.

Table 4-1. Force comparison across three conditions for the four particular periods during the gait cycle.

	Fx Longitudinal Shear Force (N) (Avg ± SD)			
	Initial contact	**Early Stance Peak**	**Single Support Peak**	**Swing**
Gel Liner	0.79 ± 0.33	7.68 ± 0.16	7.01 ± 0.25	0.97 ± 0.22
3 Ply Sock	2.86 ± 0.25	10.01 ± 0.21	9.85 ± 0.24	2.96 ± 0.21
Hole in Liner	0.39 ± 0.13	3.17 ± 0.49	4.29 ± 0.38	0.40 ± 0.23

	Fz Normal Force (N) (Avg ± SD)			
	Initial contact	**Early Stance Peak**	**Single Support Peak**	**Swing**
Gel Liner	4.99 ± 1.52	77.53 ± 2.15	57.06 ± 0.79	5.24 ± 0.88
3 Ply Sock	10.84 ± 1.39	78.21 ± 3.06	61.64 ± 1.17	11.52 ± 1.39
Hole in Liner	4.71 ± 1.45	56.39 ± 3.36	49.49 ± 0.90	4.32 ± 0.68

Table 4-2. Initial contact and early stance statistical p values noting statistical differences reported for normal force comparisons.

	Initial Contact Fz Normal Force Comparison		
	Gel Liner vs 3 Ply Sock	**Gel Liner vs Hole in Liner**	**3 Ply Sock vs Hole in Liner**
P Value	$p < 0.05$	*$p > 0.05$*	$p < 0.05$

	Early Stance Fz Normal Force Comparison		
	Gel Liner vs 3 Ply Sock	**Gel Liner vs Hole in Liner**	**3 Ply Sock vs Hole in Liner**
P Value	*$p > 0.05$*	$p < 0.05$	$p < 0.05$

Shear and normal stress during walking were calculated based on the contact area of the load cell that was imbedded within the prosthetic socket. Shear stresses ranged from 0.4 – 7.66 kPa and normal stresses ranged from 2.7 – 61.9 kPa when evaluated across the three conditions and throughout the gait cycle. For the gel liner condition, peak normal stresses were calculated to be on average 61.7 ± 1.7 kPa. On average during the entire gait cycle, normal stresses for the gel liner condition were calculated to be 27.45 kPa. These calculated normal stresses were compared to published stresses and distributed pressures.

4.4 Discussion

The goal of this study was to evaluate how normal and shear forces during walking for a transtibial amputee. Additionally, force data were obtained for three specific conditions 1) gel liner alone 2) three ply sock worn over the gel liner, and 3) a hole cut in the gel liner exposing the skin.

The inclusion of shear forces in experimental work is critical. Shear force has been proven to contribute to increased blood occlusion when compared with normal force loading alone (Manorama et al. 2010; Manorama et al. 2013) which in turn has been shown to lead to increased tissue necrosis (Oomens et al. 2016). In an amputee population this is an important consideration when evaluating limb interface mechanisms and the high risk for pressure ulcer formation on the residual limb. Our results demonstrated that while normal forces throughout the gait cycle did not vary greatly with the addition of a three ply sock, the shear forces were all significantly increased with the added sock thickness. However, we have measured a significant increase in shear forces with increased sock thickness which may lead to increased blood occlusion and resulting decreased nourishment of limb tissues. Wearing an extra sock thickness when not clinically indicated may cause limb irritation and conditions related to ulcer formation due to increased shear forces at the interface. Therefore, patients should be educated on sock usage, and clinicians should consider the proper indications for prescribing an additional sock ply.

For the condition with the hole in the gel liner, shear and normal force measurements were collected at the surface of the skin. A challenge of conducting experimental research in below knee amputees wearing a gel liner is the inability to directly access the surface of the skin for data measurement. Historically, this is a reason why thin film pressure measurement devices were used extensively in published literature because they are able to be placed beneath the surface of the gel liner, while still utilizing the typical suspension method. However, shear forces are not able to be measured with pressure sensors. Our results indicated significant decreased in shear and normal forces throughout the gait cycle when compared to the intact gel liner condition. A possible reason for the decreased forces may be the absence of material thickness, therefore allowing the tissue less bounded constrain and greater regions to displace within the socket.

Stresses were calculated based on the contact area of the load cell within the socket. For the gel liner condition, peak normal stresses were calculated to be on average 61.7 ± 1.7 kPa. Sanders *et al*. also measured normal stresses in the mid fibular region to be on average 61.3 kPa (Sanders et al. 1997). Additionally, average normal stresses for the gel liner were computed to be 27.45 kPa throughout the entire gait cycle. Gholizadeh *et al.* conducted an experimental study with pressure sensors mounted on transtibial limbs and found an average pressure throughout the gait cycle to be 36.05 ± 11.4 kPa in the mid to distal fibular region (Hossein Gholizadeh et al. 2014). Considering large standard deviations across the pressure measurement in Gholizadeh's study, our single case study falls within their reported values. However, limited shear force and stress data are available in the below knee amputee population. Schiff *et al*. evaluated correlation coefficient comparisons of stresses through the use of load cells instrumented in the socket wall but magnitudes were never presented (Schiff et al. 2014). Our case study provides new information, particularly with regard to shear forces in addition to normal forces within the prosthetic socket.

A limitation of this study includes the singular location in which force was measured. The targeted region was selected based on tissue thickness in this anatomical region of the residual limb. Future studies could also include more measurement locations to compare regional anatomical variances in soft tissue versus bony prominences. Secondly, a limitation of this methodology includes possible changes introduced due to the presence of a hole in the gel liner such as elongation changes to the gel liner or irritation caused between the skin/rigid socket wall interface.

Overall, this work contributes significantly to the understanding of shear forces at the socket to limb interface. Many patients wear different interface thicknesses during the day and this case study highlights a single sample size of how these forces change. The addition of shear force measurement in addition to normal force is important for considering the underlying tissue influences for blood perfusion and tissue health when shear is present. Finally, these results are also helpful for creating finite element models which can be based on experimentally captured data for boundary conditions and loading inputs.

5. FINITE ELEMENT ANALYSIS OF THE SOCKET TO LIMB INTERFACE WITH EXPERIMENTAL DATA INPUTS

5.1 Introduction

The mechanical interface between a patient's residual limb and their prosthetic device is a complex loading condition. When a prosthesis is not fitting well, it often leads to the formation of ulcers. While experimental and modeling research has been conducted in this patient population, there is much yet to be understood about key contributors to ulcer formation. Finite element (FE) can be used to study the effects of different prosthetic liners on superficial and deep tissue stresses.

FE has been utilized in understanding interface biomechanics, development of sockets with computer aided design (CAD)/ computer aided modeling (CAM) and approximation of deep tissue stress (Zhang et al. 1998). The model is dependent upon material properties, geometric data, loading characteristics, boundary conditions and initial conditions. While a FE model may result in a solution, it does not guarantee the model's value or accurate representation of the physical system. Therefore, combining a FE model with experimental data helps insure realistic outputs.

Early modeling in prosthetics simplified the geometry of the residual limbs and the prosthesis design, often constraining the model with a static ground reaction force at heel contact. Also, lack of experimental data at the socket to limb interface caused researchers to make many assumptions on constraints and external loading. Models did not represent the complexity of the bone structures within the limb, nor did they model any of the biological tissues as non-linear materials (Brennan & Childress 1991; Reynolds & Lord 1992; Sanders & Daly 1993; Steege & Childress 1988; Silver-Thorn 1991; Quesada & Skinner 1991; Zhang et al. 1995). A summary of initial prosthetic modelling literature is provided in Appendix A.

As imaging techniques improved so did the complexity of models. Biplanar x-ray, magnetic resonance imaging (MRI), CAD and computed tomography (CT) were used to create realistic geometries for modeling (Lee et al. 2004; Zhang & Roberts 2000; Lee & Zhang 2007; Zachariah & Sanders 2000). However, a limitation of these studies was a continued assumption that soft tissues could be modeled as linearly elastic materials. A summary of models using more advanced geometry, with linear elastic materials is located in Appendix B.

5.1.1 Deep Tissue Finite Element Analysis (FEA) in Amputees

More recent models have multiple tissue layers, interactions between those layers and mathematical constitutive models of non-linear material properties to more closely mimic biological tissues. The development of these improved models then allowed for the investigation of deep tissue injury (Portnoy et al. 2008; Portnoy, Siev-Ner, Yizhar, et al. 2009; Portnoy, Siev-Ner, Shabshin, et al. 2009; Portnoy et al. 2011; Portnoy et al. 2010; Gefen et al. 2008). Key findings for transtibial amputees indicate higher stresses accumulating at the tissue to bone interface rather than more superficial tissue layers. However, the use of experimental data inputs, as boundary conditions is still lacking.

5.1.2 Recent FEA Using FEBio

Finite Elements for Biomechanics (FEBio) is a software platform customized for complex questions in biomechanics with numerous constitutive models available in the package, and is open source (Maas et al. 2012; Meng et al. 2013; Galbusera et al. 2014; Perduta & Putanowicz 2015). Recent research is limited with regard to use of non-linear, neo-Hookean materials implemented in FEBio. The available work reported for other body regions included heel ulcers, buttock tissue damage in spinal cord injury, and a single transtibial patient was summarized in Appendix C (Sengeh et al. 2016; Levy et al. 2015; Shoham et al. 2015). Specifically, Levy *et al.*, investigated tissue stresses in heel ulcers where they implemented non-linear, neo-Hookean materials for the skin layer with shear and bulk moduli consisting of 31.9 and 3179.37 kPa (Table 5-1) (Levy et al. 2015). Shoham *et al.*, also implemented neo-Hookean materials in their model for skin and muscle with the same skin values as Levy *et al*. and muscle values as seen in Table 5-1 (Shoham et al. 2015). For our work, FEBio was used to model deep tissue stresses in a region of a transitibal limb with experimental data supporting boundary inputs.

Table 5-1. Mechanical properties of the model components selected for the FE models.

	Shear Modulus, kPa	Bulk Modulus, kPa	Elastic Modulus, kPa	Poisson's Ratio	Coefficient of Friction
Gel Liners* [1]					
Alpha	---	---	50.05	0.49	0.3
Iceross	---	---	55.86	0.49	0.3
DERMO	---	---	53.28	0.49	0.3
TEC	---	---	88.06	0.49	0.3
Skin [2]	31.9	3179.37	---	0.495	---
Muscle [2]	7.1	707.6	---	0.49	---
Bone [2]	---	---	7,000,000	0.3	---

[1] Sanders et al. 2004; O'Hara 1983; Noor & Mahmund 2015; Thomson 1966
[2] Levy et al. 2014; Shoham et al., 2015
* Ohio Willow Wood Alpha Classic; Ossur Iceross Comfort; Ossur DERMO-6; TEC Pro 18

5.1.3 Current Need for FEA in Prosthetics

Particularly relevant to prosthetics, FEA can be used to understand underlying tissue stresses which can lead to ulcer formation due to different prosthetic gel liners and interface conditions. Additionally, inputs to the FE models can utilize experimental data captured within the prosthetic socket, such as forces and displacements. Doing so would contribute new analyses to the literature which provide realistic data sets based on measured boundary conditions. For example, previous research based on experiments has shown increased shear forces contribute to increased blood occlusion and consequently increased risk for ulcer formation (Manorama et al. 2010; Manorama et al. 2013). Based on the findings by Manorama et al., it is desirable to identify how various gel liner properties influence deep tissue mechanics under shear and normal loading conditions. ***Thus, the objective of this work was to determine the stresses within the skin and muscle for a transtibial amputee limb, constrained with experimental conditions of displacement and force data.*** The goal was achieved by creating 29 models, beginning with simplified analyses and advancing to multi-layer models representing various gel liners with underlying skin, muscle and bone.

5.2 Methods

During the development of the models, simplified analyses were first implemented to investigate non-linear responses of neo-Hookean materials. Next, complex models consisting of four layers were developed with the gel liner, skin, muscle and bone. Then, the contact interface between the skin and gel liner was varied to evaluate under which conditions the gel liner would slip relative to the skin. Understanding the slip and no slip conditions and their effects on skin Von Mises and shear stress provided an improved understanding how various interface conditions may lead to ulcer formation.

5.2.1 Simplified One and Two Layer Models

The purpose of the simplified models were to investigate responses of neo-Hookean materials to various loading conditions. Simple cubes of neo-Hookean material were created to evaluate the influence of separate compressive pressure and prescribed displacements on this quasi-incompressible, hyperelastic material and compare to theoretical results (Figure 5-1a). First the entire cube of neo-Hookean material was defined with material properties for Young's modulus (E = 50 kPa) and Poisson's ratio (v = 0.49). Two separate models were executed with two different distributed pressures, 10 Pa and 5 kPa respectively, in which normal stress, strain and displacement were analyzed. Based on experimental force data collected in Chapter 4, five kPa was selected as the loading condition. The 10 Pa load was arbitrarily selected to perform an analysis in which the neo-Hookean material responded in the linear elastic range. Next, a 6 mm prescribed displacement was applied parallel to the top surface of the cube in the positive x direction.

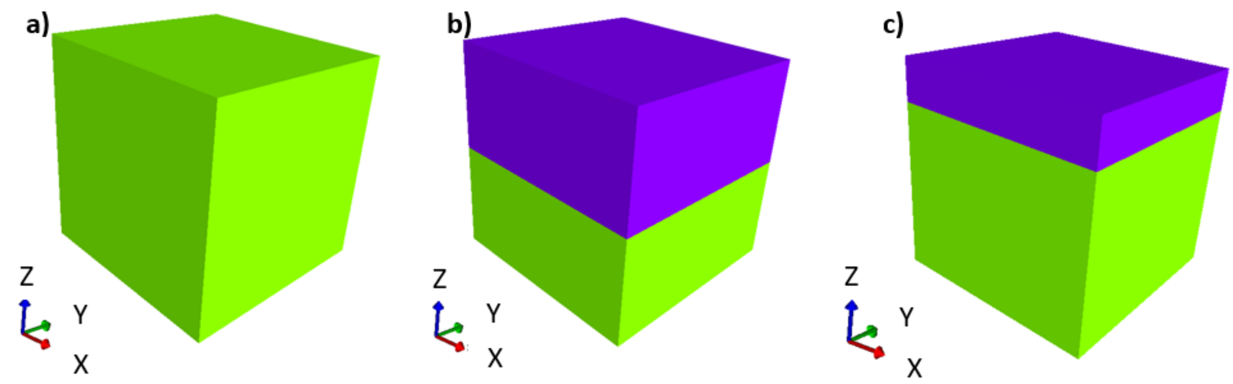

Figure 5-1. a) Square neo-Hookean model b) Square neo-Hookean model with each layer divided evenly in height c) Square neo-Hookean model with uneven layers

A simple two layer neo-Hookean model was also created to investigate the layering method using tied interfaces between layers (Figure 5-1b and 5-1c). Layers were first model as even thicknesses and secondly where the top layer was 0.2 m thick and the bottom layer was 0.8 m thick. Initially, the two layers were modeled with the same material properties (E = 50 kPa and v = 0.49). Next, the top layer was varied slightly with a material that had a reduced stiffness (E = 40 kPa and v = 0.49), while maintaining the bottom layer properties (E = 50 kPa and v = 0.49). All two layer model variations were loaded with a 5 kPa compressive distributed pressure with the bottom XY surface of the material constrained for all translations and rotations.

5.2.2 Realistic Four Layer Models

The inclusion of the four layer models was to create a realistic layered region of a transtibial amputee's limb consisting of the gel liner, skin, muscle and bone. Once the model was established, focus was given to the investigation of various gel liner material properties and contact interactions on underlying tissue stresses.

5.2.2.1 Mechanical Properties

Mechanical properties of bone, muscle, skin and various gel liners were adapted from the literature (Sanders et al. 2004; Levy et al. 2015; Shoham et al. 2015) (Table 5-1). Specifically, the bone was assumed to be a rigid body. The muscle and skin were nearly incompressible and hyperelastic, represented by a neo-Hookean material model with a strain energy density function W (Equation 1):

$$W = \frac{G_{ins}}{2}(\lambda_1^2 + \lambda_2^2 + \lambda_3^2) + \frac{1}{2}K(\ln J)^2 \quad (1)$$

Where, G_{ins} represents the shear modulus, λ_1, λ_2 & λ_3 are principal stretch ratios, K is the bulk modulus and $J = \det(\mathrm{F})$, where F is the deformation gradient tensor. This material type was selected because it has non-linear stress-strain behavior but uses a standard displacement-based element formulation.

5.2.2.2 Modeling Region of Interest and Geometry for Realistic Model

First a rectangular geometry model of 100 mm x 100 mm was developed with layers of bone, muscle, skin and a gel liner (Figure 5-2). Layer thicknesses were based on literature, 10 mm of bone, 20 mm of muscle, 3 mm of skin, and 9 mm of gel liner (Sanders et al. 2004; Zollner et al. 2013; Tepole et al. 2011; Levy et al. 2015; Shoham et al. 2015). It should be noted that muscle thickness across the entire fibula is uneven distally versus proximally. The model represents anatomy in the distal third of the fibula where muscle thickness is more consistent (Figure 5-3).

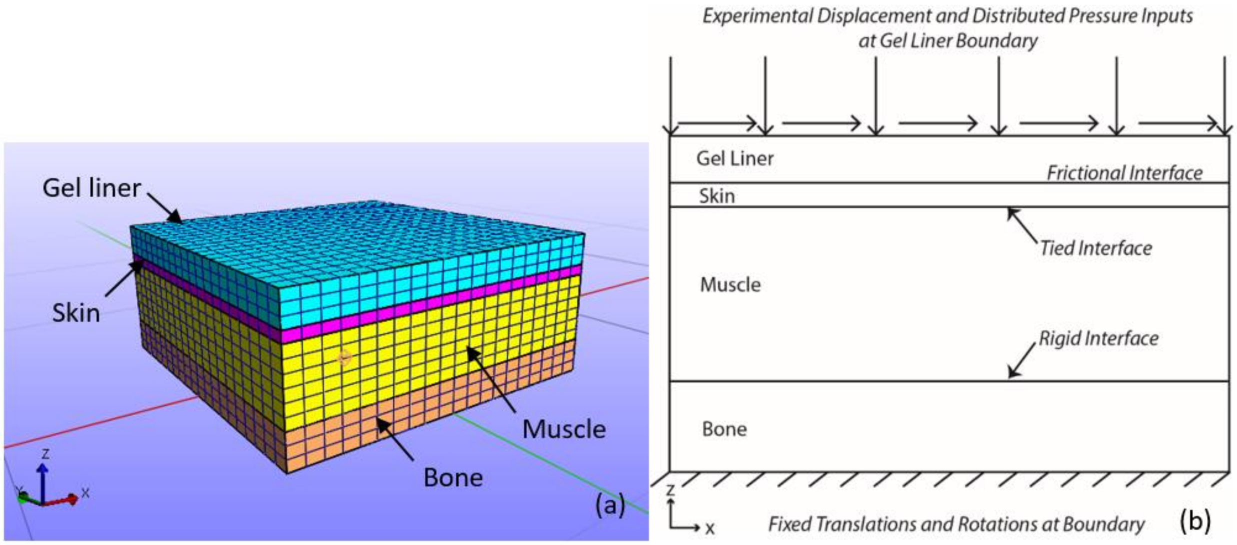

Figure 5-2. a) 3D geometry of four layer model b) Simplified geometry of FE model containing bone, muscle, skin and gel liner constrained by experimental displacements and fixed at the boundary of the bone. The gel liner to skin interface was either modeled as a tied interface or a frictional sliding interface depending on the analysis to demonstrate if slip occurred or not. A tied interface between muscle/skin used a connection of two non-conforming meshes with a high penalty factor to prevent modeled tissue separation. A rigid interface between bone/muscle was also defined to not allow separation.

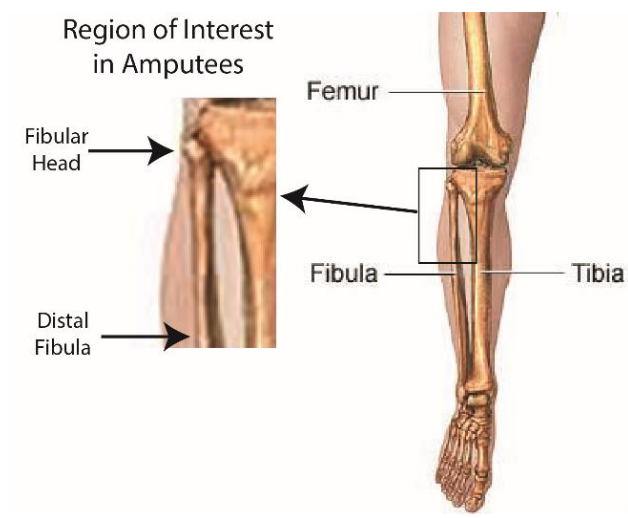

Figure 5-3. Lower extremity model of bones and generalized soft tissue focused on an amputee's anatomy of limited limb length. The anatomical area enclosed by the rectangle represents the fibular region of interest for which tissue thicknesses were modeled based on average tissue thickness in this region.

To examine robustness of the model with respect to geometry, additional model designs were implemented. A cylindrical model was developed as an axis-symmetric comparison with respect to the rectangular four layer model. Layer thicknesses for bone, muscle, skin and gel were identical to that of the rectangular model with a cylindrical radius of 56.42 mm for all the layer cross sectional areas resulting in an equivalent layer area of 0.01 m^2.

5.2.2.3 Loading and Boundary Conditions for Realistic Model

Based on measured force data found experimentally during walking, a 5 kPa distributed pressure was applied to the gel liner surface. An average regional displacement for the mid-fibula of 6 mm (obtained from our experimental data) was used for a prescribed displacement and applied at the surface of the gel liner (Figure 5-2).

5.2.2.4 Layer Contact Definitions for Realistic Model

Within the model tissue layers, the skin to muscle contact was treated as a tied interface with high penalty factor to prevent the formation of gaps between the layers. In FEBio, a tied interface can be used to connect two non-conforming meshes and it is assumed that the nodes on both mated surfaces are connected. The muscle to bone interface was treated as a rigid interface. The bone layer was constrained in all directions of translation and rotation as a rigid body on the bottom surface. At the skin to gel liner interface, two model simulations were completed to represent two clinical situations; 1) the gel liner slipped along the skin 2) no slip occured with respect to the skin during loading (Figure 5-4). For the slip condition, a frictional interface coefficient was set to a 0.3 based on Sanders et al. 2004. This allowed for slip to occur if the coefficient of friction was not great enough to prevent tangential movement between the skin and gel liner. For the no slip condition, a tied interface was modeled with the penalty factor set to prevent layer separation.

The models with the condition of slip between the liner and skin interface utilized a sliding with gaps contact. The slip conditions required xz face vertical constraints to properly define the model. Although the vertical constrains were not necessary for the tied interface on the no slip model, an analysis was conducted including xz face vertical limitations on displacement. The purpose of running two simulations, one with and one without vertical constraints on the no slip model, was to evaluate the influence of vertical constraints on tissue layer stresses.

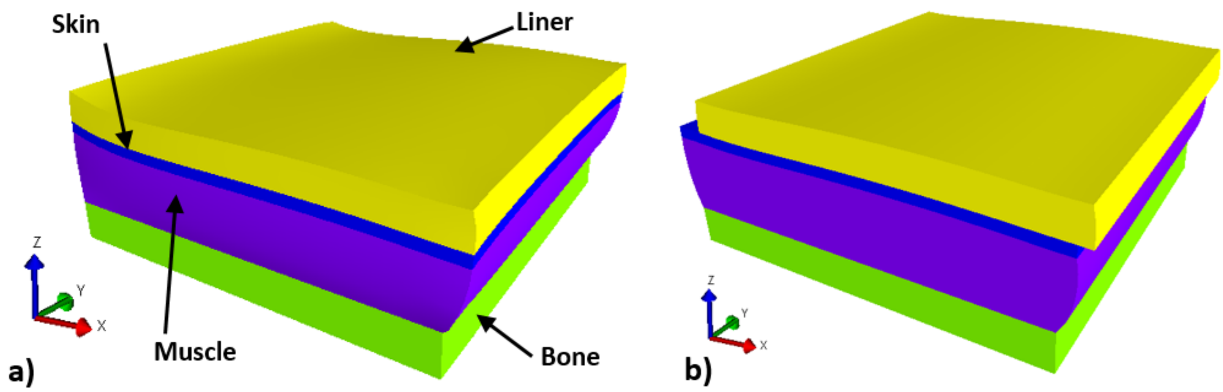

Figure 5-4: a) No slip model and b) Slip model demonstrating contact differences between the skin and gel liner interaction. As can be seen on the right, there is x direction translation between the gel liner and skin.

5.2.2.5 Liner

Four models were created, each represented a specific liner type. The selected liners were used by our participants, which included an Ohio Willowwood Alpha Liner, Ossur Iceross Comfort, Ossur DERMO-6, and TEC Pro 18 (Table 5-1). Our experimental strain of the liner during walking from Chapter 3 reported 6-11% strain which falls within this linear response region (Sanders et al. 2004). Thus, each gel liner was modeled as a linear isotropic material based on linear responses of these gel liners during tensile material testing, Figure 5-5 (Sanders et al. 2004).

Liner Stiffness: These four liners were implemented as a 9 mm thickness layer. Separate simulations were run with their increasing material stiffness (E ranging from 50050 to 88060 Pa) (Table 5-1). Simulations were modeled with both slip and no slip conditions. All liners were modeled with a Poisson's ratio of 0.49 which is based on silicon and urethane polymer material properties and representative of the liner materials (O'Hara 1983; Noor & Mahmud 2015; Thomson 1966).

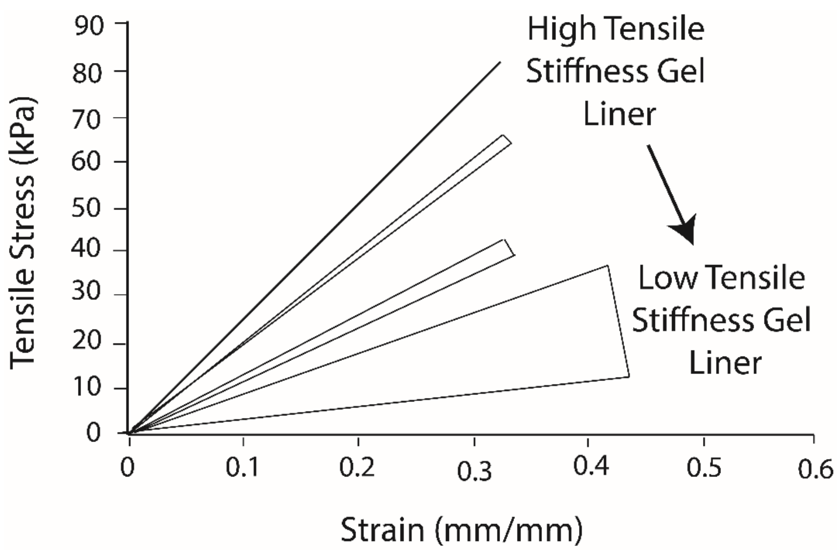

Figure 5-5. Tensile testing results for various prosthetic liners fell into four groups represented by the liner boxed regions with decreasing stiffness (Daly & Odland 1979; Sanders et al. 2004).

Liner Thickness: After the gel liner stiffness changes were modeled, one of the four liners, the Alpha liner was modeled at three gel thicknesses representing 3, 6 and 9 mm. These options are available by the manufacturer and different thicknesses are commonly worn by amputees. The change of liner thickness was modeled to evaluate the influence of liner thickness on underlying tissue stresses.

5.3 Results

5.3.1 Simplified Model Results

5.3.1.1 One and Two Layer Models

The purpose of the simplified models was to compare theory with model results. With a distributed pressure of 10 Pa applied in the negative z direction, the model responded with a compressive axial stress according to the linear elasticity theory (a negative sign indicated compression). Theoretical calculations resulted in a -10 Pa compressive stress, calculated as 10 Pa distributed pressure divided by a one square meter cross section in the model. FE model results yielded -9.946 Pa, matching well when evaluated as an average of elements in the center of the model. When the distributed pressure was increased to 5 kPa, the model responded in the nonlinear hyper-elastic manner as theoretically described in non-linear continuum mechanics for neo-Hookean materials by Equation 2 (Bonet & Wood 2008).

$$\sigma = \frac{E}{J}\ln(\lambda) \tag{2}$$

Where λ is stretch defined by the current length divided by the initial length; E is the young's modulus; J is the volume ratio defined as $\lambda^{(1-2v)}$ where v is poisson's ratio. J equals one for incompressible materials, however using our FE stretch and defined poisson's ratio, J was calculated to be 0.999997. Therefore, also representing an incompressible material without making the assumption that it was incompressible based on the volume ratio equation. Theoretical calculations using Equation 2 resulted in -3.96 kPa for the 5 kPa load compared with the -4.49 kPa stress in FEBio (Table 5-2). *When providing numerical model data for all cases, the stress was taken from the center of the analyzed layer as an average of four elements.*

Table 5-2. Comparison results of two compressive pressures with FEA and theoretical axial stress for a linear and non-linear response.

10 Pa Compressive Load Linear Response	
FEA	σ_z= -9.946 Pa
Theory	σ_z= -10.0 Pa

5 kPa Compressive Load Non-linear Response	
FEA	σ_z = -4490 Pa
Theory	σ_z = -3960 Pa

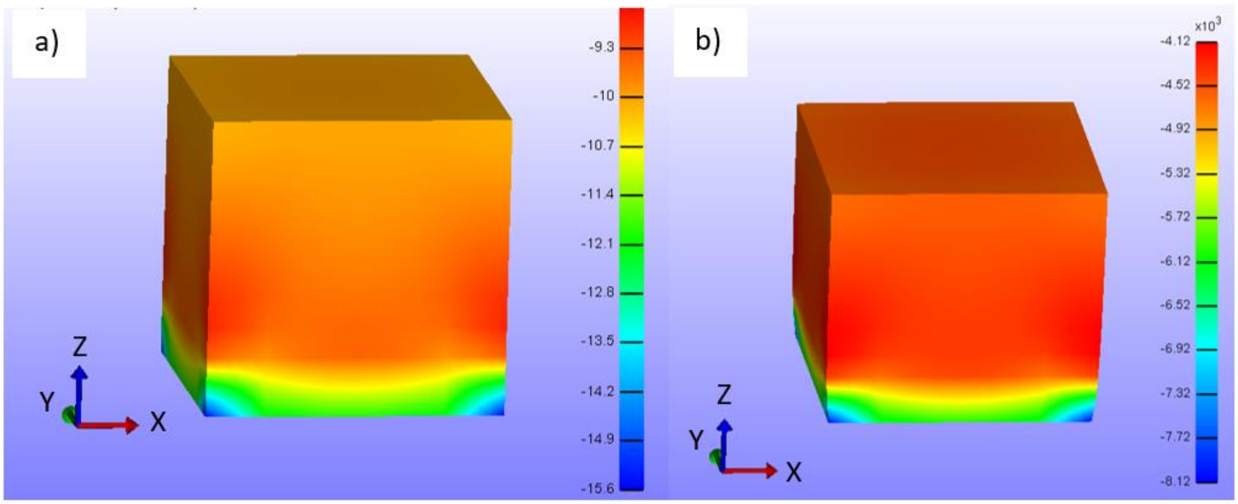

Figure 5-6. a) 10 Pa compressive load b) 5 kPa compressive load; both modeled as a single layer neo-Hookean material model but note linear and non-linear response differences. (Scales are in Pa.)

Next, simulations were run to compare the stress output of two material layers with a tied interface. The two layer model in compression resulted in similar results to the single layer model and theoretical values at 5 kPa distributed loading on the top surface (Table 5-3 and Figure 5-7). Top and bottom layers were close in compressive stress values. However, the bottom layer had slightly larger compressive stresses due to the fixed base which created a stress concentration. The tied interface with a high penalty to prevent separation did not create a noticeable stress concentration between the layers in the FEA output. Comparing top and bottom layers, both had equal material properties and therefore stresses within both layers were evenly distributed with similar results (Table 5-3).

Table 5-3. Compressive model results for a two layer neo-Hookean model with compressive stress reported. Reported model outputs were evaluated in FEBio's PostView software.

5 kPa Top layer	5 kPa Bottom layer
σ_z = -4490 Pa	σ_z = -4898 Pa

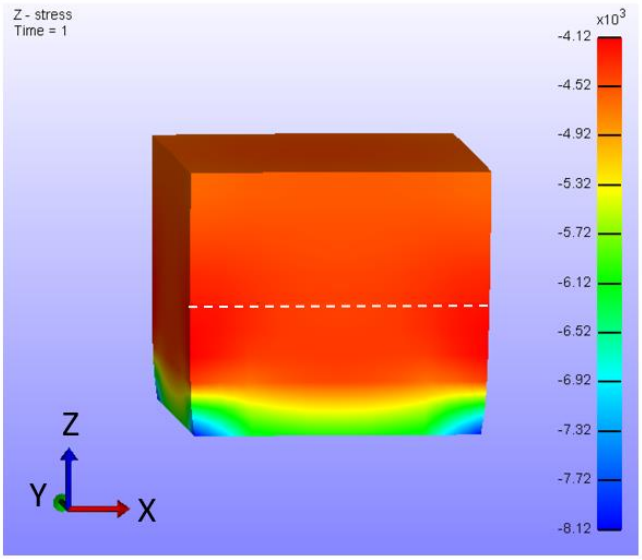

Figure 5-7. Compressive 5 kPa distributed pressure alone with tied interface between layers. Bottom layer E = 50kPa; Top layer E = 50kPa (Equal thickness layers; White dashed line represents contact interface between materials; Scales are in Pa)

Next a two layer model with uneven layer thicknesses was developed to investigate how stresses could change when uneven layer thickness joined by a tied interface were introduced. A second two layer model with uneven layer thickness and slightly different elastic moduli resulted in similar stresses to previous models at 5 kPa distributed loading on the top surface (Table 5-4 and Figure 5-8). Top and bottom layers were close in compressive stress values with 4.4 and 4.5 kPa on top and bottom respectively. Again, the tied interface between layers with a high penalty to prevent separation also did not cause an influential difference at the contact for stress analysis. The uneven thickness did not influence the results or skew model values compared with expected non-linear continuum mechanics (Equation 2).

Table 5-4. Compressive model results for a two layer neo-Hookean model with compressive stress reported. Comparison averaged elements from the middle of layers which resulted from model outputs for the top and bottom layers.

5 kPa Top layer	5 kPa Bottom layer
σ_z = -4432 Pa	σ_z = -4506 Pa

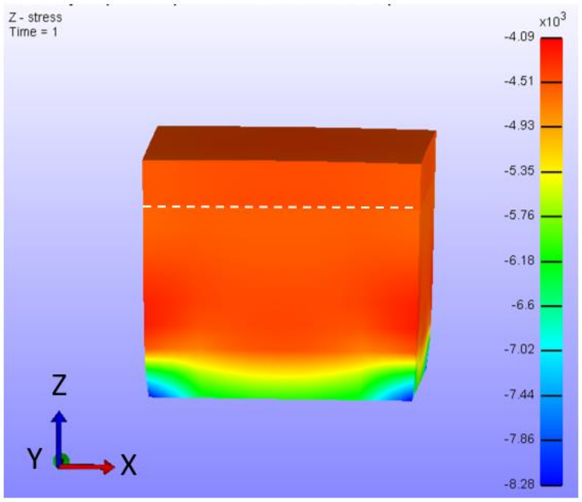

Figure 5-8. Compressive 5 kPa distributed pressure alone with tied interface between layers. Bottom layer E = 50kPa (0.8m); Top layer E = 40kPa (0.2m). (White dashed line represents contact interface between materials; Scales are in Pa)

One and two layer models were developed for the purpose of understanding the effects of geometry, interface contact definitions and uneven layer thicknesses. These results demonstrated minimal differences in stress surrounding a contact definition and good agreement with theoretical calculations.

5.3.2 Realistic Four Layer Model Results

5.3.2.1 Cylindrical versus Rectangular

Modeling comparison results for an axis symmetric geometry versus the rectangular model are reported here. *Presented stresses are from an average of four centrally located elements on the surface of each layer* (Figure 5-9).

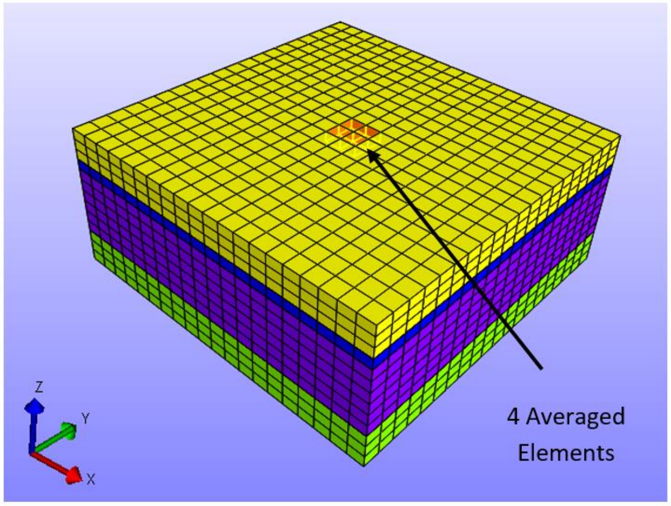

Figure 5-9. Four averaged elements were selected for the top surface of each layer. The same placement of elements represented were consistent with deeper tissue layers.

Comparisons represented are for both combined loading (5 kPa pressure and 6 mm displacement), as well as 5 kPa load alone (Table 5-5 and 5-6). The 6 mm displacement was applied in the horizontal positive x direction, parallel to the top surface. Three stresses are reported for 1) Von Mises, 2) Z normal compressive and 3) maximum shear. Von Mises stresses are reported in FEBio as effective stresses but for engineering consistency will be labeled as Von Mises in all results reported.

Table 5-5. Combined loading (5 kPa distributed pressure and 6 mm displacement) results for cylindrical versus rectangular four layer model.

Material Layer	Von Mises (kPa)	Z Normal Stress (kPa)	Max Shear Stress (kPa)
Gel Liner Cylinder	5.303	-4.626	2.925
Gel Liner Square	5.099	-4.683	2.715
Skin Cylinder	8.598	-5.328	4.873
Skin Square	8.260	-5.317	4.626
Muscle Cylinder	3.442	-4.987	1.875
Muscle Square	3.276	-5.000	1.786

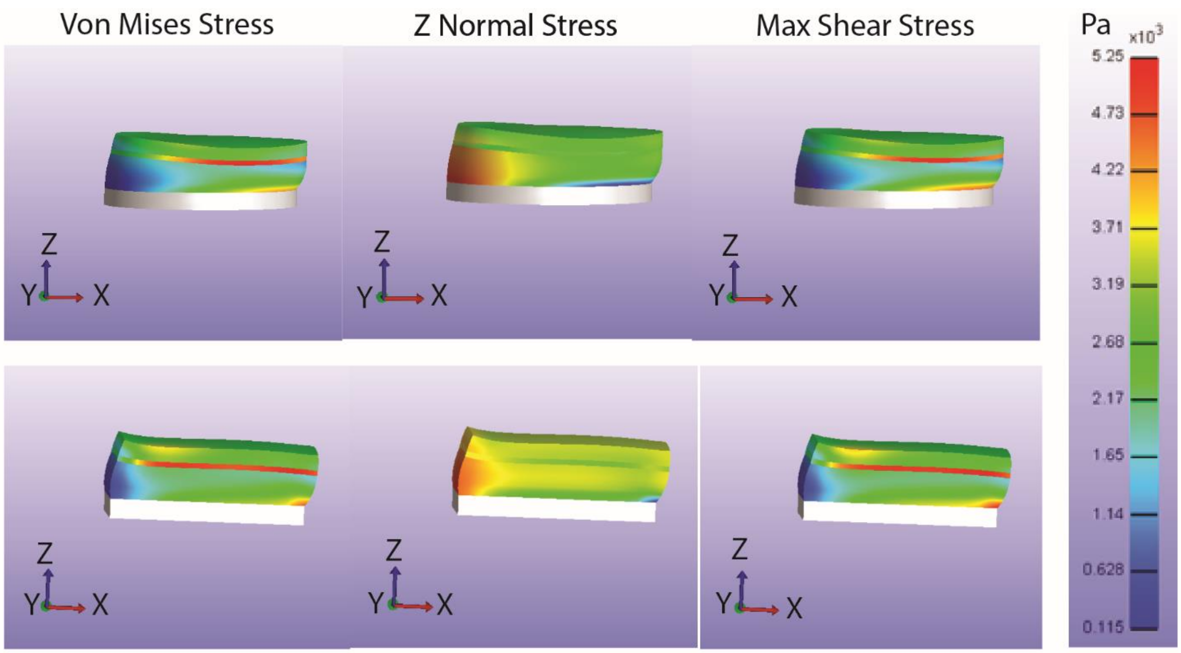

Figure 5-10. Axis Symmetric Comparison (10 cm x 10 cm Cube versus a cylinder with a radius of 5.6419 cm; A = 0.01 m^2). Combined loading with 5kPa pressure and 6mm x direction displacement. Tied interface with no slip condition and Willow wood Alpha Silicone Gel Liner.

Table 5-6. Results for cylindrical versus rectangular models with a 5 kPa distributed pressure on top surface.

Material Layer	Von Mises Stress (kPa)	Z Normal Stress (kPa)	Max Shear Stress (kPa)
Gel Liner Cylinder	5.121	-4.431	2.546
Gel Liner Square	4.753	-4.484	2.370
Skin Cylinder	8.692	-4.691	4.347
Skin Square	8.492	-4.658	4.250
Muscle Cylinder	1.826	-4.438	0.914
Muscle Square	1.835	-4.448	0.917

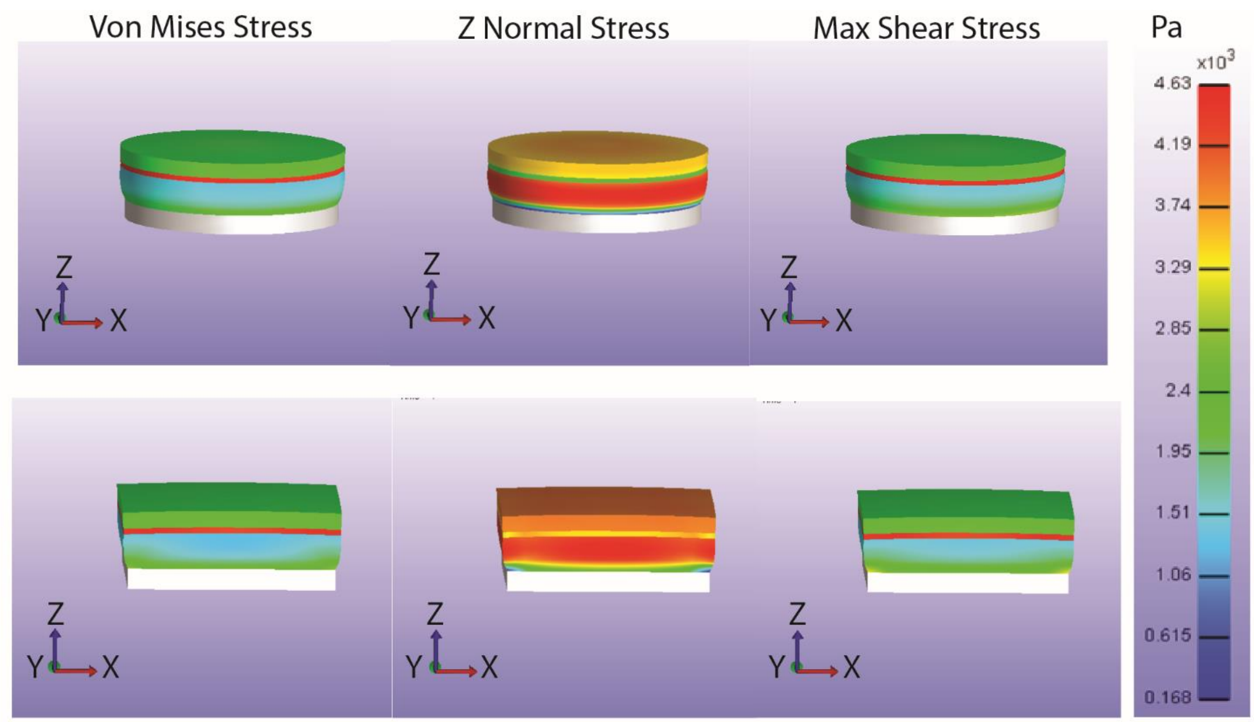

Figure 5-11. Axis Symmetric Comparison (10 cm x 10 cm Cube versus a cylinder with a radius of 5.6419 cm; A = 0.01 m^2). Loading with 5kPa pressure alone. Tied interface with no slip condition and Willow wood Alpha Silicone Gel Liner. (Scales are in Pa)

5.3.2.2 Vertical Face Constraints

To evaluate the effects of the vertical constrains, results of two different four layer models with tied interfaces between the skin and gel liner were compared. For comparison one model had a zero displacement constraint on the xz vertical faces while on the other the vertical constrains were removed (ie. front and rear surfaces) (Table 5-7). Overall without constraints, the Von Mises stress increased, the normal stress increased at the bone to muscle interface, and the shear stress increased.

Table 5-7. Model with and without vertical constraints on the xz face in positive and negative y directions. Middle locations were defined as elements selected in the center of the layer's cross sectional view at the layer surface as seen in Figure 5-9.

Material Layer	Von Mises Stress (kPa)	Z Normal Stress (kPa)	Max Shear Stress (kPa)
Gel Liner w/vert	3.390	-5.105	1.944
Gel Liner wo/vert	4.922	-4.714	2.701
Skin w/vert	4.274	-5.942	2.467
Skin wo/vert	8.219	-5.354	4.618
Muscle w/vert	2.380	-5.480	1.374
Muscle wo/vert	2.506	-4.600	1.446

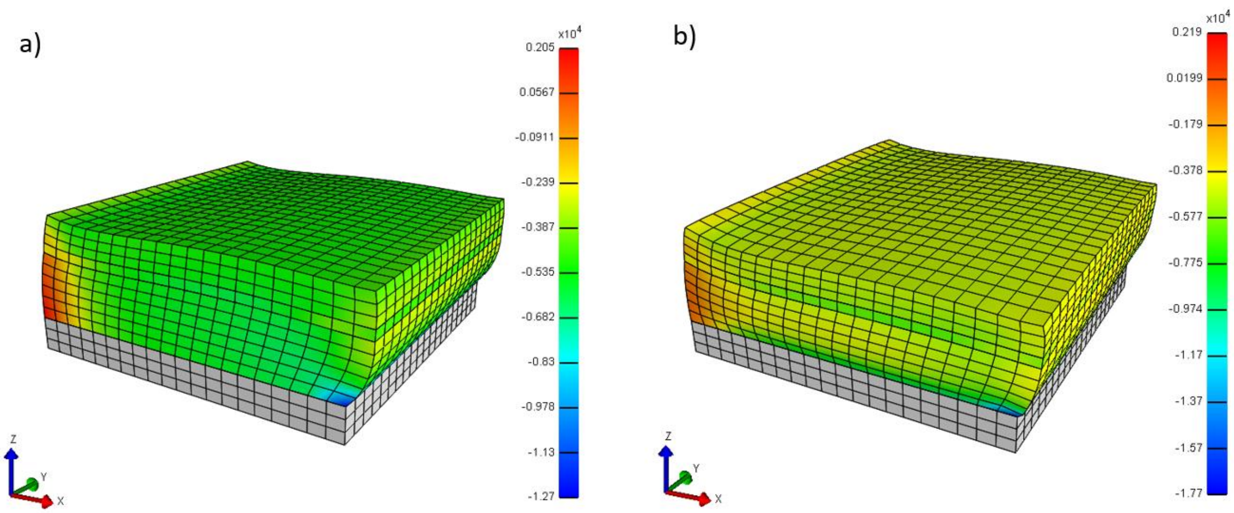

Figure 5-12. a) Model with vertical constraints on the xz face in positive and negative y directions. b) Model with vertical constraints removed. (Scales are in Pa.)

5.3.2.3 Slip versus No Slip Model Results

In models where slip occurred between the gel liner and the surface of the skin, the Von Mises stresses varied throughout the skin layer with the highest stresses occurring in the region identified as element 2 (Figure 5-13a and 5-14); whereas models without slip (Figure 5-13a) demonstrated even stresses throughout the interface contact. For the alpha liner, with identical loading conditions, the Von Mises stress at the muscle to bone interface in the no slip model was 2.65 kPa compared to 0.39 kPa in the model with slip (Table 5-8). Additionally, maximum shear stress was increased in all three locations for the model without slip with the highest value being at location 2 equal to 5.09 kPa.

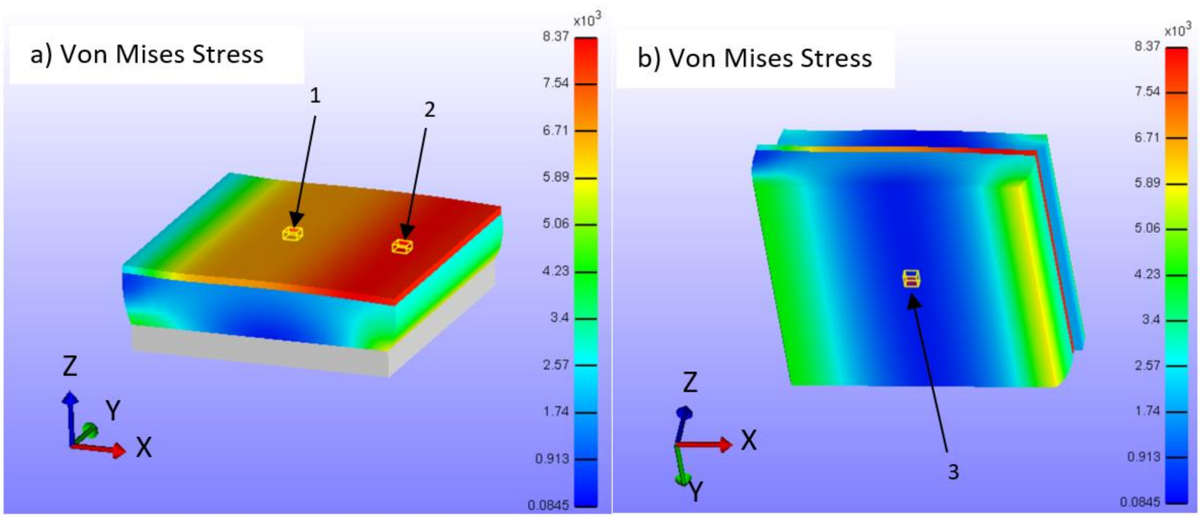

Figure 5-13: a) Gel layer hidden and presenting the model without slip, demonstrating two locations of Von Mises stress analysis on the skin. b) Location 3 is in the middle y direction of the muscle to bone interface. (Scales are in Pa.)

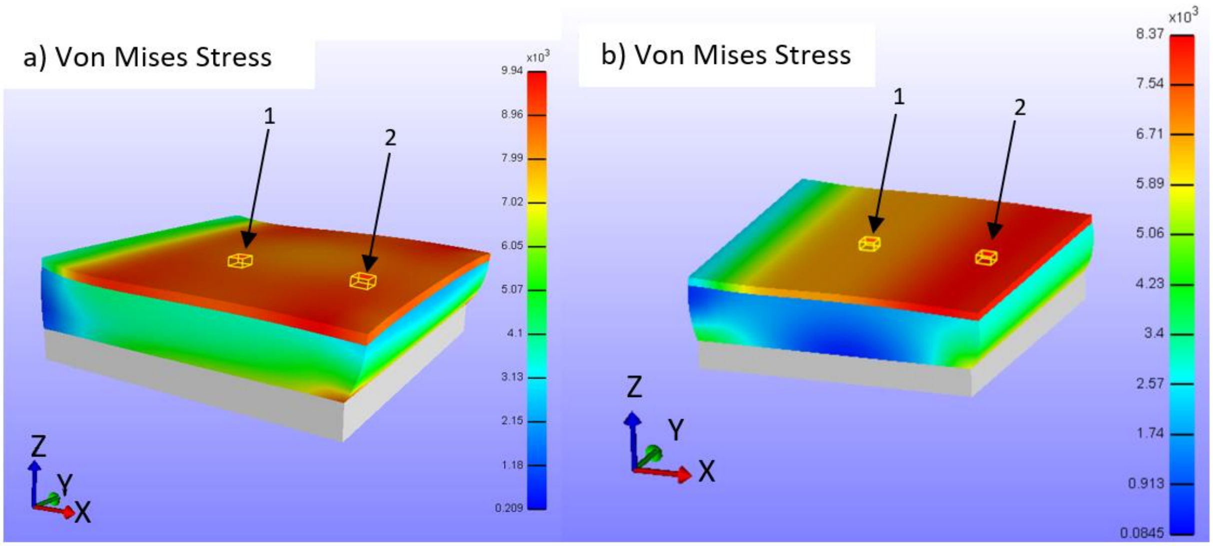

Figure 5-14. Gel layer hidden with difference is stress distribution in skin layer. a) Model with no slip. b) Model with slip. (Scales are in Pa.)

Table 5-8: Comparison for slip versus no slip conditions in three locations (same liner used in both). Location 1 and 2 are in the skin layer of the model and location 3 is at the muscle to bone interface (Figure 5-14).

	No Slip Model			Slip Model		
	Location 1	Location 2	Location 3	Location 1	Location 2	Location 3
Von Mises Stress (kPa)	9.12	9.24	2.65	6.71	8.39	0.39
Z Compressive Stress (kPa)	-4.78	-4.96	-4.63	-5.12	-4.80	-4.88
Max Shear Stress (kPa)	4.98	5.09	1.53	3.88	4.84	0.22

5.3.2.4 Liner Stiffness Results

The stresses caused by four liners were also compared. With increasing prosthetic gel liner stiffness (i.e. Alpha to Iceross Comfort to DERMO to TEC Urethane), models without slip demonstrated increased compressive stresses, and increased Von Mises and maximum shear stresses at the bone to muscle interface. Compressive stresses in the skin were similar for all liners. Maximum shear stresses were reduced in the skin as liner stiffness increased (Table 5-9). These were consistent trends for the models without slip. However, increasing gel liner stiffness in models with slip were consistent with no increasing or decreasing trends.

Table 5-9. Comparison of Von Mises, normal compressive and maximum shear stress for four different modeled prosthetic gel liners with model comparisons across a no slip and slip condition of the liner with respect to the skin.

ALPHA Liner (E = 50.05 kPa)	No Slip Model			Slip Model		
	Location 1	Location 2	Location 3	Location 1	Location 2	Location 3
Von Mises Stress (kPa)	9.120	9.236	2.653	6.687	8.347	0.385
Z Compressive Stress (kPa)	-4.777	-4.955	-4.625	-4.965	-4.924	-4.88
Max Shear Stress (kPa)	4.976	5.090	1.531	3.859	4.815	0.216

Iceross Comfort (E =55.86 kPa)	No Slip Model			Slip Model		
	Location 1	Location 2	Location 3	Location 1	Location 2	Location 3
Von Mises Stress (kPa)	8.848	8.813	2.722	6.687	8.352	0.384
Z Compressive Stress (kPa)	-4.833	-5.040	-4.742	-4.963	-4.927	-4.885
Max Shear Stress (kPa)	4.797	4.871	1.572	3.859	4.818	0.215

DERMO (E = 56.28 kPa)	No Slip Model			Slip Model		
	Location 1	Location 2	Location 3	Location 1	Location 2	Location 3
Von Mises Stress (kPa)	8.829	8.784	2.727	6.687	8.352	0.384
Z Compressive Stress (kPa)	-4.837	-5.047	-4.75	-4.963	-4.927	-4.885
Max Shear Stress (kPa)	4.785	4.855	1.574	3.859	4.818	0.215

TEC Urethane (E = 88.06 kPa)	No Slip Model			Slip Model		
	Location 1	Location 2	Location 3	Location 1	Location 2	Location 3
Von Mises Stress (kPa)	7.846	7.172	2.908	6.664	8.364	0.382
Z Compressive Stress (kPa)	-4.995	-5.385	-5.23	-4.944	-4.933	-4.916
Max Shear Stress (kPa)	4.112	4.000	1.679	3.845	4.824	0.214

5.3.2.5 Liner Thickness Results

Stresses in underlying tissues were also evaluated for three gel liner thicknesses: 9 mm, 6 mm, and 3 mm (Table 5-10). For models with no slip, trends were seen. At location one, skin Von Mises and maximum shear stresses increased with decreasing liner thickness. Location 2 was relatively unchanged for skin Von Mises and maximum shear stresses. For both locations 1 and 2, compressive stresses were unchanged. At muscle to bone interface (Location 3), Von

Mises and max shear stresses increased with decreasing liner thickness while compressive stresses decreased (Table 5-10). For the models with slip, skin Von Mises stresses at location 1 were unchanged for varying gel liner thickness. For location 2, skin Von Mises, compressive stresses and shear stresses decreased with thinner liners. At the bone to muscle interface, compressive stresses decreased with thinner liners but Von Mises and shear stresses remained unchanged.

Table 5-10. Comparison of TEC Urethane liner for three thicknesses of 9, 6 and 3 mm for no slip and slip model definitions between the gel liner and skin interface.

TEC Urethane (E = 88.06 kPa)	No Slip Model			Slip Model		
9 mm	Location 1	Location 2	Location 3	Location 1	Location 2	Location 3
Von Mises Stress (kPa)	7.846	7.172	2.908	6.664	8.364	0.382
Z Compressive Stress (kPa)	-4.995	-5.385	-5.230	-4.944	-4.933	-4.916
Max Shear Stress (kPa)	4.112	4.000	1.679	3.845	4.824	0.214

TEC Urethane (E = 88.06 kPa)	No Slip Model			Slip Model		
6 mm	Location 1	Location 2	Location 3	Location 1	Location 2	Location 3
Von Mises Stress (kPa)	7.999	7.053	3.112	6.650	8.349	0.376
Z Compressive Stress (kPa)	-5.081	-5.339	-4.977	-4.903	-4.881	-4.780
Max Shear Stress (kPa)	4.258	4.000	1.797	3.837	4.816	0.211

TEC Urethane (E = 88.06 kPa)	No Slip Model			Slip Model		
3 mm	Location 1	Location 2	Location 3	Location 1	Location 2	Location 3
Von Mises Stress (kPa)	8.208	7.174	3.325	6.617	8.296	0.378
Z Compressive Stress (kPa)	-5.063	-5.216	-4.72	-4.863	-4.821	-4.735
Max Shear Stress (kPa)	4.479	4.117	1.920	3.819	4.785	0.212

5.4 Discussion

The presented work provides new analyses of skin and muscle tissue based on experimental data inputs from prosthetic users. Further, the effects of liner stiffness and thickness were evaluated as a result of various gel liner scenarios which are commonly worn by transtibial amputees. In order to arrive at the complex four layer models, simplified models first investigated the influences of various neo-hookean material responses to different geometries, constraints and layers. The results can be used by engineers and clinicians to redesign material properties and select appropriate liners given knowledge of the patient's loading and displacement within the socket.

5.4.1 Simplified Models

Simplified simulations were used to document the effects of geometry, layering and constraints. Results of these models provided us with a basis for the more complex four layer models. Stress results of simplified models corresponded well with non-linear continuum mechanics theory. Next, one variable at a time was changed, such as the layers, material properties and contacts. These results supported the development of the four layer models by understanding these interactions. Contacts between layers did not create a stress concentration at the interface, guiding interpretation of stresses seen in gel, skin and muscle layers later.

5.4.2 Realistic Four Layer Models

5.4.2.1 Cylindrical versus Rectangular Geometry

In the four layer model, the layer thicknesses were selected based on the literature, however, the region could have been represented as a circular or square cross-section because the layer thicknesses were consistent throughout the individual layers. Therefore, a comparison of the results for two geometries was conducted. The data between cylindrical and square geometries were similar for for Von Mises and shear stresses, supporting the use of either geometry for further models.

5.4.2.2 Vertical Face Constraints

For comparing a condition of slip between the liner and skin interface, a sliding with gaps contact was implemented which required vertical face constraints. Therefore, on the models which did not require vertical constraints, additional constraints were added and analyzed to evaluate the effects of these constraints on stresses. The results demonstrated stresses with and without vertical constraints in the tied interface contact definition. Tied interface models without vertical constraints yielded tissue stresses higher than models with vertical constraints. For example, Von Mises stresses at the bone to muscle interface decreased across constraint conditions (no slip without constraints to no slip with constraints to slip with constraints). It can be suggested that vertical constraints applied in the slip models do not account for the relative change in tissue stresses and instead are associated with the contact interaction itself between the skin and gel liner.

5.4.2.3 Slip versus No Slip

When comparing the gel interface contact models, a difference found was the increased shear stress at the bone to muscle interface when not allowing slip to occur. Clinically prosthetic liners were developed as a method to cushion the transfer of loads from the prosthetic socket to the residual limb tissue (Klute et al. 2010). However, if the liner is slipping with respect to the skin surface, the question arises of whether the interface is still providing the intended protection. Our models demonstrate that compressive stresses are relatively similar across the slip versus no slip models. Therefore, cushioning is being provided mechanically to the residual limb regardless of slip. Yet, it is the increased shear at the bone to muscle interface that is of concern for deep tissue ulcer formation (De Wert et al. 2015; Manorama et al. 2010; Manorama et al. 2013). As, it has also been shown that with the addition of shear force, blood occlusion of underlying tissues is increased when compared to a compressive load alone (Manorama et al. 2013). Further study on the conditions of slip and no slip, particularly experimental studies are necessary.

5.4.2.4 Liner Stiffness

To further investigate the influences of gel liners on underlying tissue, four different gel liners were modeled with increasing stiffness. Skin demonstrated a decreased maximum shear stress with increasing stiffness for the models not allowing slip. Mechanically, the stiffest urethane prosthetic liner is closest to mechanical properties of skin with a Young's modulus of 88 kPa in the liner versus 95 kPa for skin (Levy et al. 2015; Shoham et al. 2015). With maximum shear stresses being the lowest for the urethane liner, it may suggest this would reduce skin irritation when wearing this liner. The clinical intention is for the gel liner to grip the skin and move with the residual limb. However, these stiffness results change when modeling the slip condition. When slip occurred, it can be seen that maximum shear stress decreased in all simulations and little change was observed between different liners. This is because once the liner slips relative to the skin, it no longer transfers load differently based on the liner material stiffness. This would suggest it is preferable to have a stiffer liner to minimize the level of shear stress in the skin. Clinically, if a patient presents with skin irritation, a prosthetist often will change to a softer liner. However, these model results suggest the opposite should be considered.

5.4.2.5 Liner Thickness

Prosthetic liner thickness is also commonly varied during prescription and development of a custom device. Manufacturers often provide standard liner thicknesses such as 3, 6 and 9 mm. Our models demonstrated little to no change in skin stresses but the bone to muscle interface increased shear and Von Mises stress with decreasing liner thickness. Mechanically, with the same amount of load and prescribed displacement it makes sense that a greater shear strain would be experiences and resulting shear stress because the thicknesses of the overall model is decreased.

5.4.3 Engineering Model Relevance to Influence Clinical Practices

With such a variety of prosthetic liner options, there is a developing need for engineering based analyses to better understand and inform prosthetists of the mechanical influence of various gel liners on the underlying tissue stresses. This work provides the needed mechanical assessments of the gel liner interface.

Numerous studies have attempted to quantify skin material properties; however, it is greatly dependent upon strain rate, load applied, type of tissue and location relative to the body from which it was harvested (Gallagher, A. J.; Ní Annaidh, Aisling; Bruyère 2012; Sanders et al. 1995; Pailler-Mattei et al. 2008; Holt et al. 2008). Based on our experimental strain results, we saw 6-11% strain. Walking is a cyclical event occurring approximately one cycle per second (Perry, Jacquelin; Burnfield 2010). Skin ultimate tensile strength (UTS) of 0.25-1.0 MPa was reported when loading at 0.25-10% strain per second at an initial stress of 10 kPa (Diridollou et al. 2001; Zhou et al. 2010). These studies provide an appropriate comparison to our results because we experimentally collected strain data within this range. Based on the work of numerous investigators, if loading is conducted at a slower strain rate of approximately 10% strain per minute, the UTS increased to a range of 2-30 MPa (Silver et al. 2001; Ni et al. 2012; Gallagher et al. 2012; Ankersen et al. 1999).

Simulations do not exceed published skin UTS values, however, the models represent a single loading event instead of a fatigue evaluation to failure. Therefore, values need to be considered relative to typical daily situations for prosthetic users. On average, transtibial amputees take 3395 steps per day (Stepien et al. 2007). Beyond a certain number of cyclical loadings however, reparative mechanisms are exceeded and tissue breakdown begins. Future studies could assess FEA fatigue simulations with repeated loading conditions.

Further evaluation of our models when comparing to literature and experimental data supports the meaningful results of our reported stresses. The skin layer experienced approximately 9 kPa of Von Mises stress for the 9 mm Alpha liner, which compares well to typically loaded skin samples which experienced 10 kPa of stress for *in vitro* testing (Diridollou et al. 2001). Furthermore, gel liner shear stress of 2.7 kPa in the model, compares well with experimental shear stress of 0.79-2.89 kPa during initial contact phase of walking found in our experimental work.

5.4.4 Limitations, Future Work, Summary

A limitation of our models is that our FE analysis was conducted for one iteration of loading and was not performed in a cyclical analysis. Consideration should be given to this for future model developments so that the long term cyclical effects of load on the skin can be evaluated. However, other limitations of the models presented include the generalized geometry of a block region in the limb. The anatomical limb contains bony prominences and soft tissue thicker regions. The changing bone geometry in the residual limb can create stress concentration patterns because of the distinct differences in bone material properties. Future studies could combine imaging techniques with our experimentally collected loading conditions to strengthen model results dependent on anatomical differences.

Overall, these model results can provide insight into how soft-tissue responds due to typical below knee amputee loading conditions with a modeled gel liner interface. Results suggest that liner thickness and material properties should be considered when patients present with a history of skin irritation or deep tissue injury based on documented trends in stresses throughout these simulations. Commonly manufactured liners are typically one solid material. These results could influence the further design of liners and consideration could include development of functionally graded materials.

5.5 Conclusions

Soft-tissue finite element models are needed to improve our understanding of the interface mechanics between prosthetic liners and underlying tissues in prosthetic users. Novel and unique models were developed in a sequence of simulations to address questions regarding the gel liner slip with respect to the skin and influences of liner stiffness and thickness on tissue stresses. The comparison of slip and no slip conditions present an important clinical question because clinically, slip of the liner with respect the limb is not desired. Additionally, if slip does not occur, the uneven displacements on the liner would produce a shearing of deeper tissue which is also not desirable. Trends reported for influences in tissue stresses for changing stiffness and thicknesses are an important addition to the understanding of the interface mechanics. Amputees often present with ulcers on their residual limb and added knowledge of stresses and strains can improve the understanding of what is contributing to the wounds. Further model studies and experimental data to support these models are warranted. Mechanics based data is a necessity to formulate improved prosthetic fit and design, these additional data are also helpful in guiding prosthetists in the selection of appropriate prosthetic liners for patients.

6. CONCLUSIONS

6.1 Dissertation Conclusions

In conclusion, the completed research focused on quantifying mechanics occurring at the socket to gel liner interfaced limb in transtibial amputees for better understanding of ulcer formation. To experimentally assess the limb, a novel motion capture method was developed to measure motion within the socket. The method was implemented in human subjects to evaluate displacements and strains of the gel liner and with respect to the socket. Next a case study measured shear and normal forces within the prosthetic socket wall during walking. Lastly, previously collected experimental data was used for loading conditions in finite element models to evaluate stresses of the underlying tissues due to typical walking loading conditions and various gel liner interactions with the skin.

The first part of this research validated a methodology using motion capture to quantify residual limb gel liner motion within the prosthetic socket. Clear prosthetic sockets were developed out of clinically used test socket material. Through the use of these sockets, motion capture thin-disc markers were placed on meaningful locations of the residual limb on top of the gel liner. These anatomical locations corresponded with soft tissue and bony landmark locations which were intentionally positioned with respect to pressure tolerant and intolerant locations where pressure ulcers commonly occur. Through numerous testing protocols, first static inter-marker distances were captured with caliper and motion capture methods. For two residual limb replicas, rigid and deformable, the analysis proved that inter-marker distances could be accurately captured within the clear prosthetic socket. The test setup was also translated through space, without changing the position of the limb with respect to the socket, to understand how different angles of the limb relative to the motion capture cameras could calculate inter-marker distances. Through statistical analyses, no differences were found for biplanar movement of the limb through space, nor for the static measurements comparing caliper to motion capture measures. This positively confirmed the ability for this method to be used to capture human residual limb and gel liner motion during walking. Dynamic trials were completed for the replica limb mock-up which demonstrated greater displacements distally near the pin on the gel liner insertion near the suspension mechanism. This was further supported by a single case study for a transtibial amputee during walking which analyzed greatest displacements distally in the residual limb. All this data positively supported the use of this method in multiple transtibial amputees to evaluate the influence of gel liner interface pin locking mechanisms on socket to limb interface movements.

The second part of this dissertation therefore implemented the previously validated method in nine transtiblial limbs during walking. Four measures were calculated to evaluate the various displacements and strains occurring within the prosthetic socket. Liner displacements with respect to each other were calculated, displacements with respect to the socket, rotations with respect to the socket and strains of the gel liner were all assessed during walking. Startling data revealed large displacements at the distal end of the limb, likely due to the gel liner interface with pin suspension insertion at the distal end of the limb. This data would indicate that users with frequent limb irritation leading to wounds may be better suited with a suspension type that does not cause increased strain at the distal end of the limb. Results also highlighted that limb displacements were much greater than clinicians expected, therefore overestimating the effectiveness of a “well fit prosthesis”. Results from this study should inform prosthetists of the risks for transtibial amputees when experiencing pain, discomfort or wound formation over commonly seen areas. Care should be given to redesigning sockets to minimize “play” within the socket and therefore minimizing how much the limb can translate with respect to the socket during walking.

The third experimental part included work measuring shear forces at the surface of the skin and socket to limb interface. For three conditions in a single transtibial case study, shear and normal forces were meaningfully analyzed during typical walking. Patients often use additional socks within their socket to account for volume changes and this study evaluated these differences in addition to evaluating shear forces directly at the skin. Overall, this work was important because it contributed to the understanding of shear force influence on changing socket to limb forces. Many patients wear different interface thicknesses during the day and this case study highlights a single sample of how these forces changed. The addition of shear force measurement in addition to normal force is important for considering the underlying tissue influences for blood perfusion and tissue health when additional shear is present. Finally, these results are also helpful for creating finite element models which can be based on experimentally captured data for boundary conditions and loading inputs.

The final part included finite element modeling of typical tissue thickness in the mid-fibular region for a transitibal amputee. These models were constrained with previously discussed experimental data to evaluate typical stresses occurring throughout the day in each step a limb experiences. Additionally, two conditions were heavily analyzed for the conditions of whether the gel liner slipped with respect to the skin surface or not as named, “slip and no slip conditions”. Once these differences were understood, the models were modified to evaluate various gel liner manufacturer properties such as stiffness and thickness to evaluate which liner selections would be appropriate for particular cases based on the underlying tissue stress analyses. With increasing gel liner stiffness in the no slip models, skin maximum shear stress decreased and bone to muscle compressive stress decreased. Thinner gel liners increased Von Mises and maximum shear stresses in both skin and muscle tissues. Decreasing liner thickness also decreased compressive stresses at the bone to muscle interface. Differences in stresses at the superficial versus deep tissue can be helpful in understanding mechanisms leading to ulcer formation. Soft-tissue finite element models are needed to improve our understanding of the interface mechanics between prosthetic liners and underlying tissues in prosthetic users. The comparison of slip and no slip conditions presented an important medical question because clinically, slip of the liner with respect the limb is not desired. Additionally, if slip does not occur, the uneven displacements on the liner would produce a shearing of deeper tissue which is also not desirable. Further model studies and experimental data to support these models are warranted. Mechanics based data is a necessity to formulate improved prosthetic fit and design, these additional data are also helpful in guiding prosthetists in the selection of appropriate prosthetic liners for patients.

In summary, this work provided 1) a new method used to quantify the most comprehensive data set of within socket displacements, 2) interface shear and normal forces for a below knee amputee which were used for modeling conditions, and 3) a series of models addressed tissue stresses and liner interface mechanics. The presented research benefits the biomechanical world by addressing multiple gaps in the literature which were evaluated using mechanical engineering principles. This data can further understanding of pressure ulcer formation due to interface mechanics and aid in understanding the fit of a prosthetic socket with a gel liner interface. The combination of experimental data and modeling can be very powerful in the engineering world to put emphasis on model importance when constrained with real world loading conditions. Throughout this dissertation, the intention was to create new methods and analyses to improve the life for amputees experiencing frequent pressure ulcers and wound formation. Since this area is still misunderstood and an under analyzed topic, this work contributed to the literature to further the improvement of socket fit, prosthetic device design and mechanics evaluation for transtibial amputees.

APPENDICES

APPENDIX A: FE Modeling Review

Table A-1: Summary of FE modeling methodologies investigators implemented in the first decade of prosthetic modeling. Original table, however, much of the content comes from a published review article (Zachariah & Sanders 1996). E = Young's modulus and v = Poisson's ratio.

Investigator (year)	Source of Geometric Data			Material Characterization				Loading	
	Bone	Residual Limb	Liner/ Socket	Bone E (GPa) v	Muscle E (kPa) v	Liner E (kPa) v	Socket E (GPa) v	Pre-strain	External
Brennan (1992)	matched CT scan	wrap-cast	socket	15.5 0.28	60 0.49	-	rigid surface	radial displacement	vertical load of 285 N on bone
Reynolds (1992)	matched bones	wrap-cast	CASD-template	rigid surface	50-145 0.45	-	rigid surface	radial displacement	bone displaced vertically under 350 N
Sanders (1993)	MRI	MRI	MRI	rigid surface	65.5-438† 0.49	1.8 0.39	1 0.35	-	Stance force and moment waveforms on distal socket
Steege (1998)	CT scan	CT scan	CT scan	15.5* 0.28	60 0.49	380 0.49	rigid surface	-	vertical load of 279/287 N and 3 moments on proximal femur
Steege (1995)	CT scan	CT scan	CT scan	.001-1.5* 0.28	2.6-96 0.499	-	0.001-2.1 0.28	-	Stance force and moment waveforms on distal socket
Silver-Thorn (1991)	regular geometry	regular geometry	CASD-template	rigid surface	2.9-110.5 0.45-0.499	380 0.49	1.5 0.30	-	vertical load of 287 N and 3 moments on distal socket
	regular geometry	wrap-cast	CAR		2.3-404.5 0.45-.4999				
	CT scan	CT scan	socket		3.8-1229.4 0.45-0.499				
Quesada (1991)	-	-	socket	-	60-2490††	-	14 0.13	-	heelstrike force of 984 N on heel
Zhang (1993)	matched bones	wrap-cast	CASD-template	rigid surface	50-145 0.45	380 0.49	rigid surface	radial displacement	vertical displacement of 8mm on bone
Zhang (1995)	matched bones	wrap-cast	CASD-template	0.01 0.49	160-260 0.49	380 0.49	rigid surface	radial displacement	vertical load of 800 N on bone

CASD=University College London - Computer-Aided-Socket-Design software. E= Young's modulus. v= Poisson's ratio

†Sanders also modeled skin. E = 4.3-6.9 kPa, v = 0.49.

* Steege also modeled cartilage. E = 790 kPa, v = 0.49 (1998) E = 100 kPa, v = 0.499 (1995).

††Quesada used springs to model muscle. The "elastic modulus" was converted to a spring stiffness based on tissue area and thickness

APPENDIX B: FE Modeling with Imaging Review

Table B-1: Research summary FE models with improved imaging techniques but still using linearly elastic material properties for biological tissues.

Investigator (Year)	**Source of Geometric data**	**Layers with material properties**	**Contacts between layers**	**Boundary Conditions**	**2D or 3D**	**Verified with Experimental Data**
Zhang, Roberts 2000	Biplanar X-ray views	Soft tissues, bone and liner: isotropic and linearly elastic	Contact, separating and slipping at skin to liner	Weight bearing in vertical direction only	3D	Yes, experimental stress from load cells
Lee, Zhang, Jia, Cheung 2004	MRI	Linearly elastic, isotropic, homogeneous	Unspecified	External surface of socket fixed	3D	No
Lee, Zhang 2007	MRI	Linearly elastic, isotropic, homogeneous	Soft tissue boundaries connect to bones were fixed	Bones fixed boundaries Force of load tolerance applied to each site	3D	Yes, pressure of painful regions
Zachariah, Sanders 2000	CAD, CT, MRI	Linear elastic, isotropic, homogeneous	Frictional slip versus frictionless slip at socket	800 N axial force applied at distal end of socket	3D	No

APPENDIX C: FE Modeling Using FEBio

Table C-1: Recent summary of FE models using FEBio in related biological research

Investigator (Year)	**Source of Geometric data**	**Layers with material properties**	**Contacts between layers**	**Boundary Conditions**	**2D or 3D**	**Verified with Experimental Data**
Levy, Frank, Gefen 2015	MRI	Bone and Achilies tendon: linear-elastic isotropic Skin and fat: nearly incompressible, nonlinear isotropic materials with large deformation behavior as uncoupled neo-Hookean material	Tied interfaces between all tissue components Coefficient of friction between skin and support 0.43	Reaction force at heel in WB during supine lying from experimental data	3D	No
Shoham, Levy, Kopplin, Gefen 2015	MRI	Bone and contoured foam cushion: isotropic linear elastic Muscle, fat, skin: nearly incompressible and hyperelastic represented as a neo-Hookean material	Tied interface between all tissues Frictional sliding between skin and CFC	Body weight along top boundary. Fixed surface at inferior edge of CFC	3D but uniformly extruded from a 2D MRI slice	No
Sengeh, Moerman, Petron, Herr 2016	MRI	Soft tissue (skin-adipose layer and internal muscle-soft tissue complex): non-linear elastic (Mooney-Rivlin J = 1; J is the determinant of the deformation gradient tensor) and viscoelastic materials Bones modeled as rigidly supported voids	Not specified	Load curves for loading and unloading applied at each site derived from experimental displacement-time data Fixed at top surface of residuum	3D	Yes

APPENDIX D: IRB Approval Letter

MICHIGAN STATE UNIVERSITY

Renewal Application Approval

January 16, 2017

To: Tamara Reid-Bush
2555 Engineering Building
MSU

Re: **IRB# 14-089M** Category: EXPEDITED 4,6,7
Renewal Approval Date: January 5, 2016
Project Expiration Date: January 4, 2018

Title: Measurement of motions and forces associated with the use of a lower leg prosthetic

The Institutional Review Board has completed their review of your project. I am pleased to advise you that the renewal has been approved.

The review by the committee has found that your renewal is consistent with the continued protection of the rights and welfare of human subjects, and meets the requirements of MSU's Federal Wide Assurance and the Federal Guidelines (45 CFR 46 and 21 CFR Part 50). The protection of human subjects in research is a partnership between the IRB and the investigators. We look forward to working with you as we both fulfill our responsibilities.

Renewals: IRB approval is valid until the expiration date listed above. If you are continuing your project, you must submit an Application for Renewal application at least one month before expiration. If the project is completed, please submit an Application for Permanent Closure.

Revisions: The IRB must review any changes in the project, prior to initiation of the change. Please submit an Application for Revision to have your changes reviewed. If changes are made at the time of renewal, please include an Application for Revision with the renewal application.

Problems: If issues should arise during the conduct of the research, such as unanticipated problems, adverse events, or any problem that may increase the risk to the human subjects, notify the IRB office promptly. Forms are available to report these issues.

Please use the IRB number listed above on any forms submitted which relate to this project, or on any correspondence with the IRB office.

If we can be of further assistance, please contact us at 517-355-2180 or via email at IRB@msu.edu. Thank you for your cooperation.

c: Amy Lenz, Katie Johnson

Office of Regulatory Affairs
Human Research Protection Programs

Biomedical & Health Institutional Review Board (BIRB)

Community Research Institutional Review Board (CRIRB)

Social Science Behavioral/Education Institutional Review Board (SIRB)

Olds Hall
408 West Circle Drive, #207
East Lansing, MI 48824
(517) 355-2180
Fax: (517) 432-4503
Email: irb@msu.edu
www.hrpp.msu.edu

APPENDIX E: IRB Consent Form

Measurement of Motions and Forces Associated with the Use of a Lower Leg Prosthetic
Biomechanical Design Research Laboratory
and
Mary Free Bed Rehabilitation Hospital
Motion Analysis Center

You are being asked to participate in a biomechanics research project. The researchers are required to provide a consent form to inform you about the study, to convey that participation is voluntary, to explain risks and benefits of participation, and to empower you to make an informed decision. You should feel free to ask the researchers any questions you may have. The following provides an overview of testing that will occur in the research project entitled "Measurement of Motions and Forces Associated with the Use of a Lower Leg Prosthetic".

1. PURPOSE OF RESEARCH:

The purpose of this study is to measure the force patterns and tissue motion in the residual limb of amputees. The results of this research work will help in understanding the development of pressure ulcer sores in the prosthetic socket to limb interface.

2. WHAT YOU WILL BE ASKED TO DO:

If you consent to participate, the approximate duration of the testing is 3 hours and participation is on a voluntary basis. An overview of the test will include, a short health questionnaire, sensors being applied to your body to monitor your walking through the lab space, videotaping of your walking, photographs of your leg, and a scan of your leg to create a 3D image. These tests will be performed twice on the first day of participation and then repeated in a month.

First, you will be asked to complete a health questionnaire, then some basic physical measurements will be taken such as height and weight and dimensions of the body segments and test regions. Certain areas of the skin will be cleaned with an alcohol swab to assure that tape used for retro-reflective markers will adhere. Hypo-allergenic medical tape will be used to attach these markers to the surface of the skin. You may be asked to wear special clothing such as biking shorts or athletic tops so the sensors can be positioned without the clothing interfering. We may ask that you wear clean laboratory clothing if the attire you brought will not work with our sensors. Once all reflective markers are placed on the body and your existing prosthetic device, you will be asked to perform walking trials through the walkway of the laboratory. Motion and force data will be gathered and transferred electronically to a computer. Secondly, a special instrumented prosthetic test socket will hold a force measurement device while your body segment (residual limb) fits within the device as your typical prosthetic socket would fit (customized to you). Once again you will walk multiple times though the designated walkway of the laboratory. Motion and force data will again be gathered and transferred electronically to the computer. Lastly, a clinically used tool will be used to scan your amputated limb in order to create a 3D image of your leg. The scan is painless as no contact is required as a wand is merely waved around your leg. The collected scan will be electronically transferred to the computer for anatomical and volume measurement calculations.

This study contains multiple phases of data collection. The procedure will be repeated the same day in the afternoon or evening (approximately 5 hours later). One month later the two repeated protocols will be conducted in the morning and late afternoon/evening of the same day.

3. POTENTIAL BENEFITS:

You will not directly benefit from your participation in this study. However, your participation will help in the gathering of data that will be useful in understanding the development of pressure ulcers and may help identify better prevention strategies in amputees.

4. POTENTIAL RISKS:

There is minimal risk of injury from your participation in this research. All of the work related to this project is non-invasive and will be conducted under the supervision of individuals who are experts with the involved techniques. You may experience some redness on the skin due to the adhesive tape. This redness usually disappears within a few hours, and lotion is available to you upon the removal of the tape.

5. PRIVACY AND CONFIDENTIALITY:

Participation remains confidential, and confidentiality will be maintained with all data, which will be protected to the maximum extent allowable by law. References to all data, including photographs will be made by using a coded identification number that will not reveal your identity. Research records will be kept in locked filing cabinets, on password encrypted computers and/or encrypted files in the Mechanical Engineering Department at Michigan State University. Only the study researchers and HRPP will have access to your identifiable information. Your data and photographs will be stored with the investigator for three (3) years after completion of the project. Other members of the study team may have access to your numerical data but they will not have access to your identifiable information. Access of these data by students is for the purpose of data processing. Published experimental results will not reveal your identity.

In addition to the measurements mentioned above, you may also be photographed by one of the listed researchers or other qualified laboratory assistants. This information may be used for presentation and/or publications relating to the research study.

6. YOUR RIGHTS TO PARTICIPATE, SAY NO, OR WITHDRAW:

Your participation in this study is voluntary. You may choose not to participate at all, or you may refuse to participate in certain procedures. You are free not to answer certain questions, and you may discontinue your participation at any time without penalty or loss of benefits. Whether you choose to participate or not will have no effect on your medical care or treatment at Mary Free Bed Rehabilitation Hospital. You will be told of any significant findings that develop during the course of the study that may influence your willingness to continue to participate in the research.

Further, the researchers may elect to discontinue testing on any individual with or without cause at any time, or to disqualify any individual for any reason at any time.

7. COSTS AND COMPENSATION FOR BEING IN THE STUDY:

You will not be compensated for your participation. There are no costs to participate. The testing time is approximately 3 hours.

8. THE RIGHT TO GET HELP IF INJURED:

If you are injured as a result of your participation in this research project, Michigan State University will assist you in obtaining emergency care, if necessary, for your research related injuries. If you have insurance for medical care, your insurance carrier will be billed in the ordinary manner. As with any medical insurance, any costs that are not covered or in excess of what are paid by your insurance, including deductibles, will be your responsibility. The University's policy is not to provide financial compensation for lost wages, disability, pain or discomfort, unless required by law to do so. This does not mean that you are giving up any legal rights you may have. You may contact the Principal Investigator, Tamara Reid Bush at (517) 353-9544 with any questions or to report an injury.

Further, your participation is voluntary, you may choose not to participate at all, or you may refuse to participate in certain procedures or answer certain questions or discontinue your participation at any time without penalty or loss of benefits. We appreciate your participation.

9. CONTACT INFORMATION FOR QUESTIONS AND CONCERNS

If you have concerns or questions about this study, such as scientific issues, how to do any part of it, or to report an injury (i.e. physical, psychological, social, financial, or otherwise), please contact the researcher:

Tamara Reid Bush, Ph.D.
Amy Lenz
2555 Engineering Building
East Lansing, MI 48824
Phone: 517-353-9544
Email: reidtama@msu.edu, lenzamy@msu.edu or amy.lenz@maryfreebed.com

If you have questions or concerns about your role and rights as a research participant, would like to obtain information or offer input, or would like to register a complaint about this study, you may contact, anonymously if you wish, the Michigan State University's Human Research Protection Program at 517-355-2180, Fax 517-432-4503, or e-mail irb@msu.edu or regular mail at 408 W. Circle Drive, Room 207 Olds Hall, MSU, East Lansing, MI 48824.

10. DOCUMENTATION OF INFORMED CONSENT

Your signature below means that you voluntarily agree to participate in this research study.

I voluntarily agree to participate in this study.

- *You are eligible to participate in the project even if you wish to not have photographs taken.*
  - I agree to allow digital photos/ digital video clips during the experiment.

    ☐Yes ☐No Initials____________

- I agree to allow my photographs in reports and presentations without blocking identifying features, i.e. it is ok to show your picture without a black box over your face
  ☐ Yes ☐ No Initials____________

Signature:______________________________________Date:_________

This consent form was approved by a Michigan State University Institutional Review Board. Approved 01/05/17 – valid through 01/04/18. This version supersedes all previous versions. IRB # 14-089M.

BIBLIOGRAPHY

BIBLIOGRAPHY

Ali, S., Osman, N.A.A., et al., 2012. Clinical investigation of the interface pressure in the trans-tibial socket with Dermo and Seal-In X5 liner during walking and their effect on patient satisfaction. *Clinical Biomechanics*, 27(9), pp.943–948.

Ali, S. et al., 2013. Interface pressure in transtibial socket during ascent and descent on stairs and its effect on patient satisfaction. *Clinical Biomechanics*, 28(9-10), pp.994–999.

Ali, S., Abu Osman, N.A., et al., 2012. Qualitative study of prosthetic suspension systems on transtibial amputees' satisfaction and perceived problems with their prosthetic devices. *Archives of Physical Medicine and Rehabilitation*, 93(11), pp.1919–1923.

Ankersen, J. et al., 1999. Puncture resistance and tensile strength of skin simulants. *Journal of Engineering in Medicine*, 213, pp.493–501.

Appoldt, F., Bennett, L. & Contini, R., 1969. Stump-socket pressure in lower extremity prostheses. *Journal of Biomechanics*, 2(2), pp.207–208.

Arao, H., Shimada, T. & Hagisawa, S., 2013. Morphological characteristics of the human skin over posterior aspect of heel in the context of pressure ulcer development. *Journal of Tissue Viability*, 22(2), pp.42–51.

Armstrong, D.G. et al., 1997. Amputation and reamputation of the diabetic foot. *Journal of the American Podiatric Medical Association*, 87(6), pp.255–259.

Attinger, C.E. et al., 2006. Angiosomes of the foot and ankle and clinical implications for limb salvage: reconstruction, incisions, and revascularization. *Plastic and reconstructive surgery*, 117(7 Suppl), p.261S–293S.

Bahr, C. et al., 1993. Lower-extremity amputation: incidence, risk factors, and mortality in the Oklahoma Indian Diabetes Study. *Diabetes*, 42(6), pp.876–884.

Beil, T.L., Street, G.M. & Covey, S.J., 2002. Interface pressures during ambulation using suction and vacuum-assisted prosthetic sockets. *Journal of rehabilitation research and development*, 39(6), pp.693–700.

Bonet, J. & Wood, R.D., 2008. *Nonlinear Continuum Mechanics for Finite Element Analysis* 2nd Editio., Cambridge, United Kingdom: Cambridge University Press.

Boulton, A.J.M., 2008. The diabetic foot: grand overview, epidemiology and pathogenesis. *Diabetes/metabolism research and reviews*, 24 Suppl 1(December 2007), pp.S3–6.

Bouten, C. V. et al., 2003. The etiology of pressure ulcers: Skin deep or muscle bound? *Archives of Physical Medicine and Rehabilitation*, 84(4), pp.616–619.

Boutwell, E. et al., 2012. Effect of prosthetic gel liner thickness on gait biomechanics and pressure distribution within the transtibial socket. *The Journal of Rehabilitation*

Research and Development, 49(2), p.227.

Brechow, A. et al., 2013. Improving major amputation rates in the multicomplex diabetic foot patient: focus on the severity of peripheral arterial disease. *Therapeutic advances in endocrinology and metabolism*, 4(3), pp.83–94.

Brennan, J.M. & Childress, D.S., 1991. Finite element and experimental investigation of above-knee amputee limb/prosthesis systems: a comparative study. *ASME-BED*, 20, pp.547–550.

Brown, B.J., Crone, C.G. & Attinger, C.E., 2012. Amputation in the diabetic to maximize function. *Seminars in vascular surgery*, 25(2), pp.115–21.

Brunelli, S. et al., 2009. Vacuum assisted socket system in transtibial amputees: clinical report. *Orthopadie-Technik Quarterly*, pp.2–7.

Burner, A. et al., 2013. Lifecasting in O&P. In *In Proceedings of the 39th American Academy of Orthotists and Prosthetists Annual Meeting*. Orlando, FL.

Childers, W.L. & Siebert, S., 2015. Marker-based method to measure movement between the residual limb and a transtibial prosthetic socket. *Prosthetics and orthotics international*, pp.1–9.

Coleman, S. et al., 2013. Patient risk factors for pressure ulcer development: Systematic review. *International Journal of Nursing Studies*, 50(7), pp.974–1003.

Collins, T.C. et al., 2002. Lower extremity nontraumatic amputation among veterans with peripheral arterial disease: is race an independent factor? *Medical care*, 40(1 Suppl), pp.I106–I116.

Convery, P. & Murray, K.D., 2001. Ultrasound study of the motion of the residual femur within a trans-femoral socket during daily living activities other than gait. *Prosthetics and orthotics international*, 25(3), pp.220–7.

Convery, P. & Murray, K.D., 2000. Ultrasound study of the motion of the residual femur within a trans-femoral socket during gait. *Prosthetics and orthotics international*, 24(3), pp.226–32.

Daly, C.H. & Odland, G.F., 1979. Age-related changes in the mechanical properties of human skin. *The Journal of Investigative Dermatology*, 73(1), pp.84–87.

Dillingham, T.R., Pezzin, L.E. & Shore, A.D., 2005. Reamputation, mortality, and health care costs among persons with dysvascular lower-limb amputations. *Archives of Physical Medicine and Rehabilitation*, 86(3), pp.480–486.

Diridollou, S. et al., 2001. Skin ageing : changes of physical properties of human skin in vivo. *International Journal of Cosmetic Science*, 23, pp.353–362.

Dombroski, S. et al., 2014. Silicone Model Project. In *In Proceedings of the 40th American Academy of Orthotists and Prosthetists Annual Meeting*. Chicago, IL.

Dou, P. et al., 2006. Pressure distribution at the stump/socket interface in transtibial amputees during walking on stairs, slope and non-flat road. *Clinical Biomechanics*, 21(10), pp.1067–1073.

Dudek, N.L., Marks, M.B. & Marshall, S.C., 2006. Skin problems in an amputee clinic. *American journal of physical medicine & rehabilitation / Association of Academic Physiatrists*, 85(5), pp.424–429.

Dumas, R., Cheze, L. & Frossard, L., 2009. Loading applied on prosthetic knee of transfemoral amputee: Comparison of inverse dynamics and direct measurements. *Gait and Posture*, 30(4), pp.560–562.

Edwards, M., 2000. Below knee prosthetic socket designs and suspension systems. *Physical medicine and rehabilitation clinics of North America*, 11(3), pp.585–593.

Emrich, R. & Slater, K., 1998. Comparative analysis of below-knee prosthetic socket liner materials. *Journal of medical engineering & technology*, 22(2), pp.94–98.

Erikson, U. & Lemperg, R., 1969. Roentgenological study of movements of the stump within the prosthuis socket in below-knee amputees fitted. *Acta orthop. Scandinav*, 40, pp.520–529.

Eshraghi, A. et al., 2013. An experimental study of the interface pressure profile during level walking of a new suspension system for lower limb amputees. *Clinical Biomechanics*, 28(1), pp.55–60.

Fagundes, C. et al., 2005. Prognostic factors for amputation or death in patients submitted to vascular surgery for acute limb ischemia. *Vascular health and risk management*, 1(4), pp.345–9.

Fergason, J. & Smith, D.G., 1999. Socket considerations for the patient with a transtibial amputation. *Clinical Orthopaedics and Related Research*, 361, pp.76–84.

Friberg, O., 1984. Biomechanical significance of the correct length of lower limb prostheses: a clinical and radiological study. *Prosthetics and orthotics international*, 8, pp.124–129.

Gailey, R.S. et al., 2002. The Amputee Mobility Predictor: An instrument to assess determinants of the lower-limb amputee's ability to ambulate. *Archives of Physical Medicine and Rehabilitation*, 83(5), pp.613–627.

Galbusera, F. et al., 2014. Comparison of various contact algorithms for poroelastic tissues. *Computer methods in biomechanics and biomedical engineering*, 17(12), pp.1323–34.

Galdik, J., 1955. The Below-Knee Suction Socket. *Orthop Prosthet Appl J*, 9, pp.43–46.

Gallagher, A.. J.., Ní Annaidh, A. & Bruyère, K., 2012. Dynamic Tensile Properties of Human Skin. *International Research Council on the Biomechanics of Injury*, (IRC-12-59), pp.494–502.

Gard, S.A., 2006. Use of quantitative gait analysis for the evaluation of prosthetic walking performance. *JPO: Journal of Prosthetics and Orthotics*, 18(1), pp.93–104.

Gefen, A. et al., 2008. Strain-time cell-death threshold for skeletal muscle in a tissueengineered model system for deep tissue injury. *Journal of Biomechanics*, 41(9), pp.2003–2012.

Gholizadeh, H. et al., 2015. A comparison of pressure distributions between two types of sockets in a bulbous stump. *Prosthetics and Orthotics International*, pp.1–8.

Gholizadeh, H. et al., 2014. Clinical implication of interface pressure for a new prosthetic suspension system. *Biomedical engineering online*, 13(1), p.89.

Gholizadeh, H. et al., 2014. Transtibial prosthesis suspension systems: Systematic review of literature. *Clinical Biomechanics*, 29(1), pp.87–97.

Gholizadeh, H. et al., 2012. Transtibial prosthetic socket pistoning: Static evaluation of Seal-In ® X5 and Dermo ® Liner using motion analysis system. *Clinical Biomechanics*, 27(1), pp.34–39.

Golbranson, F.L. et al., 1988. Volume changes occurring in postoperative below-knee residual limbs. *Journal of Rehabilitation Research*, 25(2), pp.11–18.

Haltmayer, M. et al., 2001. Impact of atherosclerotic risk factors on the anatomical distribution of peripheral arterial disease. *International Angiology*, 20, pp.200–207.

Heim, M. et al., 1997. Silicone suspension of external prostheses. A new era in artificial limb usage. *The Journal of bone and joint surgery. British volume*, 79, pp.638–640.

Henrot, P. et al., 2000. Imaging of the painful lower limb stump. *Radiographics : a review publication of the Radiological Society of North America, Inc*, 20 Spec No, pp.S219–S235.

Holman, K.H. et al., 2012. Racial Disparities in the Use of Revascularization Before Leg Amputation in Medicare Patients. *Journal of Vascular Surgery*, 54(2), pp.420–426.

Holt, B., Tripathi, A. & Morgan, J., 2008. Viscoelastic response of human skin to low magnitude physiologically relevant shear. *Journal of Biomechanics*, 41(12), pp.2689–2695.

Johnson, K. & Davis, A.J., 2014. Lower Extremity Prosthetic Sockets and Suspension Systems. In *Prosthetic Restoration and Rehabilitation of the Upper and Lower Extremity*. New York, NY: Demos Medical Publishing, pp. 59–70.

Jude, E. et al., 2001. Peripheral Arterial Disease in Diabetic and Nondiabetic Patients. *Diabetes Care*, 24(8), pp.1433–1437.

Kahle, J.T., 1999. Conventional and hydrostatic transtibial interface comparison. *Journal of Prosthetics and Orthotics*, 11(4), pp.85–91.

Kapp, S., 1999. Suspension systems for prostheses. *Clinical Orthopaedics and Related Research*, 361, pp.55–62.

Kapp, S.L. & Fergason, J.R., 2004. Transtibial Amputation: Prosthetic Management. In *Atlas of Amputations and Limb Deficiences: Surgical, Prosthetic and Rehabilitation Principles*. Rosemont, IL: American Academy of Orthopedic Surgeons, pp. 503–515.

Khan, N.A. et al., 2014. Does the Clinical Examination Predict Lower Extremity Peripheral Arterial Disease? *Journal of the American Medical Association*, 295(5), pp.6–8.

Klute, G.K., Glaister, B.C. & Berge, J.S., 2010. Prosthetic liners for lower limb amputees : A review of the literature. *Prosthetics and Orthotics International*, 34(June), pp.146–153.

Koc, E. et al., 2008. Skin problems in amputees: A descriptive study. *International Journal of Dermatology*, 47(5), pp.463–466.

Krouskop, T. a et al., 1987. Computer-aided design of a prosthetic socket for an above-knee amputee. *Journal of rehabilitation research and development*, 24(2), pp.31–38.

Langewouters, G., Wesseling, K. & Goedhard, W., 1984. The static elastic properties of 45 human thoracic and 20 abdominal aortas in vitro and the parameters of a new model. *Journal of Biomechanics*, 17(6), pp.425–435.

Le, K.M. et al., 1984. An In-depth look at pressure sores using monolithic silicone pressure sensors. *Plastic and reconstructive surgery*, 74(6), pp.745 – 754.

Leavitt, L.A. et al., 1970. Quantitative method to measure the relationship between prosthetic gait and the forces produced at the stump-socket interface. *American Journal of Physical Medicine and Rehabilitation*, 49(3), pp.192–203.

Lee, W.C.C. et al., 2004. Finite element modeling of the contact interface between trans-tibial residual limb and prosthetic socket. *Medical Engineering and Physics*, 26(8), pp.655–662.

Lee, W.C.C. & Zhang, M., 2007. Using computational simulation to aid in the prediction of socket fit: A preliminary study. *Medical Engineering and Physics*, 29(8), pp.923–929.

Levy, A., Frank, M.B.O. & Gefen, A., 2015. The biomechanical efficacy of dressings in preventing heel ulcers. *Journal of Tissue Viability*, 24(1), pp.1–11.

Levy, S., 1995. Amputees: skin problems and prostheses. *Cutis*, 55(5), pp.297–301.

Levy, S. & Barnes, G., 1956. Verrucous hyperplasia of amputation stump. *Archives of Dermatology*, 74(4), pp.448–449.

Liao, F., Burns, S. & Jan, Y., 2013. Skin blood flow dynamics and its role in pressure ulcers. *Journal of Tissue Viability*, 22(2), pp.25–36.

Lilja, M., Johansson, T. & Oberg, T., 1993. Movement of the tibial end in a PTB prosthesis socket: a sagittal X-ray study of the PTB prosthesis. *Prosthetics and orthotics international*, 17(1), pp.21–6.

Lyon, C.C. et al., 2000. Skin disorders in amputees. *Journal of the American Academy of Dermatology*, 42(3), pp.501–507.

Maas, S.A. et al., 2012. FEBio: Finite Elements for Biomechanics. *Journal of*

Biomechanical Engineering, 134(1), p.011005.

Mak, A.F.T., Zhang, M. & Tam, E.W.C., 2010. Biomechanics of Pressure Ulcer in Body Tissues Interacting with External Forces during Locomotion. *The Annual Review of Biomedical Engineering*, 12, pp.29–53.

Manorama, A. et al., 2013. Quantifying the effects of external shear loads on arterial and venous blood flow: Implications for pressure ulcer development. *Clinical Biomechanics*, 28(5), pp.574–578.

Manorama, A.A. et al., 2010. Blood perfusion and transcutaneous oxygen level characterizations in human skin with changes in normal and shear loads - Implications for pressure ulcer formation. *Clinical Biomechanics*, 25(8), pp.823–828.

Marso, S.P. & Hiatt, W.R., 2006. Peripheral arterial disease in patients with diabetes. *Journal of the American College of Cardiology*, 47(5), pp.921–929.

Meier, R.H., 1973. Stump-socket fit of below-knee prostheses: comparison of three methods of measurement. *Archives of Physical Medicine and Rehabilitation*, 54(12), pp.553–558.

Meng, Q. et al., 2013. Comparison between FEBio and Abaqus for biphasic contact problems. *Proceedings of the Institution of Mechanical Engineers. Part H, Journal of engineering in medicine*, 227(9), pp.1009–19.

Miller, A., 2009. Gait event detection using a multilayer neural network. *Gait and Posture*, 29, pp.542–545.

Muller, E.A. & Hettinger, T., 1952. A new method for measurement of pressure within suction socket. *Zeitschrift fur Orthopadie und Unfallchirurgie*, 83(1), pp.132–137.

Naeff, M. & van Pijkeren, T., 1980. Dynamic pressure measurements at the interface between residual limb and socket--the relationship between pressure distribution, comfort, and brim shape. *Bulletin of prosthetics research*, 10(33), pp.35–50.

Narita, H., Yokogushi, K., Shii, S., Kakizawa, M. & Nosaka, T., 1997. Suspension effect and dynamic evaluation of the total surface bearing (TSB) trans-tibial prosthesis: a comparison with the patellar tendon bearing (PTB) trans-tibial prosthesis. *Prosthetics and orthotics international*, 21(3), pp.175–178.

Neumann, E.S. et al., 2013. Use of a load cell and force-moment curves to compare transverse plane moment loads on transtibial residual limbs: A preliminary investigation. *Prosthetics and orthotics international*, 38(3), pp.253–262.

Newton, R.L. et al., 1988. Skeletal Radiology Radiological evaluation of prosthetic fit in below-the-knee amputees. *Skeletal Radiology*, 17, pp.276–280.

Ni, A.A. et al., 2012. Characterization of the anisotropic mechanical properties of excised human skin. *Journal of Bechanical Behaviour of Biomedical Materials*, 5, pp.139–148.

Nixon, J. et al., 2006. Pressure relieving support surfaces: a randomised evaluation. *Health technology assessment (Winchester, England)*, 10(22), pp.2–6.

Noor, S.A. & Mahmud, J., 2015. Modelling and Computation of Silicone Rubber Deformation Adapting Neo-Hookean Constitutive Equation. *International Conference on Communication Systems and Network Technologies*, pp.1323–1326.

O'Hara, G.P., 1983. Mechanical Properties of Silicone Rubber in a Closed Volume. *Technical Report ARLCB*, 2(December).

Oomens, C.W.J. et al., 2016. How does lateral tilting affect the internal strains in the sacral region of bed ridden patients? — A contribution to pressure ulcer prevention. *Clinical Biomechanics*, 35, pp.7–13.

Owings, M.F. & Kozak, L.J., 1998. Ambulatory and inpatient procedures in the United States, 1996. *Vital and health statistics. Series 13, Data from the National Health Survey*, (139), pp.1–119.

Pailler-Mattei, C., Bec, S. & Zahouani, H., 2008. In vivo measurements of the elastic mechanical properties of human skin by indentation tests. *Medical Engineering and Physics*, 30(5), pp.599–606.

Papaioannou, G. et al., 2010. Assessment of amputee socket-stump-residual bone kinematics during strenuous activities using Dynamic Roentgen Stereogrammetric Analysis. *Journal of biomechanics*, 43(5), pp.871–8.

Pearson, J.R., 1974. Pressure variation in the below-knee, patellar tendon bearing suction socket prosthesis. *Journal of Biomechanics*, 7(6), pp.487–496.

Perduta, A. & Putanowicz, R., 2015. Comparison of elastomer modelling in various FEM packages. *Procedia Engineering*, 108, pp.510–517.

Perry, Jacquelin; Burnfield, J.M., 2010. *Gait Analysis Normal and Pathological Function* 2nd Editio., Thorofare, NJ: SLACK Incorporated.

van Pijkeren, T., Naeff, M. & Kwee, H.H., 1980. A new method for the measurement of normal pressure between amputation residual limb and socket. *Bulletin of prosthetics research*, 10(33), pp.31–34.

Pirouzi, G. et al., 2014. Review of the socket design and interface pressure measurement for transtibial prosthesis. *Scientific World Journal*, 2014.

Portnoy, S. et al., 2011. Effects of sitting postures on risks for deep tissue injury in the residuum of a transtibial prosthetic-user: a biomechanical case study. *Computer methods in biomechanics and biomedical engineering*, 14(11), pp.1009–19.

Portnoy, S. et al., 2008. Internal mechanical conditions in the soft tissues of a residual limb of a trans-tibial amputee. *Journal of Biomechanics*, 41(9), pp.1897–1909.

Portnoy, S., Siev-Ner, I., Shabshin, N., et al., 2009. Patient-specific analyses of deep tissue loads post transtibial amputation in residual limbs of multiple prosthetic users. *Journal of Biomechanics*, 42(16), pp.2686–2693.

Portnoy, S. et al., 2007. Real-time patient-specific finite element analysis of internal stresses in the soft tissues of a residual limb: A new tool for prosthetic fitting. *Annals of Biomedical Engineering*, 35(1), pp.120–135.

Portnoy, S. et al., 2010. Real-time subject-specific analyses of dynamic internal tissue loads in the residual limb of transtibial amputees. *Medical Engineering and Physics*, 32(4), pp.312–323.

Portnoy, S., Siev-Ner, I., Yizhar, Z., et al., 2009. Surgical and morphological factors that affect internal mechanical loads in soft tissues of the transtibial residuum. *Annals of Biomedical Engineering*, 37(12), pp.2583–2605.

Pritham, C.H., 1979. Suspension of the below knee prosthesis: An overview. *Ortho Pros*, 33(22), pp.1–19.

Prompers, L. et al., 2007. High prevalence of ischaemia, infection and serious comorbidity in patients with diabetic foot disease in Europe. Baseline results from the Eurodiale study. *Diabetologia*, 50(1), pp.18–25.

Prosthetists, A.A. of O. and, 2004. Post-Operative Management of the Lower Extremity Amputee: Official Findings of the Consensus Conference. In *American Academy of Orthotists and Prosthetists*.

Quesada, P. & Skinner, H., 1991. Analysis of a below-knee patellar tendon-bearing prosthesis : A finite element study. *Journal of Rehabilitation Reasearch*, 28(3), pp.1–12.

Radcliffe, C.W. & Foort, J., 1961. *Patellar-tendon-bearing Below-knee Prosthesis* 1st ed., Berkeley, CA: University of California.

Reynolds, D.P. & Lord, M., 1992. Interface load analysis for computer-aided design of below-knee prosthetic sockets. *Medical and Biological Engineering and Computing*, 30(4), pp.419–426.

Robbins, J.M. et al., 2008. Mortality rates and diabetic foot ulcers: is it time to communicate mortality risk to patients with diabetic foot ulceration? *Journal of the American Podiatric Medical Association*, 98(6), pp.489–493.

Sanders, J.E. et al., 2006. A noncontact sensor for measurement of distal residual-limb position during walking. *Journal of rehabilitation research and development*, 43(4), pp.509–516.

Sanders, J.E. et al., 2005. Changes in interface pressures and shear stresses over time on trans-tibial amputee subjects ambulating with prosthetic limbs: Comparison of diurnal and six-month differences. *Journal of Biomechanics*, 38(8), pp.1566–1573.

Sanders, J.E. et al., 2009. Clinical utility of in-socket residual limb volume change measurement: case study results. *Prosthetics and orthotics international*, 33(4), pp.378–390.

Sanders, J.E. et al., 1998. Effects of alignment changes on stance phase pressures and shear stresses on transtibial amputees: Measurements from 13 transducer sites. *IEEE Transactions on Rehabilitation Engineering*, 6(1), pp.21–31.

Sanders, J.E. et al., 2000. Effects of changes in cadence, prosthetic componentry, and time on interface pressures and shear stresses of three trans-tibial amputees. *Clinical Biomechanics*, 15(9), pp.684–694.

Sanders, J.E. et al., 1997. Interface pressures and shear stresses at thirteen socket sites on two persons with transtibial amputation. *Journal of rehabilitation research and development*, 34(1), pp.19–43.

Sanders, J.E. et al., 1998. Material properties of commonly-used interface materials and their static coefficients of friction with skin and socks. *Journal of rehabilitation research and development*, 35(2), pp.161–176.

Sanders, J.E. et al., 2004. Testing of elastomeric liners used in limb prosthetics: classification of 15 products by mechanical performance. *Journal of rehabilitation research and development*, 41(2), pp.175–186.

Sanders, J.E. & Daly, C.H., 1993. Normal and shear stresses on a residual limb in a prosthetic socket during ambulation: Comparison of finite element results with experimental measurements. *Journal of Rehabilitation Reasearch*, 30(2), pp.191–204.

Sanders, J.E., Daly, C.H. & Burgess, E.M., 1992. Interface shear stresses during ambulation with a below-knee prosthetic limb. *Journal of rehabilitation research and development*, 29(4), pp.1–8.

Sanders, J.E. & Fatone, S., 2011. Residual Limb Volume Change: Systematic Review of Measurement and Management. *Journal of Rehabilitation Reasearch device*, 48(8), pp.949–986.

Sanders, J.E., Goldstein, B.S. & Leotta, D.F., 1995. Skin response to mechanical stress: Adaptation rather than breakdown - A review of the literature. *Journal of Rehabilitation Research and Development*, 32(3), pp.214–226.

Schiff, a. et al., 2014. Quantification of Shear Stresses Within a Transtibial Prosthetic Socket. *Foot & Ankle International*, 35(8), pp.779–782.

Schwartz, M.H. & Rozumalski, A., 2008. The gait deviation index: A new comprehensive index of gait pathology. *Gait and Posture*, 28(3), pp.351–357.

Schwarze, M. et al., 2013. Loads on the prosthesis-socket interface of above-knee amputees during normal gait: Validation of a multi-body simulation. *Journal of Biomechanics*, 46(6), pp.1201–1206.

Sengeh, D.M. et al., 2016. Multi-material 3-D viscoelastic model of a transtibial residuum from in-vivo indentation and MRI data. *Journal of the Mechanical Behavior of Biomedical Materials*, 59, pp.379–392.

Shoham, N. et al., 2015. Contoured Foam Cushions Cannot Provide Long-term

Protection Against Pressure-Ulcers for Individuals with a Spinal Cord Injury: Modeling Studies. *Advances in skin & wound care*, 28(7), pp.303–316.

Silver, F.H., Freeman, J.W. & Devore, D., 2001. Viscoelastic properties of human skin and processed dermis. *Skin Research and Technology*, 7(9), pp.18–23.

Silver-Thorn, M.B., 1991. *Estimation and experimental verification of residual limb/prosthetic socket interface pressures for below-knee amputees*. Northwestern University.

Spires, M.C., Kelly, B.M. & Davis, A.J., 2014. *Prosthetic Restoration and Rehabilitation of the Upper and Lower Extremity* 1st ed., New York, NY: demosMedical.

Steege, J.W. & Childress, D.S., 1988. *Finite element estimation of pressure at the below-knee socket interface by finite element analysis*, Seattle, WA.

Stepien, J.M. et al., 2007. Activity Levels Among Lower-Limb Amputees : Self-Report Versus Step Activity Monitor. *Archives of Physical Medicine and Rehabilitation*, 88(July), pp.896–900.

Taylor, G.I. & Pan, W.R., 1998. Angiosomes of the Leg: Anatomic Study and Clinical Implications. *Plastic and reconstructive surgery*, 102(3), pp.599–616.

Tepole, A.B. et al., 2011. Growing skin: A computational model for skin expansion in reconstructive surgery. *J Mech Phys Solids*, 59(10), pp.2177–2190.

Thomson, K.C., 1966. On the Complex Poisson ' s Ratio of a Urethane Rubber Compound. *Journal of Applied Polymer Science*, 10, pp.1133–1136.

De Wert, L.A. et al., 2015. A new method to evaluate the effects of shear on the skin. *Wound Repair and Regeneration*, 23(6), pp.885–890.

Wolf, S.I. et al., 2009. Pressure characteristics at the stump/socket interface in transtibial amputees using an adaptive prosthetic foot. *Clinical Biomechanics*, 24(10), pp.860–865.

Zachariah, S.G. et al., 2004. Shape and volume change in the transtibial residuum over the short term: Preliminary investigation of six subjects. *journal of Rehabilitation Research and Development*, 41(5), pp.683–694.

Zachariah, S.G. & Sanders, J.E., 2000. Finite element estimates of interface stress in the trans-tibial prosthesis using gap elements are di ! erent from those using automated contact. , 33.

Zachariah, S.G. & Sanders, J.E., 1996. Interface mechanics in lower-limb external prosthetics: A review of finite element models. *IEEE Transactions on Rehabilitation Engineering*, 4(4), pp.288–302.

Zhang, M. et al., 1995. Development of a non-linear finite element modelling of the below-knee prosthetic socket interface. *Medical Engineering and Physics*, 17(8), pp.559–566.

Zhang, M., Mak, A.F.T. & Roberts, V.C., 1998. Finite element modelling of a residual lower-limb in a prosthetic socket: A survey of the development in the first decade. *Medical Engineering and Physics*, 20(5), pp.360–373.

Zhang, M. & Roberts, C., 2000. Comparison of computational analysis with clinical measurement of stresses on below-knee residual limb in a prosthetic socket. *Medical Engineering and Physics*, 22(9), pp.607–612.

Zhou, B.B. et al., 2010. Strain rate sensitivity of skin tissue under thermomechanical loading. *Philosophical Transactions of the Royal Society*, 368, pp.679–690.

Ziegler-Graham, K. et al., 2008. Estimating the Prevalence of Limb Loss in the United States: 2005 to 2050. *Archives of Physical Medicine and Rehabilitation*, 89(3), pp.422–429.

Zollner, A.M. et al., 2013. Growth on demand: Reviewing the mechanobiology of stretched skin. *J Mech Phys Solids*, 28, pp.495–509.